

**A COMPARISON OF TWO WARMING TREATMENTS AND THEIR EFFECTS
ON PLANT GROWTH AND ECOSYSTEM CO₂ EXCHANGE, AND A
CONCURRENT STUDY OF SEASONAL VARIATION IN THE SOIL
MICROBIAL COMMUNITY**

EMILY WILTON
Bachelor of Science (Great Distinction)
University of Lethbridge, 2012

A Thesis
Submitted to the School of Graduate Studies
of the University of Lethbridge
in Partial Fulfilment of the
Requirements for the Degree

MASTER OF SCIENCE

Department of Biological Sciences
University of Lethbridge
LETHBRIDGE, ALBERTA, CANADA

© Emily Wilton, 2015

A COMPARISON OF TWO WARMING TREATMENTS AND THEIR EFFECTS
ON PLANT GROWTH AND ECOSYSTEM CO₂ EXCHANGE, AND A
CONCURRENT STUDY OF SEASONAL VARIATION IN THE SOIL MICROBIAL
COMMUNITY

EMILY WILTON

Date of Defence: March 24, 2015

Dr. Lawrence B. Flanagan Supervisor	Professor	Ph.D.
Dr. L. Brent Selinger Thesis Examination Committee Member	Professor	Ph.D.
Dr. Stewart B. Rood Thesis Examination Committee Member	Professor	Ph.D.
Dr. Elizabeth A. Schultz Thesis Examination Committee Member	Associate Professor	Ph.D.
Dr. Anthony Russell Chair, Thesis Examination Committee	Assistant Professor	Ph.D.

Abstract

This study compared the effects of two different warming treatments (open-top chambers and infrared heaters) on the environmental conditions in native prairie grassland. Both treatments increased average air temperature, with infrared heaters providing a more consistent warming than open-top chambers, but also a more significant decrease in soil moisture. Additionally, the effects of warming on plant biomass and ecosystem CO₂ exchange were examined. No significant effects of increased temperature were found, although 2013 had higher precipitation than normal and produced more aboveground biomass than average years, with correspondingly low $\delta^{13}\text{C}$ and $\delta^{18}\text{O}$ values. Finally, a concurrent study examined the seasonal variation in soil microbial activity, as controlled by the direct and indirect effects of soil temperature and soil moisture. Significant seasonal patterns were found in soil respiration, soil microbial biomass, extracellular enzyme activity and the species composition of the soil bacterial community.

Acknowledgments

I would like to thank my thesis supervisor Dr. Larry Flanagan for opportunity to pursue research in his field. His support and encouragement has pushed me to be the best I can be. I would also like to thank the rest of my supervisory committee, Dr. Stewart Rood, Dr. Brent Selinger, and Dr. Elizabeth Schultz for all of their support and feedback on my progress. I would specifically like to thank Dr. Elizabeth Schultz for providing me the opportunity to do undergraduate research and encouraging me to pursue my Master's degree.

I would also like to thank the students and staff in the Flanagan lab for all of their help and encouragement; my fellow graduate student, Trina Orchard, our technician, Eric Sharp, and our summer student employee, Kayla Johnson. I don't know if I could have gotten through all my field work without your help! I would also like to thank Dr. Alice Hontela and her students for the use of their lab equipment and expertise, and everyone in the Department of Biological Sciences store room.

Finally, I would like to thank my family and friends for all the love and support you've given me over the last two years. Even when things were most difficult, you have always believed in me and pushed me to keep going, and I couldn't be more proud of where I have ended up.

Funding was provided in the form of research grants to Dr. L.B. Flanagan from the Natural Sciences and Engineering Research Council of Canada (NSERC), as well as personal funding from the University of Lethbridge School of Graduate Studies, and scholarships from the Government of Alberta.

Table of Contents

Thesis Examination Committee Members Page	ii
Abstract	iii
Acknowledgements	iv
Table of Contents	v
List of Tables	vii
List of Figures	viii
List of Abbreviations and Symbols	xiii

CHAPTER 1. INTRODUCTION 1

CHAPTER 2. COMPARISON OF INFRARED HEATERS AND OPEN- TOP CHAMBERS AS EXPERIMENTAL WARMING METHODS

2.1 Introduction	4
2.2 Methods and materials	9
2.2.1 Field site description	9
2.2.2 Warming treatments	10
2.3 Results	12
2.4 Discussion	22
2.5 Conclusion	24

CHAPTER 3. EFFECTS OF EXPERIMENTAL WARMING ON PLANT BIOMASS PRODUCTION AND ECOSYSTEM CO₂ EXCHANGE IN A TEMPERATE GRASSLAND ECOSYSTEM

3.1 Introduction	25
3.2 Methods and materials	31
3.2.1 Field site description	31
3.2.2 Warming treatments	31
3.2.3 Peak aboveground plant biomass	31
3.2.4 Carbon dioxide flux	33
3.3 Results	35
3.3.1 Peak aboveground plant biomass	35
3.3.2 Carbon dioxide flux	36
3.4 Discussion	40
3.4.1 Peak aboveground plant biomass	40
3.4.2 Carbon dioxide flux	43
3.5 Conclusion	44

CHAPTER 4. SEASONAL VARIATION IN SOIL MICROBIAL BIOMASS, BACTERIAL COMMUNITY COMPOSITION AND EXTRACELLULAR ENZYME ACTIVITY IN RELATION TO SOIL RESPIRATION IN A NORTHERN GREAT PLAINS GRASSLAND

4.1 Introduction	45
4.2 Methods and materials	56
4.2.1 Field site description	56
4.2.2 Environmental measures	56

4.2.3	Carbon dioxide flux	56
4.2.4	Soil sample collection	57
4.2.5	Substrate-induced respiration	58
4.2.6	Soil enzyme activity	61
4.2.6.1	β-1,4-N-acetylglucosaminidase assay	62
4.2.6.2	Phenol oxidase assay	63
4.2.6.3	Modeling seasonal enzyme activity	66
4.2.7	Soil bacterial community composition	67
4.3	Results	70
4.3.1	Environmental conditions	70
4.3.2	Carbon dioxide flux	70
4.3.3	Substrate-induced respiration	72
4.3.4	Soil enzyme activity	73
4.3.5	Soil bacterial community composition	76
4.4	Discussion	95
4.4.1	Soil respiration	95
4.4.2	Substrate-induced respiration	97
4.4.3	Soil enzyme activity	98
4.4.4	Soil bacterial community composition	101
4.5	Conclusion	103
CHAPTER 5. CONCLUSION		104
REFERENCES		106

List of Tables

Table 3.1	Comparison of peak aboveground biomass collected on August 6, 2013, from control, infrared heated and open-top chamber plots in a grassland near Lethbridge, Alberta, and the elemental composition of the collected vegetation. Values represent mean \pm standard error, n=9.	37
Table 3.2	Comparison of peak aboveground biomass and growing season precipitation in the study year (2013), a year of average precipitation (1999) and a dry year (2001). Values represent mean \pm standard error, n=9. Values from 1999 and 2001 from Flanagan and Farquhar (2014).	37
Table 3.3	Comparison of carbon ($\delta^{13}\text{C}$) and oxygen ($\delta^{18}\text{O}$) isotope ratios from peak aboveground biomass collected on August 6, 2013, from control, infrared heated and open-top chamber plots. Values represent mean \pm standard error, n=9.	38
Table 3.4	Comparison of carbon ($\delta^{13}\text{C}$) and oxygen ($\delta^{18}\text{O}$) isotope ratios from peak aboveground biomass in the study year (2013), a year of average precipitation (1999) and a dry year (2001). Values represent mean \pm standard error, n=9. Values from 1999 and 2001 from Flanagan and Farquhar (2014).	38
Table 4.1	Comparison of the effects of sugar and yeast extract solutions (10% w/v) on the respiration rate of fresh soil, based on respiration rates measured 24 hours after the addition of the solution. Values represent mean \pm standard error, n=3.	69
Table 4.2	Comparison of the effects of substrate addition on the respiration rate of autoclaved and fresh soil. Values represent mean \pm standard error, n=2.	69

List of Figures

Figure 2.1	Diagram of a simple energy flow model with solar, sky, and infrared-heater radiation affecting a vegetation canopy. The numbers in the table are the theoretical resulting mid-day air, canopy, canopy air, and soil temperatures (°C) for “Reference”, anticipated “Global Warming”, “Infrared Heated Plot” and “Open-top Chamber”. Modified from Kimball (2011) with data from Hollister and Webber (2000).	8
Figure 2.2	The diurnal pattern of canopy temperature (a) and air temperature (b), based on measurements made in control, infrared heated and open-top chamber plots in a grassland ecosystem near Lethbridge, Alberta from August 14-24, 2013. Values represent average ± standard error, n=3.	17
Figure 2.3	The diurnal pattern of canopy temperature (a) and air temperature (b), based on measurements made in control, infrared heated and open-top chamber plots on September 1 and 2, 2013, which were a clear and overcast day, respectively. Values represent average ± standard error, n=3.	18
Figure 2.4	(a) Air temperature (°C) distribution in control, infrared heated and open-top chamber plots based on half-hourly measurements from May to October, 2013 (n=26,496). (b) Canopy temperature (°C) distribution in control and infrared heated plots based on hourly measurements from May to October, 2013 (n=12,816).	19
Figure 2.5	Soil temperature (°C) distribution in control, infrared heated, and open-top chamber plots at 5 cm (a) and 10 cm (b) depths, based on half-hourly measurements from May to October, 2013 (n=26,496).	20
Figure 2.6	Soil water content (m ³ m ⁻³) distribution in control, infrared heated and open-top chamber plots, based on half-hourly measurements from May to October, 2013 (n=25,776).	21

Figure 3.1	Comparison of integrated carbon flux rates (g C m^{-2} period ⁻¹) calculated based on half-hourly autochamber measurements of total carbon dioxide flux for control and warmed treatment plots during the growing season (May to October, 2013). Net ecosystem CO_2 exchange was partitioned total ecosystem respiration (TER) and gross ecosystem productivity (GEP), the difference between which represents net ecosystem productivity (NEP). Error bars represent \pm standard error. Statistical significance was based on single-factor ANOVA. NEP: $F(1)=0.4$, $p=0.57$, TER: $F(1)=0.9$, $p=0.40$, GEP: $F(1)=1.9$, $p=0.25$.	39
Figure 4.1	Temperature sensitivity coefficient (Q_{10}) as a function of temperature, as calculated by equation 4.3.	51
Figure 4.2	Respiration rate as a function of temperature and the effects of variation in water availability (A_w). Generated from Equation 4.1, with $R_{10} = 5 \mu\text{mol CO}_2 \text{ m}^{-2} \text{ s}^{-1}$ and Q_{10} varying as shown in Figure 4.1.	52
Figure 4.3	A theoretical pattern illustrating the effects of temperature on biomass.	53
Figure 4.4	A theoretical pattern illustrating the effects of biomass on respiratory capacity (R_{10}).	54
Figure 4.5	Respiration rate as a function of temperature and the effects of variation in respiratory capacity (R_{10}). Generated from Equation 4.1, with $A_w = 0.65$ and Q_{10} varying as shown in Figure 4.1.	55
Figure 4.6	Seasonal variation in (a) daily average soil temperature at a depth of 5 cm, (b) daily average soil water content and (c) total daily precipitation at a grassland near Lethbridge, Alberta. Vertical lines mark June 1 and August 31, 2013, between which dates soil sampling was done. Values for soil temperature and water content represent 5-day averages \pm standard error, $n=9$. Statistical significance was based on single-factor ANOVA. (a) $F(35)=213$, $p<0.001$, (b) $F(34)=25$, $p<0.001$.	78

- Figure 4.7 Seasonal variation in (a) gross ecosystem productivity (GEP) and (b) total ecosystem respiration (TER), calculated from half-hourly autochamber measurements. Vertical lines mark June 1 and August 31, 2013, between which dates soil sampling was done. Values represent 5-day averages \pm standard error, $n=6$. Statistical significance was based on single-factor ANOVA. (a) $F(32)=53.3$, $p<0.001$, (b) $F(32)=65.9$, $p<0.001$. 79
- Figure 4.8 Seasonal variation in soil respiration, based on manual field measurements. Vertical lines mark June 1 and August 31, 2013, between which dates soil sampling was done. Values represent mean \pm standard error, $n=9$. Statistical significance was based on single-factor ANOVA. $F(14)=24.3$, $p<0.001$. 80
- Figure 4.9 The relationship between soil respiration and (a) soil temperature at a depth of 5 cm, (b) soil water content at 0-15 cm soil depth, and (c) the product of soil temperature and water content. The red triangles represent the anomalous measurements from days 212 - 221, and were not included in the correlation calculation. Symbols after r value indicate statistical significant (NS - not significant, * - $p<0.05$, ** - $p<0.01$, *** - $p<0.001$). $n=108$ when anomalous measurements are removed. 81
- Figure 4.10 Seasonal variation in living soil microbial biomass, measured using substrate-induced respiration as a proxy. Values represent mean \pm standard error, $n=9$. Statistical significance was based on single-factor ANOVA. $F(3)=6.6$, $p=0.001$. 82
- Figure 4.11 The relationship between substrate-induced respiration and (a) soil temperature at a depth of 5 cm, (b) soil water content, (c) gross ecosystem productivity, and (d) total ecosystem respiration. Symbols after r value indicate statistical significant (NS - not significant, * - $p<0.05$, ** - $p<0.01$, *** - $p<0.001$). $n=36$ for (a) and (b), $n=24$ for (c) and (d). 83

- Figure 4.12 Seasonal variation in measured activity of NAGase (left) and phenol oxidase (right) at 10°C (a,d) and 23°C (b,e), and their calculated temperature sensitivity coefficients (c,f). Values represent mean \pm standard error, n=9. Statistical significance was based on single-factor ANOVA. (a) F(3)=12.7, p<0.001, (b) F(3)=10.0, p<0.001, (c) F(3)=6.6, p=0.001, (d) F(3)=4.2, p=0.01, (e) F(3)=2.4, p=0.09, (f) F(3)=1.7, p=0.2. 84
- Figure 4.13 The relationship between NAGase activity at 10°C and (a) soil temperature at a depth of 5 cm, (b) soil water content, (c) gross ecosystem productivity (GEP), (d) total ecosystem respiration (TER), and (e) substrate-induced respiration (e). Symbols after *r* value indicate statistical significant (NS - not significant, * - p<0.05, ** - p<0.01, *** - p<0.001). n=36 for (a),(b) and (e), n=24 for (c) and (d). 85
- Figure 4.14 The relationship between phenol oxidase activity at 10°C and (a) soil temperature at a depth of 5 cm, (b) soil water content, (c) gross ecosystem productivity (GEP), (d) total ecosystem respiration (TER), and (e) substrate-induced respiration (e). Symbols after *r* value indicate statistical significant (NS - not significant, * - p<0.05, ** - p<0.01, *** - p<0.001). n=36 for (a),(b) and (e), n=24 for (c) and (d). 86
- Figure 4.15 Seasonal variation of modeled *in situ* enzyme activity of (a) NAGase and (b) phenol oxidase, calculated based on activity rate at 10°C, temperature sensitivity coefficient and actual daily average soil temperature at a depth of 10 cm, as shown in Equation 4.14. Values represent the average across plots (n=9). 87
- Figure 4.16 The relationship between modeled *in situ* NAGase activity and (a) gross ecosystem productivity (GEP) and (b) total ecosystem respiration (TER). Values represent the daily average, averaged across plots (n=6). Symbols after *r* value indicate statistical significant (NS - not significant, * - p<0.05, ** - p<0.01, *** - p<0.001). n=78. 88
- Figure 4.17 The relationship between modeled *in situ* phenol oxidase activity and (a) gross ecosystem productivity (GEP) and (b) total ecosystem respiration (TER). Values represent the daily average, averaged across plots (n=6). Symbols after *r* value indicate statistical significant (NS - not significant, * - p<0.05, ** - p<0.01, *** - p<0.001). n=78. 89

Figure 4.18	(a) Correlation coefficients between modeled <i>in situ</i> phenol oxidase activity and gross ecosystem productivity (GEP) as a function lag-time (1-day lag means phenol oxidase activity is compared to GEP from one day earlier). Boxed values are not significantly different from the peak value, based on standard error of the correlation coefficient. (b) The relationship between modeled <i>in situ</i> phenol oxidase activity and mean GEP, using 23-day lag, n=78. (c) Seasonal variation in modeled <i>in situ</i> phenol oxidase activity and GEP, where DOY for GEP = DOY + 23, to account for lag.	90
Figure 4.19	Seasonal variation in (a) species richness and (b) species diversity of the soil bacterial community. Values represent mean \pm standard error, n=9. Statistical significance was based on single-factor ANOVA. (a) F(3)=0.9, p=0.5, (b) F(3)=2.8, p=0.06.	91
Figure 4.20	Seasonal variation in the relative abundance of the major bacterial phyla. Values represent the mean (n=9).	92
Figure 4.21	Seasonal variation in the relative abundance of 8 major bacterial phyla. Values represent mean \pm standard error (n=9). Statistical significance was based on single-factor ANOVA. (a) F(3)=15.4, p<0.001, (b) F(3)=6.5, p=0.001, (c) F(3)=4.8, p=0.007, (d) F(3)=6.9, p=0.001, (e) F(3)=15.6, p<0.001, (f) F(3)=2.4, p=0.09, (g) F(3)=12.6, p<0.001, (h) F(3)=18.6, p<0.001.	93
Figure 4.22	Seasonal variation in the relative abundance of the four major <i>Proteobacteria</i> classes. Values represent mean \pm standard error (n=9). Statistical significance was based on single-factor ANOVA. (a) F(3)=9.5, p<0.001, (b) F(3)=1.9, p=0.17, (c) F(3)=7.2, p<0.001, (d) F(3)=8.0, p<0.001.	94

List of Abbreviations and Symbols

A = leaf net CO₂ assimilation rate

A_w = available soil water content

abs. = absorbance

c_a = partial pressure of CO₂ in the atmosphere outside a leaf

c_i = partial pressure of CO₂ within leaf intercellular spaces

E = leaf transpiration rate

e_a = partial pressure of water in the atmosphere outside a leaf

e_i = partial pressure of water within leaf intercellular spaces

f_{Aw} = relative water stress function

fluor. = fluorescence

GEP = gross ecosystem productivity

GPP = gross primary productivity

IPCC = Intergovernmental Panel on Climate Change

LAI = leaf area index

L-DOPA = L-dihydroxyphenylalanine

n = number of moles (mol)

NAGase = β -1,4-*N*-acetylglucosaminidase

NEP = net ecosystem productivity

NMDS = nonmetric multidimensional scaling

NPP = net primary productivity

OD = optical density

OTU = operational taxonomic unit

P = atmospheric pressure

Q_{10} = temperature sensitivity coefficient

R_{10} = basal rate at 10°C

R = gas constant (8.314 m³ Pa mol⁻¹ K⁻¹)

SIR = substrate-induced respiration

SOM = soil organic matter

T = temperature (K or °C, as listed)

TER = total ecosystem respiration

WUE = water-use efficiency

v = volume (m³)

VPD = vapour pressure deficit

$\delta^{13}\text{C}$ = carbon isotope ratio (¹³C/¹²C)

$\delta^{18}\text{O}$ = oxygen isotope ratio (¹⁸O/¹⁶O)

ΔCO_2 = change in CO₂ concentration

CHAPTER 1. INTRODUCTION

The Intergovernmental Panel on Climate Change (IPCC) defines climate change as “a change in the state of the climate that can be identified by changes in the mean and/or variability of the properties, and that persists for an extended period, typically decades or longer” (IPCC 2013a). It is known that there is currently more energy entering the Earth system than leaving (positive radiative forcing), and that the major contributor is the increase in concentration of atmospheric carbon dioxide since 1750 (IPCC 2013b). It is extremely likely that the observed warming since the mid-20th century has been due to anthropogenic impacts on the environment (IPCC 2013b). The questions that must be asked are no longer: is climate change occurring, and if so, what is causing it? We know that the concentration of atmospheric CO₂ is being changed by human activity, with consequences that include warmer air temperatures and altered precipitation and snow melt patterns (Barnett *et al.* 2005, Rosenzweig *et al.* 2008). Therefore, we must explore the consequences of increased atmospheric CO₂, increased temperatures in terrestrial ecosystems, changes in the frequency of extreme weather events and changes in the timing and amount of water availability.

The atmosphere and terrestrial ecosystems are both part of the global carbon cycle. Carbon is constantly being exchanged between these parts, and atmospheric CO₂ is the main component of the atmospheric phase of the cycle. The terrestrial constituents of the carbon cycle are more diverse, including living vegetation, all living organisms and dead organic matter in litter and soils.

Carbon movement between the terrestrial and atmospheric elements occurs largely as the movement of CO₂: carbon uptake from the atmosphere as CO₂ being used in photosynthesis and carbon released from terrestrial ecosystems as CO₂ through respiratory processes (Ciais *et al.* 2013).

Terrestrial ecosystems cover a very wide range of environments, from tropical rain forests to arctic tundra to hot, dry, deserts. One particular type of terrestrial ecosystem is particularly important to human society: the grassland. Grassland ecosystems cover 6.1-7.4% of global land area and store 7.3-11.4% of soil organic carbon (Zeglin *et al.* 2007). Grasslands are important in agriculture, for both grazing livestock and planting crops, play environmental roles as water catchments and biodiversity reserves, and also provide for cultural and recreational needs (Boval and Dixon 2012). Grassland ecosystems show large interannual variation in productivity, primarily due to changes in water availability (Wever *et al.* 2002). Therefore, in addition to providing important habitat for wildlife and domesticated livestock and ideal agricultural land, grasslands also play a major role in the global carbon cycle. They provide an excellent opportunity to study the response of ecosystems to environmental change, such as the expected future changes in climate (Wever *et al.* 2002).

Previous research has shown that higher atmospheric CO₂ levels increase plant photosynthetic activity, thereby transferring additional carbon belowground to act as a natural carbon sink (Kowalchuk 2012). The sequestration of carbon belowground then acts as a buffer to reduce CO₂

emissions to the atmosphere (King 2011). In contrast, the results of other studies have shown that the transfer of carbon to the soil may stimulate the decomposition of organic matter by soil microbes, releasing more carbon into the atmosphere and thus, acting as a net source of CO₂ (Kowalchuk 2012). It is critical to understand the source/sink status of carbon cycling under warming conditions, as it will directly influence atmospheric carbon dioxide and further changes in climate.

My thesis has three primary objectives, which will address the effects of warming on specific aspects of a grassland ecosystem. First, I will compare two experimental methods of warming (open-top chambers and infrared heaters) and their effectiveness at replicating the effects of global climate change, allowing for improvement in experimental methods in future studies. Second, I will determine the effects of experimental warming on plant growth and physiology and ecosystem CO₂ exchange. Third, I will analyze the seasonal variation of the composition and activity of the soil microbial community, and the possible direct and indirect effects of soil temperature and water availability.

CHAPTER 2. COMPARISON OF INFRARED HEATERS AND OPEN- TOP CHAMBERS AS EXPERIMENTAL WARMING METHODS

2.1 Introduction

The concentration of atmospheric greenhouse gases is increasing, and one of the consequences will be increased global temperature (IPCC 2013b). However, to call it simply warming does not address the other possible changes that will occur alongside this increase in temperature. These may include changes in precipitation, such as the timing and size of precipitation events, increased frequency of droughts and heatwaves, a rise in sea level and the melting of glaciers (Meehl and Tebaldi 2004, Barnett *et al.* 2005, Solomon *et al.* 2009). As an additional complication, the effects of warming on plants and microorganisms will vary by species. The overall effect of increased temperature is an increase in the rates of biological processes up to a point at which further warming is detrimental, but the point at which that occurs will be species and ecosystem dependent (Burke *et al.* 1997). With so many complicating factors, it is vital to be able to study the effects of warming under conditions that are as natural as possible. In order to do so, researchers may experimentally warm a plot of land on which measurements can be made. Unfortunately, when studying the effects of warming on Earth's ecosystems in field experiments, it is not possible to simply raise the temperature and keep all other variables the same. Any warming treatment that may be used will affect more than just the temperature (Aronson and McNulty 2009). It is important to understand how a

warming treatment works and what changes it imposes on the ecosystem of study.

There are many warming methods being used today in ecosystem research, but I will focus on two: infrared heaters and open-top chambers. Infrared heaters and open-top chambers function in very different ways, and both have advantages and disadvantages. Infrared heaters increase the temperature of the plant canopy directly, and do not directly increase the air temperature (Kimball 2011). Open-top chambers increase the air temperature passively, being made from clear plastic panels (Godfree *et al.* 2011). Open-top chambers are advantageous because they rely on passive, solar heating and may therefore be used in locations without access to electricity. These enclosures also create an artificial microenvironment that may differ significantly from an open area in parameters other than air temperature, such as light intensity, relative humidity, evaporative water loss, wind speed, rainfall and even ozone concentration (Olszyk *et al.* 1980, Kimball 2011). In contrast, the infrared heater system does not affect as many environmental parameters (being an open-air system), although it may result in the over-all drying of the plot if additional water is not added (Kimball 2011). Infrared heaters also require significant energy input to run which may be quite expensive, depending on the location and the desired amount of warming (Aronson and McNulty 2009). An advantage of infrared heaters is that they consistently increase the temperature in the plot by using the same type of warming that is expected to occur naturally (increased infrared radiation) (Aronson and McNulty 2009, Kimball 2011). While infrared

heaters do not directly increase the temperature of the air, they do cause the expected increase in both canopy and soil temperatures, as seen in Figure 2.1 (Kimball 2011).

Both of these warming treatments do increase the average temperature of the system while they are in use. However, it is important to understand how all of the treatments' effects correspond to anticipated environmental changes due to global climate change. Some effects may correspond to expected changes due to climate change, and some effects may be contrary to anticipated changes. One important consideration is asymmetric warming during the day compared to the night. In terrestrial environments, warming is more pronounced at night because changes to daily minimum temperature (night-time) are greater than changes to daily maximum temperatures (daytime) (Aronson and McNulty 2009, 2010). Therefore, it is important that the chosen warming treatment can generate greater temperature increases at night than during the day. It is also important to consider the relative humidity of the air as well as soil moisture. With increased air temperatures, absolute humidity is expected to increase, while relative humidity will remain relatively constant (Kimball 2005). If an experimental warming treatment only heats the air and does not increase humidity, the vapor pressure deficit between the air and the leaves will not accurately represent future scenarios, and transpiration rates and soil water depletion will be inaccurate (Kimball 2005).

In this study, two experimental methods of warming (open-top chambers and infrared heaters) are being compared to assess their effectiveness at replicating the effects of global climate change, allowing for improvement in experimental methods for future studies.

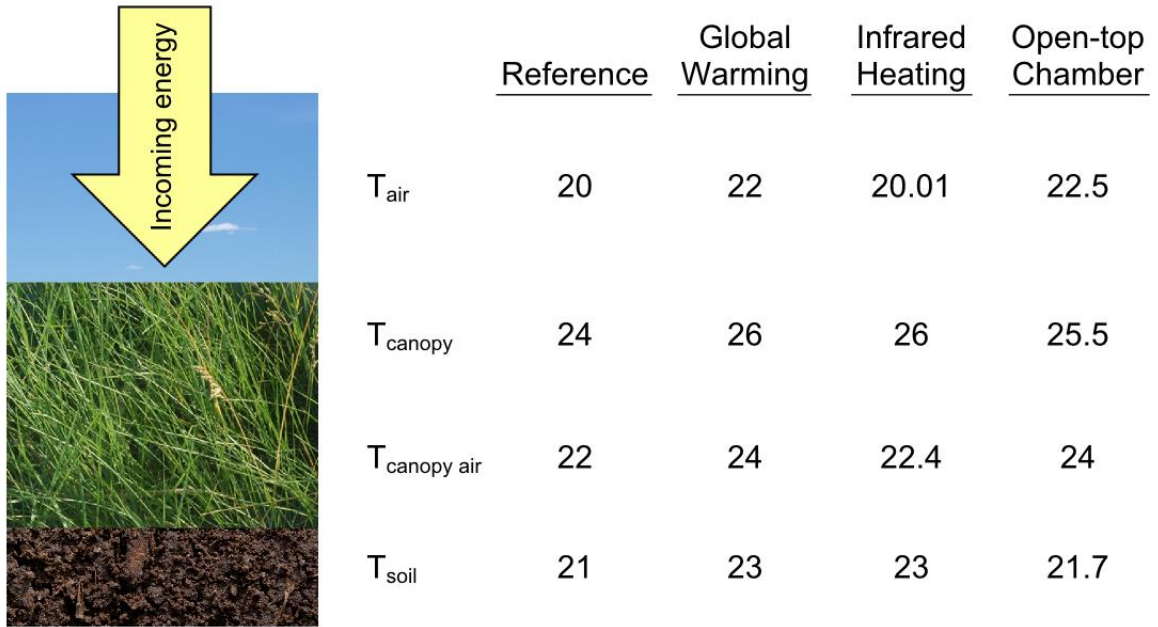


Figure 2.1: Diagram of a simple energy flow model with solar, sky, and infrared-heater radiation affecting a vegetation canopy. The numbers in the table are the theoretical resulting mid-day air, canopy, canopy air, and soil temperatures ($^{\circ}\text{C}$) for “Reference”, anticipated “Global Warming”, “Infrared Heated Plot” and “Open-top Chamber”. Modified from Kimball (2011) with data from Hollister and Webber (2000)

2.2 Methods and materials

2.2.1 Field site description

The experimental site is located approximately 2 km west of the city limits of Lethbridge, Alberta, Canada (Lat. N: 49.470919; Long. W: 112.94025). Its elevation is 951 m above sea level. It is part of the northwestern short/mixed grassland eco-region of the Great Plains. The climate is semi-arid and continental, with mean daily temperatures (1981-2010) of -6.0°C in January and 18.2°C in July, measured at the Lethbridge airport (Environment Canada 2015). The mean annual precipitation (1981-2010) is 380.2 mm, with 35% falling in May and June (Environment Canada 2015).

The site is very flat, with slopes equal to or less than 2% grade (Flanagan and Johnson 2005). The soil, an orthic dark-brown chernozem, was underlain by a thick glacial till with very low permeability and no water table (Flanagan and Adkinson 2011). The soil A horizon (0.09 m) was clay loam with 28.8% sand, 40% silt and 31.2% clay. The B horizon (0.16 m) had a clay texture with 27.4% sand, 29.6% silt and 40% clay (Carlson 2000). The bulk density of the surface soil horizon (10 cm) was 1.24 g cm⁻³ (Flanagan *et al.* 2013). Due to a lack of grazing at the site for at least the last 25 years, a substantial layer of dead plant material (litter) has developed on the ground surface (Flanagan *et al.* 2013). The plant community was primarily composed of the grasses *Agropyron dasystachyum* [(Hook.) Scrib.] and *Agropyron smithii* (Rydb.) Other major plant species include: *Vicia americana* (Nutt.), *Artemesia frigida* (Willd.), *Carex*

filifolia (Nutt.), *Stipa comata* (Trin. And Rupr.), *Stipa viridula* (Trin.) and *Bouteloua gracilis* [(H.B.K.) Lag.] (Carlson 2000, Flanagan and Johnson 2005).

2.2.2 Warming treatments

The experiment consisted of three treatments: control with ambient temperature, warming using infrared heaters, and warming using open-top chambers. The infrared heaters and frames were assembled as described by Kimball *et al.* (2008). They were set to produce a consistent canopy temperature increase of 1.5°C during the day and 2°C at night, modulated in relation to the canopy temperature of the control plot. The open-top chambers were constructed as described by Flanagan *et al.* (2013), including the polyvinyl chloride pipes filled with water, acting as thermal mass to dampen daily air temperature changes within the chamber and to increase air temperature at night. The chambers were expected to produce an average air temperature increase of 2 – 2.5°C, fluctuating with levels of incoming solar radiation and wind speed (Flanagan *et al.* 2013).

There were three replicate plots for each treatment. A set of environmental measurements was taken in the control and experimental plots. This included continuous measurements of air temperature 30 cm above ground (107 temperature probe in a radiation shield, Campbell Scientific, Edmonton, Canada), soil temperature at 5 and 10 cm depths (soil thermocouples, Campbell Scientific), and soil moisture down to a depth of 15 cm (C616 soil moisture

probes, Campbell Scientific). The environmental sensors were read and logged by a data logger (CR23X, Campbell Scientific).

Air temperature, soil temperature and soil water content were measured every 30 minutes. Canopy temperature was measured every hour with an infrared radiometer sensor (SI-1H1, Apogee Instruments, Logan, UT, USA). All temperature and soil moisture data was averaged over 24 hours for each day to determine an average daily value. The daily averages were then used to calculate a 5-day moving average to remove some noise from the data. Results were assessed by repeated measures ANOVA using the 5-day moving average from every 5th day. Treatments were compared in a pairwise manner and evaluated for statistically significant effects of treatment.

2.3 Results

Daily average air temperature was approximately 1.2°C higher in the open-top chamber plots than the control plots over the course of the study (Repeated measures ANOVA: $F=355.6$, $df=1$, $p<0.001$), while the difference between infrared heated plots and the control plots was only 0.7°C (Repeated measures ANOVA: $F=362.3$, $df=1$, $P<0.001$). In addition to being significantly warmer than the control plots, the two treatments were significantly different from each other in terms of air temperature (Repeated measures ANOVA: $F=90.9$, $df=1$, $p=0.001$). However, the infrared heaters were not actively warming the air temperature, but only the canopy temperature. The effect of the infrared heaters on air temperature was indirect, as during the peak of the season, the canopy was tall enough to envelop the air temperature sensors. The daily average canopy temperatures averaged approximately 1.6°C higher in the infrared heated plots than the control plots over the course of the study (Repeated measures ANOVA: $F=70.2$, $df=1$, $p=0.001$).

The diurnal patterns of air/canopy temperature and warming also differ between the infrared heated plots and the open-top chambers (Figure 2.2). The infrared heaters were programmed to provide 1.5°C of warming during the day and 2°C of warming at night. Over the ten day period shown in Figure 2.2a, the average daytime warming was 1.7°C and the nighttime warming was 2.0°C. The open-top chambers can only provide significant warming during the day when the sun is shining. Over the ten day period shown in Figure 2.2b, the average daytime warming for the open-top chambers was 2.1°C and the nighttime

warming was 0.5°C. In addition, the diurnal temperature patterns also differed greatly due to environmental conditions, specifically in the amount of daytime warming. Infrared heaters showed consistent daytime warming on both a sunny and an overcast day, while the open-top chambers showed approximately 4°C of warming on the sunny day and a decrease in temperature of almost 0.5°C on the overcast day (Figure 2.3).

In addition to average daily warming and diurnal warming patterns, warming treatments were also assessed by the frequency at which temperatures occurred. The temperature distribution for the infrared heaters showed a similar pattern in both canopy temperature (Figure 2.4b) and air temperature (Figure 2.4a). The average canopy temperature in the control plots was 13.2°C with a standard deviation of 9.2°C. The infrared heated plots had a higher average canopy temperature of 14.8°C but the standard deviation was similar, at 9.0°C. The average air temperature in the control plots was 14.3°C with a standard deviation of 8.4°C. The infrared heated plots had a slightly higher average air temperature of 15.0°C but the standard deviation was the same, at 8.4°C. The increase in air temperature was less than that of canopy temperature, because the infrared heaters did not directly warm the air. Any increase in air temperature was due to an increase in the canopy temperature, as the canopy surrounded the air temperature sensor, once the plants had grown sufficiently. As such, there was no effect on air temperature early in the season, reducing the average for the season. The open-top chambers had a direct impact on air temperature and the distribution was different than in the control or infrared heated plots (Figure

2.4a). The average air temperature in the open-top chambers was 15.4°C with a standard deviation of 9.4°C. Not only was the average air temperature higher in the open-top chambers, there was also a widening of the distribution, as indicated by the higher standard deviation.

The daily average soil temperature at a 5 cm depth was approximately 1.4°C higher in the infrared heated plots than the control plots over the course of the study (Repeated measures ANOVA: $F=22.4$, $df=1$, $p=0.009$). The daily average soil temperature at a 5 cm depth in the open-top chambers ranged from approximately 0.5°C above to 0.5°C below the control plots, resulting in a negligible average difference of 0.03°C cooler in the open-top chamber plots than the control plots (Repeated measures ANOVA: $F=0.04$, $df=1$, $p=0.861$). The infrared heated plots were therefore also warmer than the open-top chamber plots (Repeated measures ANOVA: $F=38.0$, $df=1$, $p=0.861$). The daily average soil temperature at a 10 cm depth was also approximately 1.4°C higher in the infrared heated plots than the control plots over the course of the study (Repeated measures ANOVA: $F=39.7$, $df=1$, $p=0.003$). The open-top chamber plots still showed a very small overall difference, being 0.1°C warmer than the control plots over the course of the study (Repeated measures ANOVA: $F=0.5$, $df=1$, $p=0.517$). Similarly to soil temperature at 5 cm, the temperature at 10 cm in the infrared heated plots was also higher than the open-top chamber plots (Repeated measures ANOVA: $F=51.3$, $df=1$, $p=0.002$).

Infrared heaters showed a shift upwards in the distribution of soil temperatures with higher average temperatures of 16.7°C at 5 cm depth and 16.4°C at 10 cm depth, compared to the control values of 15.2°C and 15.0°C (Figure 2.5). The distributions were similar in shape at 5 cm depth as the standard deviations were 5.2°C in the control plots and 5.3°C in the infrared heated plots. At 10 cm depth, the overall variation in temperature was lower, although the variation in the infrared heated plots was higher with a standard deviation of 5.0°C compared to only 4.8°C in the control plots. Open-top chambers showed a narrowing of the distribution at both temperatures, with fewer occurrences at the low and high ends and more occurrences at more moderate temperatures (Figure 2.5). At 5 cm depth, the average temperature was 15.2°C, the same as the control plots, but with a standard deviation of only 4.8°C. At 10 cm depth, the average temperature was 15.1°C, similar to the control, but with a slightly lower standard deviation of 4.7°C.

The daily soil water content averaged 0.06 m³ m⁻³ lower in the infrared heated plots than the control plots over the course of the study (Repeated measures ANOVA: F=20.4, df=1, p=0.011). The open-top chambers averaged only 0.02 m³ m⁻³ lower than the control plots (Repeated measures ANOVA: F=3.2, df=1, p=0.148). The infrared heated plots were significantly drier than the open-top chamber plots (Repeated measures ANOVA: F=8.5, df=1, p=0.044). Infrared heaters showed a strong shift downwards in the distribution of soil moisture with an average of 0.24 m³ m⁻³, compared to 0.30 m³ m⁻³ in the control plots (Figure 2.6). However, the variation in soil moisture was similar in the

control and infrared heated plots, with standard deviations of $0.06 \text{ m}^3 \text{ m}^{-3}$ in both treatments. Open-top chambers did show a decrease in soil moisture compared to the control plots, with an average of $0.28 \text{ m}^3 \text{ m}^{-3}$, but the variation was reduced compared to the other two treatments, with a standard deviation of $0.05 \text{ m}^3 \text{ m}^{-3}$ (Figure 2.6).

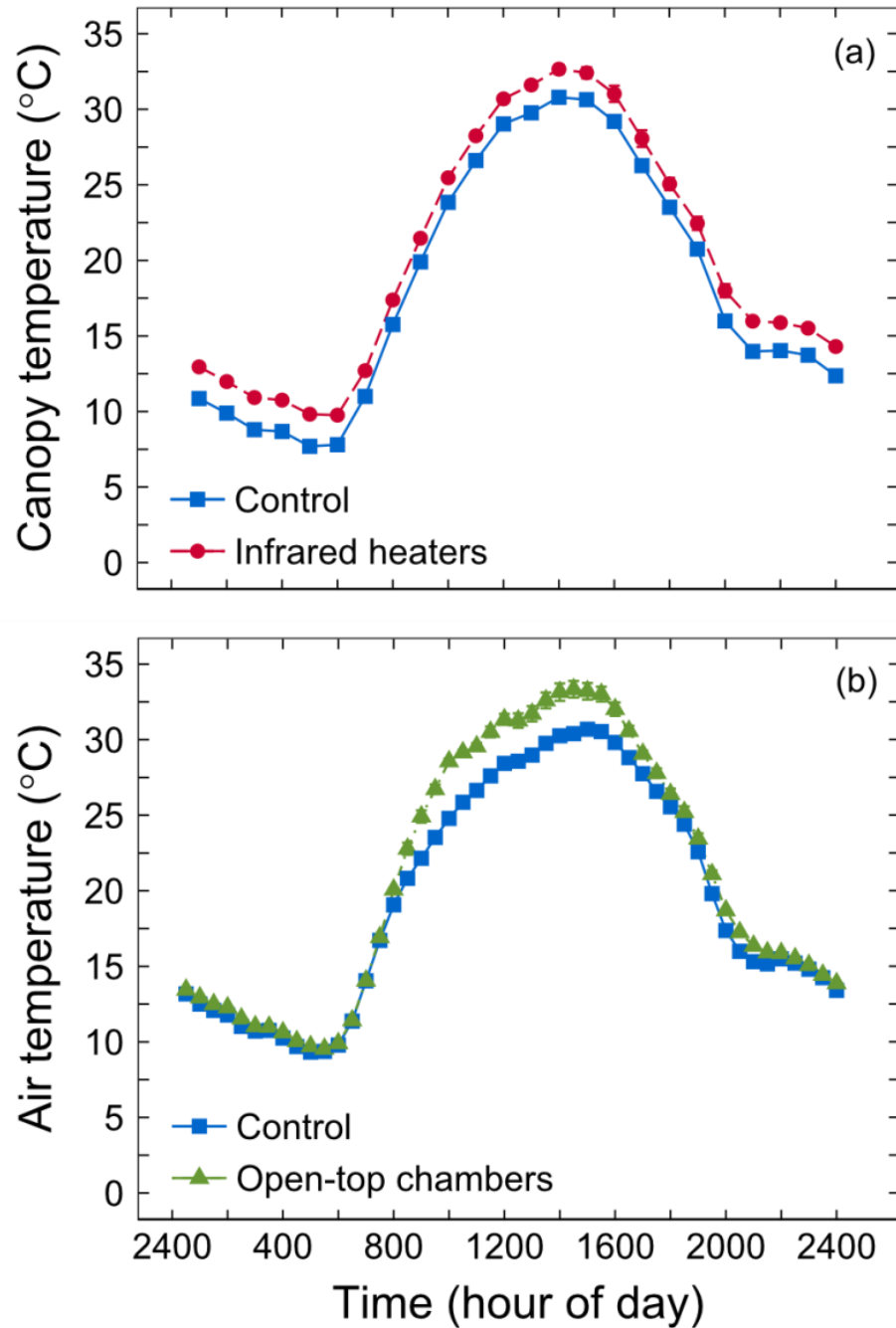


Figure 2.2: The diurnal pattern of canopy temperature (a) and air temperature (b), based on measurements made in control, infrared heated and open-top chamber plots in a grassland ecosystem near Lethbridge, Alberta from August 14-24, 2013. Values represent average \pm standard error, $n=3$.

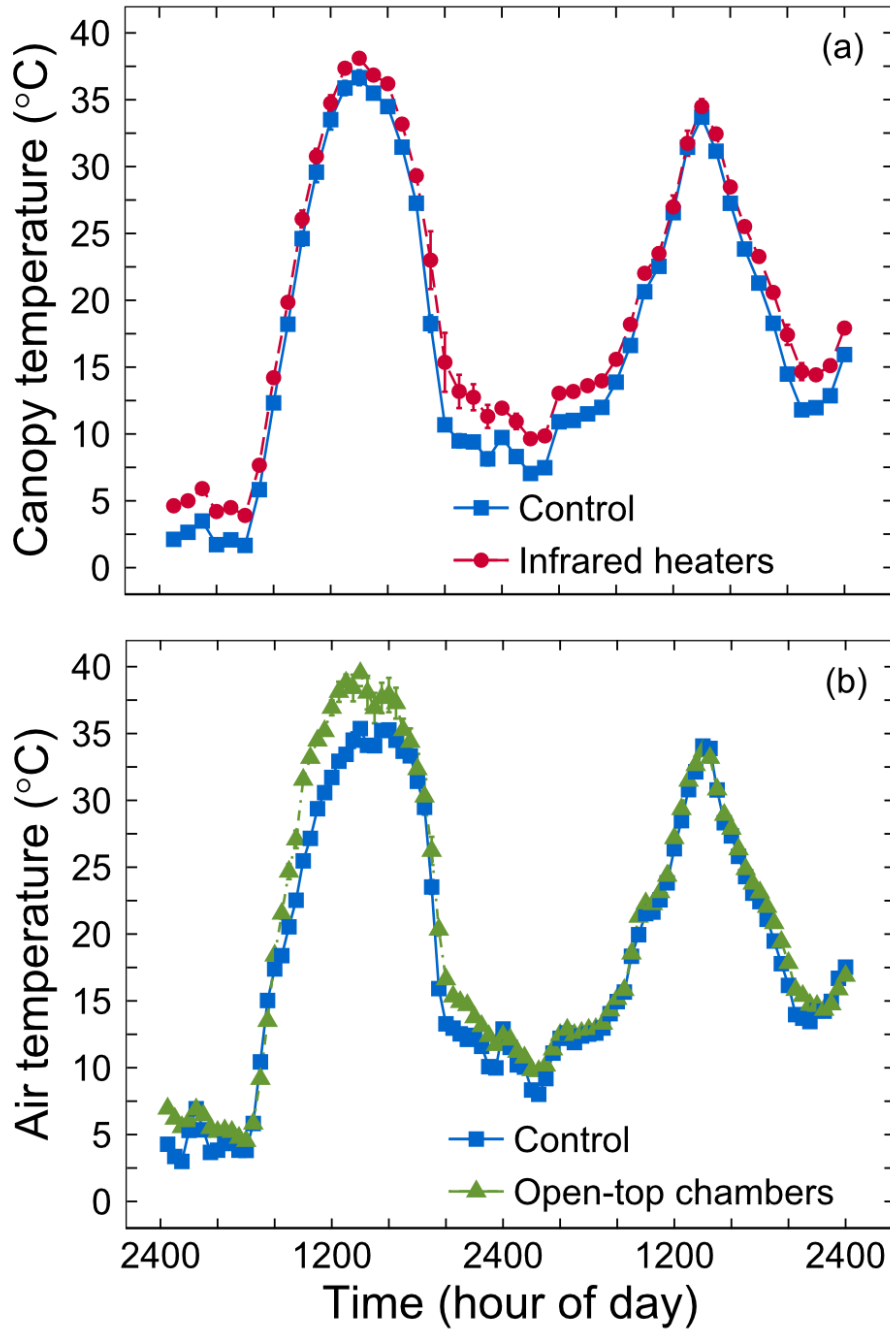


Figure 2.3: The diurnal pattern of canopy temperature (a) and air temperature (b), based on measurements made in control, infrared heated and open-top chamber plots on September 1 and 2, 2013, which were a clear and overcast day, respectively. Values represent average \pm standard error, $n=3$.

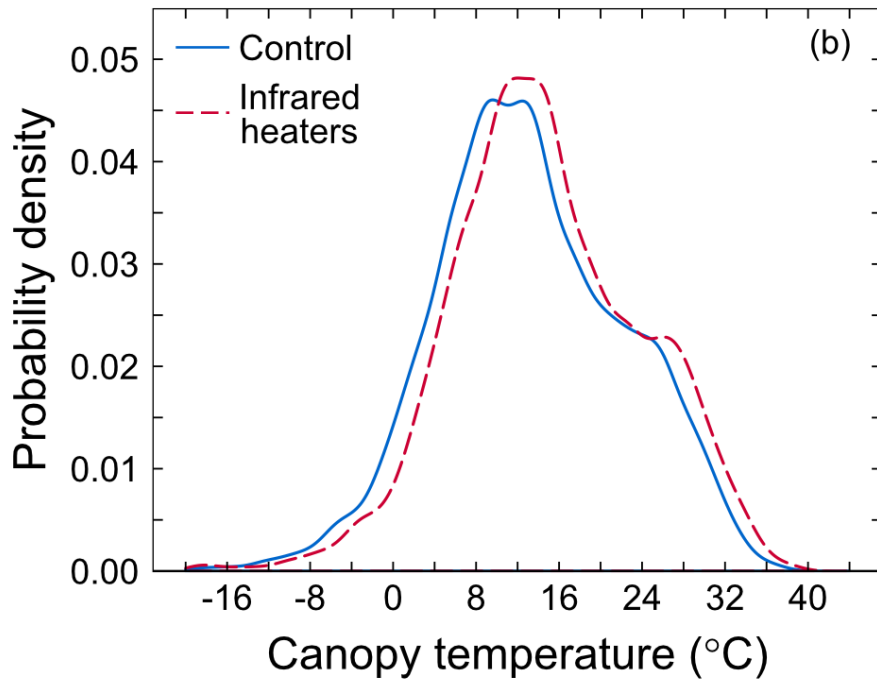
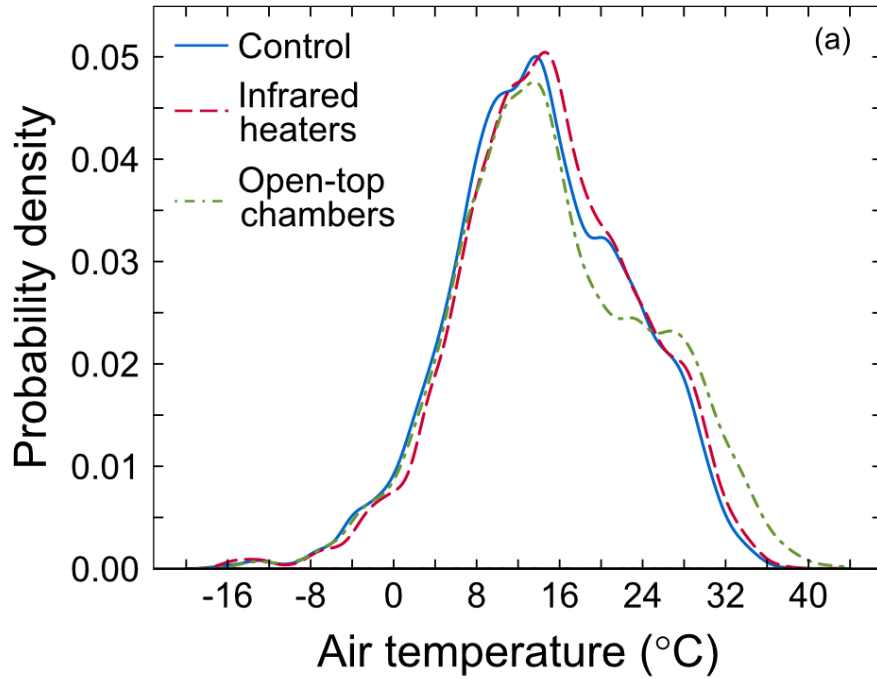


Figure 2.4: (a) Air temperature ($^{\circ}\text{C}$) distribution in control, infrared heated and open-top chamber plots based on half-hourly measurements from May to October, 2013 ($n=26,496$). (b) Canopy temperature ($^{\circ}\text{C}$) distribution in control and infrared heated plots based on hourly measurements from May to October, 2013 ($n=12,816$).

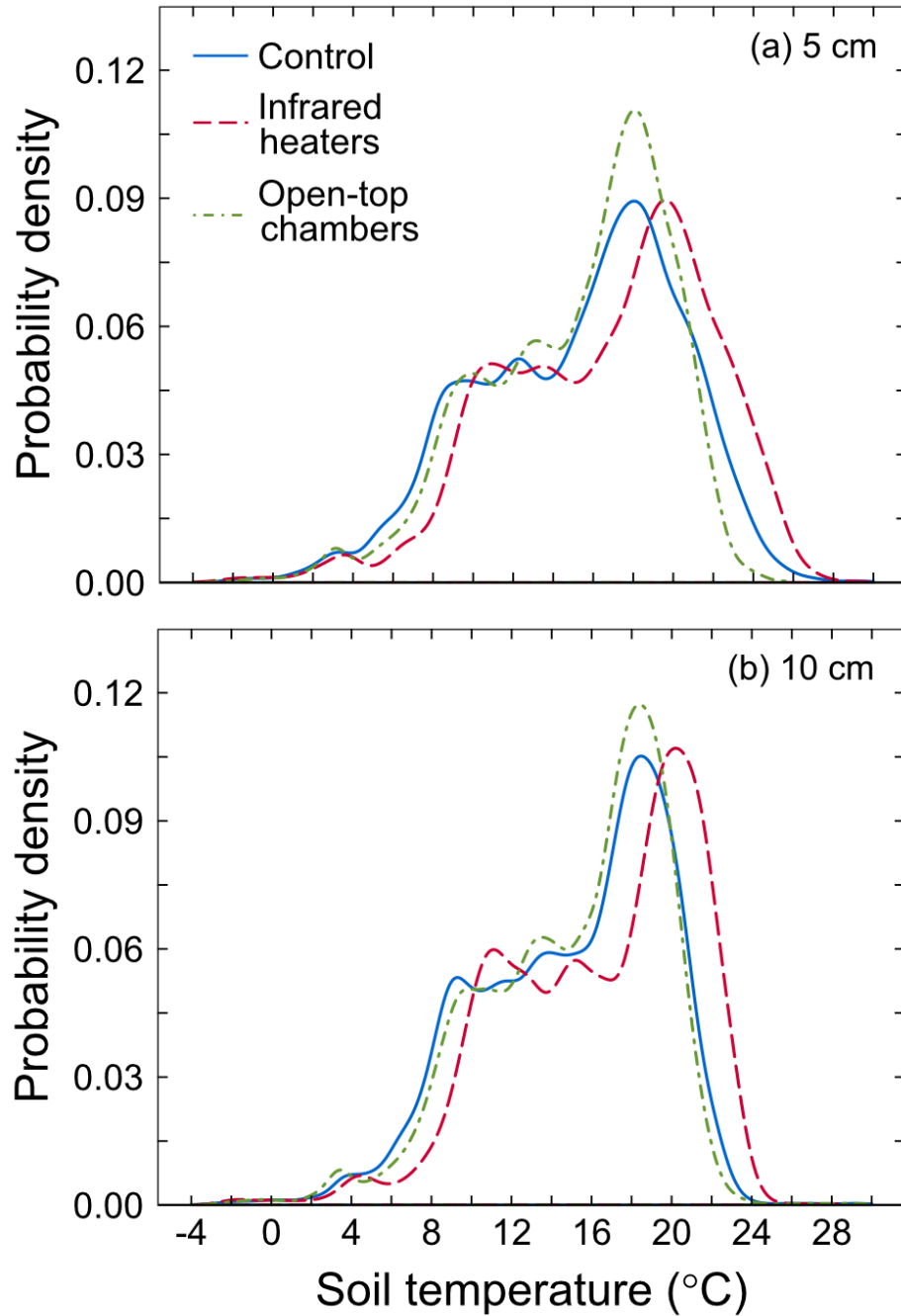


Figure 2.5: Soil temperature (°C) distribution in control, infrared heated, and open-top chamber plots at 5 cm (a) and 10 cm (b) depths, based on half-hourly measurements from May to October, 2013 (n=26,496).

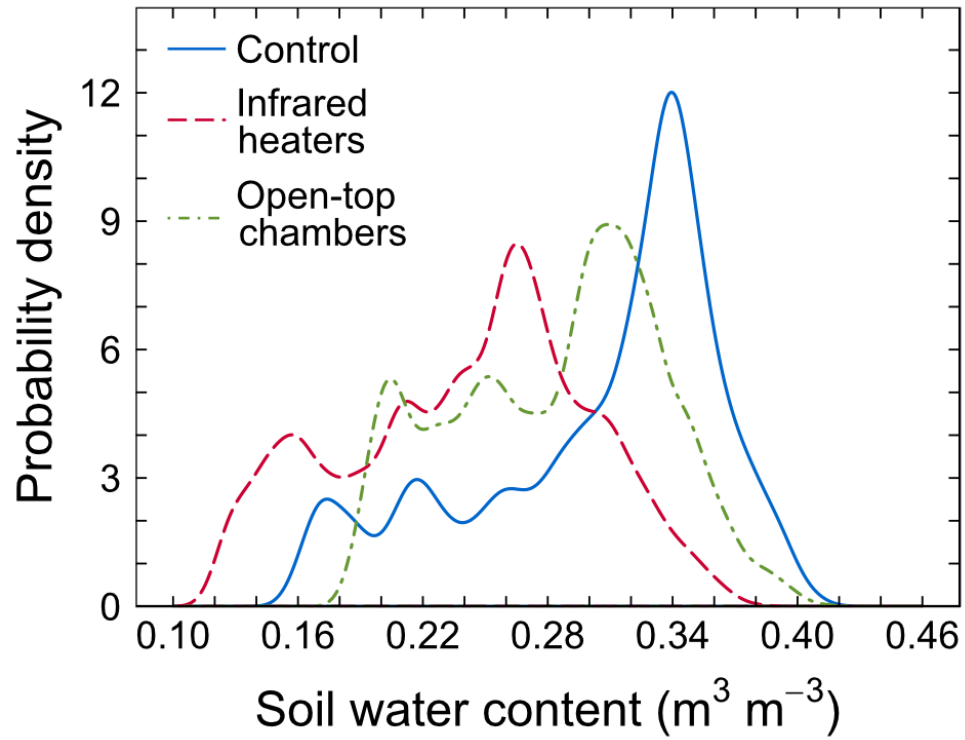


Figure 2.6: Soil water content ($\text{m}^3 \text{m}^{-3}$) distribution in control, infrared heated and open-top chamber plots, based on half-hourly measurements from May to October, 2013 ($n=25,776$).

2.4 Discussion

The purpose of this study was to compare two experimental warming methods (open-top chambers and infrared heaters) to assess their effectiveness at replicating the effects of global climate change, allowing for improvement in experimental methods for future studies. Experimental methods generally have some artifacts, and it is important to identify and understand those artifacts in order to choose an optimal method for a given study, as well as to make accurate comparisons between studies in the literature.

Open-top chambers are a cost-effective, passive method of increasing daily average air temperature (Aronson and McNulty 2009). However, because it is a passive system, the amount of warming depends strongly on environmental conditions, specifically the amount of sunlight (Aronson and McNulty 2009). There may be very high amounts of warming on bright, sunny days and almost no warming on overcast days (Figure 2.3). As well, there is generally minimal night-time warming (Figure 2.2). While thermal ballast does prevent the total cool down of the chamber overnight, it cannot produce greater night-time than daytime warming as would be expected due to global climate change. Open-top chambers do reduce soil moisture, but not as significantly as infrared heaters (Figure 2.6). However, open-top chambers do show other significant artifacts, although they were not assessed in this study (Olszyk *et al.* 1980, Kimball 2011). One such artifact is decreased wind speed, which can affect plant growth, as plants have larger leaves at lower wind speeds (Whitehead 1962). Our study site has an average annual wind speed (1928-1999) of 5.2 m s^{-1} , meaning that a

reduced wind speed in the open-top chambers may result in increased plant growth that could be mistaken for a consequence of the warming treatment (Flanagan *et al.* 2002, Flanagan and Johnson 2005).

In contrast, the infrared heaters are a more expensive, active warming system (Aronson and McNulty 2009). They can provide a very consistent increase in temperature by being modulated by canopy temperature sensors in both a control and warmed plot. They can be used to produce an increase in temperature that corresponds to predicted global changes, including higher levels of warming at night than during the day caused by greater increases to minimum temperature than to maximum temperatures (Dhakhwa and Campbell 1998, Aronson and McNulty 2009, 2010). One potential downside of infrared heaters is the significant drying of the soil (Figure 2.6). However, this artifact can be countered by appropriate watering, based on the elevated evapotranspiration in the warmed versus the control plot, and may be particularly important in water-limited ecosystems (Kimball 2011). Infrared heaters also replicate natural heating by using the same form of heat: radiation instead of conduction or convection (Aronson and McNulty 2009). While infrared heaters produce warming that is more similar to future global climate change, they may not be practical in all experiments due to the cost of equipment and operation.

2.5 Conclusion

When the two warming treatments were compared side-by-side, it was evident that they have significantly different effects on the treatment plots. It is important to consider these differences when planning a field study, because different artifacts may be more or less problematic depending on what is being studied. Both warming methods can provide valuable information about the response of ecosystems to future global climate change, and while infrared heaters may most closely mimic these future changes, they are not always a financially or logistically viable option. It is important to understand the artifacts of different warming methods, so that accurate conclusions may be drawn from field studies. It is also important to understand the differences between warming methods, in order to accurately draw comparisons between different studies in the literature. By understanding the full effect of a warming treatment, it becomes possible to make accurate predictions about the effects of warming on ecosystems in the future.

CHAPTER 3. EFFECTS OF EXPERIMENTAL WARMING ON PLANT BIOMASS PRODUCTION AND ECOSYSTEM CO₂ EXCHANGE IN A TEMPERATE GRASSLAND ECOSYSTEM

3.1 Introduction

The concentration of atmospheric carbon dioxide (CO₂) is being changed by human activity, with consequences that include warmer air temperatures and altered precipitation and snow melt patterns (Barnett *et al.* 2005, Rosenzweig *et al.* 2008). The direct influence of elevated CO₂ on ecosystems is almost entirely limited to leaves, while the effects of the resulting increases in temperature will be much more complex, as temperature affects almost all chemical and biological processes (Shaver *et al.* 2000). Terrestrial ecosystems represent a major component of biological processes that can affect the biosphere as a whole; they can absorb or emit important greenhouse gases such as CO₂, methane and nitrous oxide, and they control the exchange of water and energy between the land surface and the atmosphere (Heimann and Reichstein 2008).

The movement of carbon between terrestrial ecosystems and the atmosphere involves organic systems as an intermediary. Carbon dioxide moves from the atmosphere into the ecosystem through photosynthesis, where the carbon is stored in living vegetation and soil organic matter (Heimann and Reichstein 2008). It is returned to the atmosphere primarily through respiratory processes, both autotrophic (plant and photosynthetic bacteria) and heterotrophic (soil microorganisms, fungi and animals) (Heimann and

Reichstein 2008). Some carbon is also lost through disturbances, such as fire, or as volatile organic compounds, methane or dissolved carbon (Falkowski *et al.* 2000, Heimann and Reichstein 2008). Terrestrial ecosystems store large quantities of carbon and the release of this carbon to the atmosphere would have a significant impact on global climate (Heimann and Reichstein 2008). Increases in temperature may affect either input or output of carbon from these ecosystems, affecting the net carbon flux and its role in the global carbon cycle. Therefore, it is vital to be able to study the effects of warming under otherwise natural conditions, to quantify these changes in carbon flux. In order to do so, researchers may experimentally warm a plot of land on which measurements can be made. By using an experimental warming method, the effects of increased temperature on whole ecosystems can be assessed.

Within a certain range of temperatures (commonly 10° to 35°C), increases in temperature can increase photosynthetic rates by increasing the activity of the enzymes in the pathway (Burke *et al.* 1997). However, after a certain point, further increases in temperature are detrimental, and this point is dependent on the species and its normal environment (Burke *et al.* 1997). Additionally, the effects of temperature are more pronounced when either light or intercellular CO₂ levels are increased (Berry and Bjorkman 1980). Temperature affects respiratory processes in plants by affecting the capacity of enzymes and the affinity of enzymes for their substrate, as well as membrane properties and the resulting substrate concentration gradients (Atkin and Tjoelker 2003). The cellular regulation of respiration in soil microorganisms is less well understood.

On the ecosystem scale, the primary effects of temperature on respiration are through these cellular and biochemical controls (Davidson *et al.* 2006). At low temperatures, these processes are limited by their biochemistry. As temperatures increase, the rate of respiratory activity increases, up to a point at which the enzymes are degraded. The high and low temperatures that are detrimental to an organism are specific to the organism and the environment to which it is acclimated.

The effects of increased temperature on photosynthesis and respiration are conceptually similar, but the specific values for each are different. Under warming conditions, ecosystem respiration is increased proportionally more than ecosystem primary production (photosynthesis) (Yvon-Durocher *et al.* 2010). The imbalance causes a shift in the carbon budget of the ecosystem, which could result in an increase in the amount of carbon fixed by photosynthesis that is subsequently released by respiration, compromising the ability of an ecosystem to sequester carbon as warming occurs (Yvon-Durocher *et al.* 2010). Elevated atmospheric CO₂ has been shown to increase photosynthetic rates, resulting in increased aboveground biomass production (Bowes 1993). Therefore, all else being equal, increased photosynthetic rates due to warming should also increase aboveground biomass production. Meta-analysis of warming studies has shown that warming does generally increase terrestrial plant biomass and therefore enhanced carbon uptake by terrestrial ecosystems through net primary production (NPP) and plant growth (Lin *et al.* 2010). However, increases in plant productivity under warming conditions may be a direct effect of increased

photosynthesis or longer growing seasons, or indirectly caused by increased nutrient availability due to increased rates of decomposition in the soil (Rustad *et al.* 2001).

In addition to the effects of temperature, the availability of water and the ability of plants to use it efficiently may also limit the ability of an ecosystem to use elevated atmospheric CO₂ for the production of biomass (Bowes 1993). A plant's water-use efficiency refers to the amount of biomass it can produce per unit of water used, or at the leaf level, the ratio of photosynthetic activity to transpiration (Polley 2002). A study in a semi-arid grassland in China showed that increased temperature without increased precipitation decreased water-use efficiency, as photosynthetic activity declined while water loss remained the same, likely because stomatal regulation to prevent excess water loss also reduced CO₂ uptake (Niu *et al.* 2011). Global climate change caused by elevated atmospheric CO₂ will likely result in increased temperatures and changes to both the timing and magnitude of precipitation events, making it hard to predict how these factors will interact in different ecosystems (Barnett *et al.* 2005, Rosenzweig *et al.* 2008).

If plant biomass production does increase, there may be benefits, either for crop production or carbon sequestration to buffer against further climate change, but there are also consequences. A study by An *et al.* (2005) showed that warming treatments result in decreased leaf nitrogen in green and senescent leaves. The decrease in nitrogen content has an impact both on the nutritional

value of agricultural crops and the quality of the litter being supplied to decomposers. Studies have also shown that litter nitrogen content is strongly correlated to green leaf nitrogen content and has an effect on decomposition (Cornwell *et al.* 2008). The combination of changes to litter quality and increased decomposition rates due to warming treatments may have unforeseen consequences on the soil component of the carbon cycle. In addition to the effects of nutrient availability and litter quality, the production of CO₂ in soils due to the microbial decomposition of organic matter is temperature-dependent, and rates of activity increase with temperature (Davidson and Janssens 2006).

Changes in environmental conditions, specifically increases in CO₂, can cause an increase in exudation of carbon compounds from plant roots into the soil (Phillips *et al.* 2011). In turn, the increased flux of carbon into the soil can cause increased microbial activity and faster rates of soil organic matter decomposition and turnover (Phillips *et al.* 2011). These changes can also cause a shift in soil enzyme activity involved in decomposition, leading to increased decomposition and release of carbon from old, recalcitrant soil organic matter (Phillips *et al.* 2011). Hopkins *et al.* (2012) have shown that in temperate forest soils, warming increased the respiration of soil carbon over a decade old, a major component of soil organic matter, and indicated that a large portion of soil organic carbon may be vulnerable to decomposition with future changes in climate. In fact, the turnover time of intermediate (years to decades old) soil organic matter was approximately halved by a 10°C increase in temperature,

suggesting that large, recalcitrant pools of soil carbon may be just as sensitive to temperature as the more labile, active carbon pool (Townsend *et al.* 1995).

The direct and indirect effects of ecosystem warming on plant productivity and respiration processes may strongly impact the carbon flux of a terrestrial ecosystem. It is critical to understand the source/sink status of carbon cycling under warming conditions, as it will directly influence atmospheric carbon dioxide and further changes in climate. This study will determine the effects of experimental warming on plant growth and physiology as well as on ecosystem CO₂ exchange.

3.2 Methods and materials

3.2.1 Field site description

As described in Chapter 2.

3.2.2 Warming treatments

As described in Chapter 2.

3.2.3 Peak aboveground plant biomass

In each treatment plot, a 20 x 50 cm subplot was chosen. In the control and infrared heated plots, the subplot was 20 cm away from the autochamber and parallel to it, on the side of the plot opposite to the soil respiration collar. In the open-top chambers, the subplot was parallel to the edge of the chamber, on the side opposite the soil respiration collar, and 20 cm away from the soil moisture probe and the autochamber. These subplots were harvested by clipping this summer's growth at the soil level on August 6, 2013 when biomass was near peak. Litter from previous years was not harvested. Any litter that was accidentally collected was removed from the sample before further processing. The harvested material was dried at 60°C for approximately 60 hours and then weighed. The dry mass was then converted from the mass per subplot to the mass per square meter (g m^{-2}). The aboveground biomass was averaged by treatment and assessed with a single-factor ANOVA test for statistical significance.

Dried plant biomass was ground, first coarsely in a coffee grinder, then finely in a ball mill (Retsch MM200, Haan, Germany), and homogenized for analysis. Subsamples of biomass were analysed for $^{13}\text{C}/^{12}\text{C}$ carbon isotope composition (expressed using delta-notation, $\delta^{13}\text{C}_{\text{PDB}}$, ‰) on CO_2 gas generated from combustion of the dried plant tissue in an elemental analyser (4100, Costech Analytical Technologies, Valencia, CA, USA) and quantified with a gas isotope ratio mass spectrometer (Delta Plus XL, Thermo Finnigan, San Jose, CA, USA) at the University of Calgary. The precision of the $\delta^{13}\text{C}$ measurements was 0.1‰ based on the standard deviation of repeated analyses of two internal laboratory standards used for this study (UL-Mar1, $\delta^{13}\text{C} = -28.45\text{‰}$; UL Rye, $\delta^{13}\text{C} = -23.01\text{‰}$). These working standards have been calibrated by comparison to the international standard (International Atomic Energy Agency; IAEA), IAEA-CH-3 Cellulose ($\delta^{13}\text{C} = -24.724\text{‰}$). This analysis also provided measurements of the total carbon content (mg C g^{-1} biomass) and nitrogen content (mg N g^{-1} biomass) of the aboveground plant biomass. As well, subsamples of biomass were analysed for $^{18}\text{O}/^{16}\text{O}$ oxygen isotope composition (expressed using delta-notation, $\delta^{18}\text{O}_{\text{VSMOW}}$, ‰) on CO gas generated from the dried plant tissue in a Heka HT oxygen analyser pyrolysis column and quantified using a gas isotope ratio mass spectrometer (Delta Plus XL, Thermo Finnigan, San Jose, CA, USA) at the University of Calgary. The precision of the $\delta^{18}\text{O}$ measurements was 0.3‰ based on the standard deviation of replicate measurements of two internal laboratory standards used for this study (ANU sucrose, $\delta^{18}\text{O} = 36.40\text{‰}$; IAEA V-9 cellulose, $\delta^{18}\text{O} = 27.8\text{‰}$). There is no official IAEA standard for $\delta^{18}\text{O}$ in organic matter, but ANU sucrose (also known as IAEA-

CH-6 sucrose [$\delta^{13}\text{C} = -10.449\text{‰}$]) has been used as an informal, international reference material. Aboveground biomass, elemental values and isotope ratios were averaged by treatment and assessed with a single-factor ANOVA test for statistical significance.

Leaf level water-use efficiency (WUE) is the ratio of leaf net CO_2 assimilation rate (A) and transpiration rate (E), which depend on the gradients of CO_2 and water diffusing into and out of leaves:

$$\text{WUE} = \frac{A}{E} = \frac{(c_a - c_i)}{(e_i - e_a)1.6} \quad (3.1)$$

where c is the partial pressure of CO_2 , e is the partial pressure of water vapour, and subscripts refer to the atmosphere outside the leaf (a) and within the leaf intercellular spaces (i); 1.6 is the ratio of the diffusion coefficients for H_2O and CO_2 in air (Flanagan and Farquhar 2014). The carbon isotope content of leaf organic matter ($\delta^{13}\text{C}$) is related to $c_a - c_i$, while the oxygen isotope content ($\delta^{18}\text{O}$) is related to $e_i - e_a$. The actual water-use efficiency cannot be calculated without additional variables and measurements, but the carbon and oxygen isotope ratios do give some insight into controls on plant water use (Flanagan and Farquhar 2014).

3.2.4 Carbon dioxide flux

Ecosystem net CO_2 exchange was measured using an automated chamber system with clear chamber lids that are attached to soil collars (Carbone *et al.* 2008, Cai *et al.* 2010). The autochambers recorded the net ecosystem exchange

rate once every 30 minutes on a continuous basis throughout the growing season period, from late April to early October. The measurements of net ecosystem CO₂ exchange was partitioned into estimates of ecosystem photosynthesis and total respiration using methods outlined in Cai *et al.* (2010). Single-factor ANOVA was used to examine the effect of warming treatment on integrated CO₂ flux values for the season. Only the carbon dioxide flux measurements from the control and infrared heated plots were considered, due to potential inaccuracies in the open-top chambers caused by wind-related artifacts.

3.3 Results

3.3.1 Peak aboveground plant biomass

Peak aboveground plant biomass, measured on August 6, 2013, averaged 329 g m⁻² in the control plots, while the warmed plots had a slightly higher average close to 350 g m⁻² (Table 3.1). However, this difference was not statistically significant (Single-factor ANOVA: $F=0.09$, $df=2$, $p=0.92$). Carbon content in the peak aboveground biomass averaged 440 mg C g⁻¹ biomass for all treatments, with no significant treatment effect (Single-factor ANOVA: $F=0.7$, $df=2$, $p=0.55$; Table 3.1). Nitrogen content averaged 11.8 mg N g⁻¹ biomass and also showed no significant treatment effect (Single-factor ANOVA: $F=1.0$, $df=2$, $p=0.42$; Table 3.1). As a result, the average carbon to nitrogen ratio (C:N) was 38 with no significant treatment effect (Single-factor ANOVA: $F=1.0$ $df=2$, $p=0.42$; Table 3.1). Also measured were the ratios of carbon and oxygen isotopes within the plant biomass. Analysis of carbon-13 indicated an average $\delta^{13}\text{C}$ of -28.5‰ with no significant treatment effect (Single-factor ANOVA: $F=1.0$, $df=2$, $p=0.41$; Table 3.3). Oxygen-18 analysis showed an average $\delta^{18}\text{O}$ of 18.5‰ with no significant treatment effect (Single-factor ANOVA: $F=0.6$, $df=2$, $p=0.56$; Table 3.3).

The growing season of 2013 had higher precipitation than usual, with 346 mm falling from May to October, while the mean precipitation from May to October (1971-2000) was 268.3 mm (Environment Canada 2015). In a year with average growing precipitation (1999), peak aboveground biomass was 114 g m⁻², while in a dry year (2001) with only 89 mm of precipitation peak aboveground

biomass was only 101 g m⁻² (Table 3.2) (Flanagan and Farquhar 2014). The comparison of carbon and oxygen isotope ratios in wet and dry years shows similar variation to biomass measurements. In contrast to the wet year of 2013, a year of average precipitation had a $\delta^{13}\text{C}$ of -26.7‰ and a $\delta^{18}\text{O}$ of 24.9‰, while a dry year had a $\delta^{13}\text{C}$ of -26.1‰ and a $\delta^{18}\text{O}$ of 25.2‰ (Table 3.4) (Flanagan and Farquhar 2014).

3.3.2 Carbon dioxide flux

To assess the effect of the warming treatment on the carbon cycle, it is helpful to look at an integrated value over the course of the season when measurements were made, from May to October (Figure 3.1). Gross ecosystem productivity is slightly higher in infrared heated plots at approximately 770 g of carbon taken up per m² over the season, compared to approximately 670 g of carbon in the control plots. This difference was not, however, statistically significant (Single-factor ANOVA: $F=1.9$, $df=1$, $p=0.25$). Total ecosystem respiration was also slightly higher in the heated plots at approximately 715 g of carbon released per m² over the season, compared to approximately 660 g of carbon in the control plots. This difference was also not statistically significant (Single-factor ANOVA: $F=0.9$, $df=1$, $p=0.40$). As a result, both control and infrared heated plots showed a positive value for net ecosystem productivity as both were taking up more carbon than was being released. The warmed plots had a net uptake of about 55 g C m⁻² while the control plots only took up about 10 g C m⁻². This difference was not statistically significant (Single-factor ANOVA: $F=0.4$, $df=1$, $p=0.57$).

Table 3.1: Comparison of peak aboveground biomass collected on August 6, 2013, from control, infrared heated and open-top chamber plots in a grassland near Lethbridge, Alberta, and the elemental composition of the collected vegetation. Values represent mean \pm standard error, n=9.

Measurement	Control	Infrared heaters	Open-top chambers
Aboveground biomass (g m ⁻²)	329 \pm 17	347 \pm 64	350 \pm 19
Carbon content (mg g ⁻¹)	442 \pm 1	440 \pm 2	444 \pm 3
Nitrogen content (mg g ⁻¹)	12.4 \pm 0.4	11.2 \pm 0.9	11.7 \pm 0.3
C:N ratio	37 \pm 2	37 \pm 2	39 \pm 3

Table 3.2: Comparison of peak aboveground biomass and growing season precipitation in the study year (2013), a year of average precipitation (1999) and a dry year (2001). Values represent mean \pm standard error, n=9. Values from 1999 and 2001 from Flanagan and Farquhar (2014).

Measurement	Study year (2013)	Average year (1999)	Dry year (2001)
Aboveground biomass (g m ⁻²)	329 \pm 17	114 \pm 17	101 \pm 8
Precipitation from May to October (mm)	346	239.6	89.7

Table 3.3: Comparison of carbon ($\delta^{13}\text{C}$) and oxygen ($\delta^{18}\text{O}$) isotope ratios from peak aboveground biomass collected on August 6, 2013, from control, infrared heated and open-top chamber plots. Values represent mean \pm standard error, n=9.

Measurement	Control	Infrared heaters	Open-top chambers
$\delta^{13}\text{C}$ (‰)	-28.5 ± 0.2	-28.8 ± 0.3	-28.3 ± 0.2
$\delta^{18}\text{O}$ (‰)	18.3 ± 0.2	18.9 ± 0.4	18.6 ± 0.5

Table 3.4: Comparison of carbon ($\delta^{13}\text{C}$) and oxygen ($\delta^{18}\text{O}$) isotope ratios from peak aboveground biomass in the study year (2013), a year of average precipitation (1999) and a dry year (2001). Values represent mean \pm standard error, n=9. Values from 1999 and 2001 from Flanagan and Farquhar (2014).

Measurement	Study year (2013)	Average year (1999)	Dry year (2001)
$\delta^{13}\text{C}$ (‰)	-28.5 ± 0.2	-26.7 ± 1.0	-26.1 ± 0.1
$\delta^{18}\text{O}$ (‰)	18.3 ± 0.2	24.9 ± 1.5	25.2 ± 1.1
Precipitation from May to October (mm)	346	239.6	89.7

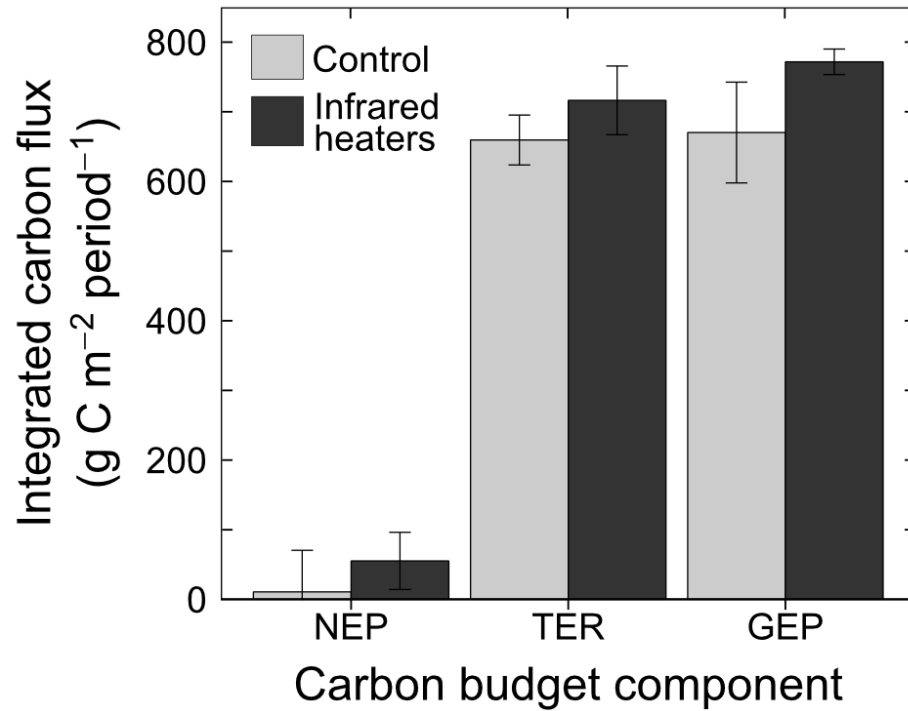


Figure 3.1: Comparison of integrated carbon flux rates ($\text{g C m}^{-2} \text{ period}^{-1}$) calculated based on half-hourly autochamber measurements of total carbon dioxide flux for control and warmed treatment plots during the growing season (May to October, 2013). Net ecosystem CO_2 exchange was partitioned total ecosystem respiration (TER) and gross ecosystem productivity (GEP), the difference between which represents net ecosystem productivity (NEP). Error bars represent \pm standard error. Statistical significance was based on single-factor ANOVA. NEP: $F(1)=0.4$, $p=0.57$, TER: $F(1)=0.9$, $p=0.40$, GEP: $F(1)=1.9$, $p=0.25$.

3.4 Discussion

The purpose of this study was to investigate the effects of elevated temperatures on plant growth and physiology, as well as on ecosystem CO₂ exchange. Plant biomass may be affected by changes in ecosystem temperature, thereby resulting in changes in elemental composition. These changes may have an effect on plant production and nutrition (Bowes 1993, An *et al.* 2005). As well, water-use efficiency may be altered by warming, affecting how plants acclimate to future changes in precipitation regimes. Any changes to plant growth and physiology may impact their role in the global carbon cycle (Schimel 1995, Luo 2007). It is important to understand the source/sink status of ecosystems under warming conditions, as it will directly influence atmospheric carbon dioxide and further changes in climate (Kowalchuk 2012).

3.4.1 Peak aboveground plant biomass

Aboveground plant biomass may be expected to increase under warming conditions, due to an increase in photosynthetic rates (Lin *et al.* 2010). My study did not show an increase in peak aboveground biomass under either warming treatment (Table 3.1). There was, however, significantly higher biomass than a dry or average year at this study site (Table 3.2). The site maximum over 8 previous years of study was approximately 250 g m⁻², while the study year of 2013 had much higher plant biomass reaching almost 350 g m⁻² (Flanagan and Adkinson 2011). This is consistent with that fact that, in general, biomass at this site is strongly correlated with precipitation and soil moisture (Flanagan and Adkinson 2011). There were also no significant variations in elemental

composition between the warmed and control plots (Table 3.1). At this study site, there is a tendency for years with low biomass to have higher nitrogen content: biomass values around 250 g m⁻² had about 10 mg g⁻¹ of nitrogen, while biomass values around 100 g m⁻² had about 20 mg g⁻¹ of nitrogen (Flanagan and Adkinson 2011). In 2013, high biomass of around 350 g m⁻² has a nitrogen content of around 12 mg g⁻¹, which is higher than might be expected (Table 3.1). It is possible that the high precipitation levels allowed greater nitrogen mineralization, and therefore, plant growth was less nitrogen limited than in other years (Burke *et al.* 1997).

Water-use efficiency can also be assessed from plant biomass, based on $\delta^{13}\text{C}$ and $\delta^{18}\text{O}$ values. The ratio between $\delta^{13}\text{C}$ and $\delta^{18}\text{O}$ is representative of the ratio between leaf net CO₂ assimilation rate (A) and transpiration rate (E), and therefore of water-use efficiency (as seen in Equation 3.1). Due to lack of treatment effect on both $\delta^{13}\text{C}$ and $\delta^{18}\text{O}$, it can be concluded that the ratio of A and E has not been affected, and therefore that there was no change in water-use efficiency due to the warming treatment. However, a study in a semi-arid grassland in China showed that increased temperature without increased precipitation decreased water-use efficiency at the ecosystem level, as photosynthetic activity declined while water loss remained the same, likely because stomatal regulation to prevent excess water loss also reduced CO₂ uptake (Niu *et al.* 2011). This study by Niu *et al.* (2011) was a four year study, therefore it is possible that similar changes in water-use efficiency may be seen in the southern Alberta grassland site after a prolonged warming treatment.

In addition, interannual variations in isotope ratios emphasize the different environmental and physiological elements than control water-use efficiency. In past years, low peak biomass values at this study site have corresponded to high $\delta^{13}\text{C}$ and high $\delta^{18}\text{O}$ values: biomass of around 100 g m^{-2} had a $\delta^{13}\text{C}$ of about -26.5‰ and a $\delta^{18}\text{O}$ of about 25‰ (Flanagan and Farquhar 2014). In contrast, higher biomass of around 250 g m^{-2} had a lower $\delta^{13}\text{C}$ of about -28‰ and a lower $\delta^{18}\text{O}$ of about 23.5‰ (Flanagan and Farquhar 2014). This trend is consistent with the study season of 2013, which had very high peak biomass production (329 g m^{-2}) and correspondingly high values for $\delta^{13}\text{C}$ (-28‰) and $\delta^{18}\text{O}$ (18‰) (Tables 3.1 and 3.3).

The carbon isotope ratio within plant tissue is determined by isotopic fractionation as carbon dioxide moves into the leaf and is used by the photosynthetic process, controlled in part by the ratio of intercellular (c_i) to atmospheric (c_a) CO_2 (Gebrekirstos *et al.* 2011). The high $\delta^{13}\text{C}$ value in the dry year is indicative of low c_i , as low stomatal conductance limits the entrance of CO_2 into the leaves (Gebrekirstos *et al.* 2011). The low $\delta^{13}\text{C}$ value of -28‰ is also consistent with other years of high biomass production where water stress was not a limiting factor on photosynthesis and growth, and stomatal conductance could remain high (Flanagan and Farquhar 2014). The oxygen isotope ratio within plant tissue is indicative of leaf-to-air vapour pressure deficit (VPD). Low leaf-to-air VPD, as occurs when the air outside the leaf has high humidity, results in a low $\delta^{18}\text{O}$ value, such as was seen in the wet growing season of 2013 (Kahmen *et al.* 2011). The high $\delta^{18}\text{O}$ value in the dry year is, therefore, as expected and

indicative of high VPD. When both carbon and oxygen isotope ratios are affected by environmental and physiological conditions, it is impossible to determine water-use efficiency without further data. However, the information on these environmental and physiological conditions can be useful for understanding ecosystem processes.

3.4.2 Carbon dioxide flux

Measuring ecosystem carbon dioxide flux allows us to determine if the ecosystem is acting as a source or sink of carbon dioxide. The study season of 2013 did not show any significant differences in carbon dioxide flux between the control and warmed plots (Figure 3.1). High ecosystem productivity and respiration are closely linked to leaf area and biomass, making high values in 2013 unsurprising due to its high aboveground plant biomass (Xu and Baldocchi 2004, Flanagan and Adkinson 2011). While both ecosystem productivity and respiration were high in 2013, productivity surpassed respiration, making the site a net carbon sink. Previous measurements at this study site, although made by eddy covariance, also show that it is a carbon sink (Flanagan *et al.* 2013).

Grasslands in general have the capacity to be large carbon sinks for atmospheric CO₂, as they can store large amounts of carbon in biomass and soil organic matter (Smith 2014). A study of the entire grassland area of northern China showed that it was an area of net carbon uptake from 2000 to 2010 (Zhang *et al.* 2014). Similarly, a study of the Great Plains of North America showed that the entire Great Plains area was a carbon sink between 2000 and 2008, although

the carbon budget varied spatially, and the western portion was actually a carbon source during a drought (Zhang *et al.* 2011). Grasslands do not always act as carbon sinks, and under warming conditions with respiration rates increasing more than ecosystem productivity, the carbon balance may shift to grasslands being a net source of carbon (Yvon-Durocher *et al.* 2010).

3.5 Conclusion

This experiment was the first year in what will be a long-term warming study. There were no significant changes in plant biomass, water-use efficiency or carbon dioxide flux in the warmed plots compared to the control plots. The high levels of carbon dioxide flux and high biomass production in 2013 may have been due to the high precipitation input compared to average years at this study site. The interannual differences in precipitation and other environmental conditions emphasize the need for long term studies. While a relatively small change in temperature may only produce small changes in ecosystem processes, it is important to understand that these small changes may add up over a long-term study. In addition, water availability and possible changes in plant and ecosystem water-use efficiency may affect how this semi-arid ecosystem will acclimate to future warming. It is essential to study the effects of warming on wet, dry, and average years, in order to accurately predict the future consequences of global climate change.

CHAPTER 4. SEASONAL VARIATION IN SOIL MICROBIAL BIOMASS, BACTERIAL COMMUNITY COMPOSITION AND EXTRACELLULAR ENZYME ACTIVITY IN RELATION TO SOIL RESPIRATION IN A NORTHERN GREAT PLAINS GRASSLAND

4.1 Introduction

The concentration of atmospheric carbon dioxide (CO₂) is being changed by human activity, with consequences that include warmer air temperatures and altered precipitation and snow melt patterns (Barnett *et al.* 2005, Rosenzweig *et al.* 2008). Soil respiration accounts for 35% of total global carbon released to the atmosphere and 60% of terrestrial carbon released to the atmosphere (Schlesinger and Andrews 2000). It is, therefore, vital to understand how changes in global environmental conditions may affect the processes involved in soil respiration. Soil respiration refers to the diffusion of carbon dioxide out of the soil due to the elevated levels of CO₂ produced by biological processes (Davidson *et al.* 2002). The CO₂ has two sources: autotrophic (root) respiration and heterotrophic (microbial) respiration (Hanson *et al.* 2000). Therefore, soil respiration can be affected by changes to plant and microbial activity. Soil respiration shows strong seasonal patterns, and when water stress is not a factor, respiration is correlated with temperature (Janssens and Pilegaard 2003). Seasonal soil CO₂ flux patterns have been shown to be similar to soil temperature patterns, with the highest fluxes occurring during times of peak biomass production (Frank *et al.* 2002). However, these effects of temperature may be either direct or indirect.

Respiration rates may be calculated from the following modified van't Hoff (1898) equation with an added function for water availability,

$$\text{Respiration rate} = R_{10} \times Q_{10}^{\left(\frac{T-10}{10}\right)} \times f_{A_w} \quad (4.1)$$

where R_{10} is the respiration rate at 10°C ($\mu\text{mol CO}_2 \text{ m}^{-2} \text{ s}^{-1}$), Q_{10} is the temperature sensitivity coefficient, T is the temperature (°C), and f_{A_w} is a relative water stress function that varies on a scale from 0 to 1 (Equation 4.2).

$$f_{A_w} = A_w \text{ max.} \times e^{-\left(\frac{A_w - A_w \text{ opt.}}{A_w \text{ width}}\right)^2} \quad (4.2)$$

The water stress function represents a theoretical binomial distribution for this study site, where A_w is available water, $A_w \text{ max}$ equals 1, $A_w \text{ opt}$ equals 0.85, and $A_w \text{ width}$ equals 0.47. Q_{10} is directly affected by temperature, as the temperature sensitivity of respiration tends to be decreased at higher measurement temperatures (Figure 4.1) (Tjoelker *et al.* 2001).

$$Q_{10} = 3 - (0.045 \times T) \quad (4.3)$$

In a scenario where R_{10} remains constant, respiration rate will rise as a function of temperature and is also increased by increased water availability (Figure 4.2). This represents the direct effect of soil temperature and soil water content on soil respiration. However, in a real world scenario, R_{10} is not constant. R_{10} represents the ecosystem's capacity for respiration at 10°C (Cai *et al.* 2010). This respiratory capacity can be affected by several factors, including root biomass, microbial biomass, and substrate availability, all factors that vary seasonally and are correlated with changes in temperature (Boone *et al.* 1998). For example, biomass may show a normal distribution as a function of temperature (Figure 4.3), while R_{10} may increase linearly with increases in biomass (Figure 4.4). At

constant soil moisture, the rate of soil respiration as a function of temperature will be different at different values of R_{10} (Figure 4.5). The same general pattern may be expected for substrate availability, which also affects R_{10} . Therefore, changes in R_{10} associated with temperature shifts, due to variations in biomass and substrate availability, represent the indirect effects of temperature on soil respiration. While these specific values and relationships are theoretical, they do serve to illustrate the difference between the direct and indirect effects of temperature on soil respiration.

The factors involved in changes in respiratory capacity are varied and intertwined. It has been shown that, in forests, soil respiration is influenced by plant activity and below-ground carbon allocation, and that this may be even more important than soil temperature (Hogberg *et al.* 2001). The seasonal changes in the rate of gross primary productivity (GPP), or photosynthesis, is controlled by variation in the amount of leaf area, as the highest rate of GPP tends to occur during the period of greatest leaf area index (LAI) (Flanagan *et al.* 2002, Flanagan and Adkinson 2011). The biological processes occurring in the aboveground portions of plants are fundamentally linked to the processes occurring belowground. Plants put a portion of the energy they obtain through photosynthesis into root growth and respiration (Holland *et al.* 1996). The allocation of energy to roots may be affected by temperature, as root to shoot ratios in grassland ecosystems tend to decrease in response to increased temperature (Mokany *et al.* 2006). A change in root biomass is likely to have an

impact on the root respiration component of total soil respiration (Kucera and Kirkham 1971, Cao *et al.* 2004).

In addition, roots secrete a wide variety of compounds into the soil, generally referred to as root exudates (Walker *et al.* 2003). The primary components of root exudates are carbon-based compounds (sugars, amino acids, and proteins, to name a few) but they also contain ions, inorganic acids, oxygen and water (Badri and Vivanco 2009). The quantity and composition of root exudates are affected by plant species and age, as well as environmental factors like biotic and abiotic stressors (Badri and Vivanco 2009). The rate of exudation is also strongly coupled to rates of photosynthesis and carbon allocation to roots (Dilkes *et al.* 2004). Root exudates provide substrate for soil microorganisms, thereby increasing heterotrophic respiration rates (Curiel Yuste *et al.* 2007). Additionally, warming can increase root turnover, providing dead root tissue to be decomposed and provide yet more substrate for respiration (Fitter *et al.* 1999).

The increase in substrate availability through exudation may directly increase respiration rates, although it may also cause a priming effect that increases extracellular enzyme activity (Blagodatskaya and Kuzyakov 2008). Changes in the activity of these soil enzymes can cause an increase in the decomposition rate of old soil organic matter (SOM) that is generally difficult to break down, and thus affect the efflux of carbon from soil through heterotrophic respiratory processes (Phillips *et al.* 2011). Soil enzyme activity may be controlled by nitrogen availability, water availability (soil moisture) and the

quality and quantity of soil organic matter (Waldrop and Firestone 2006, Bell *et al.* 2009, Wallenstein *et al.* 2009). There are a wide range of extracellular enzymes found in soil to degrade the variety of macromolecules constituting soil organic matter such as lignin, cellulose, starch, lipids, chitin and proteins (Wallenstein and Weintraub 2008). As many ecosystems are limited by nitrogen availability, enzymes that liberate nitrogen are particularly important. Two such enzymes are β -1,4-*N*-acetylglucosaminidase (NAGase) and phenol oxidase. NAGase is a hydrolytic enzyme that breaks down β -1,4-glucosamines from cell walls of soil organisms into amino sugars, which are part of a moderate to fast cycling pool of nitrogen in soil (Roberts *et al.* 2007, Phillips *et al.* 2011). In contrast, phenol oxidase is involved in the decomposition of lignin and the release of nitrogen that can be bound to it (Schmidt-Rohr *et al.* 2004). Phenol oxidase is often used as a sentinel of SOM decomposition, as high phenol oxidase activity tends to mean low SOM accumulation, and the nitrogen released from lignin is part of a slow cycling pool of soil nitrogen (Sinsabaugh 2010).

The seasonal patterns in ecosystem carbon dioxide flux and plant activity, as well as the seasonal environmental patterns, have significant impacts on the soil and its microbial community. The microbial community in the soil is the primary component of the decomposer system which regulates nutrient cycling, and temporal variation of the microbial biomass is directly related to nutrient availability for the whole ecosystem and consequently the overall productivity of the ecosystem (Wardle 1998). In established ecosystems, microbial biomass is in equilibrium and remains relatively stable, with short-term seasonal fluctuations

(Corre *et al.* 2002). In addition to seasonal fluctuations of soil microbial biomass, the species composition of the microbial community can also exhibit seasonal patterns. The results of one study have shown that changes in precipitation and moisture caused a shift in the relative abundance of bacterial phyla, and that elevated temperatures caused an increase in fungal abundance with a decrease in bacterial abundance (Castro *et al.* 2010). Cleveland *et al.* (2007) suggest that the input of labile carbon (such root exudates) increases soil respiration by causing a shift in the microbial community towards groups that can free limiting nutrients (such as nitrogen or phosphorus) from SOM.

A meter deep layer of the world's soils contain more than two times the amount of carbon in the atmosphere (Rustad *et al.* 2000). An increase in soil respiration rates due to environmental changes could release a portion of this carbon, exacerbating the increasing atmospheric CO₂ levels (Rustad *et al.* 2000). The consequences of increased atmospheric CO₂ levels are generally understood (Barnett *et al.* 2005, Rosenzweig *et al.* 2008), and it is important to determine how changes in soil respiration rates may further intensify these consequences. Seasonal patterns in environmental factors, such as soil temperature and soil moisture, allow the study of the impact of these factors on soil respiration, as well as the interactions between soil respiration and other ecosystem processes. This study will examine the direct effects of soil temperature and soil moisture on soil respiration, as well as the potential indirect effects of seasonal changes in microbial biomass, bacterial community species composition, extracellular enzyme activity, and substrate availability.

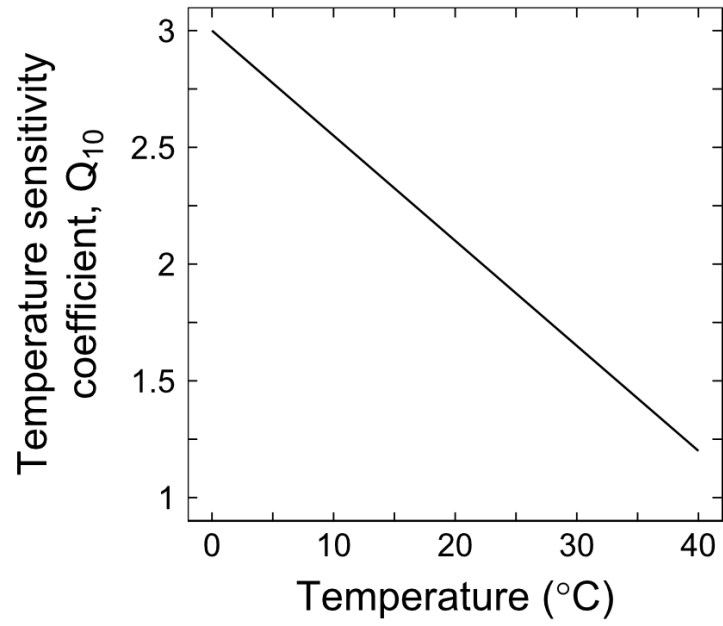


Figure 4.1: Temperature sensitivity coefficient (Q_{10}) as a function of temperature, as calculated by equation 4.3.

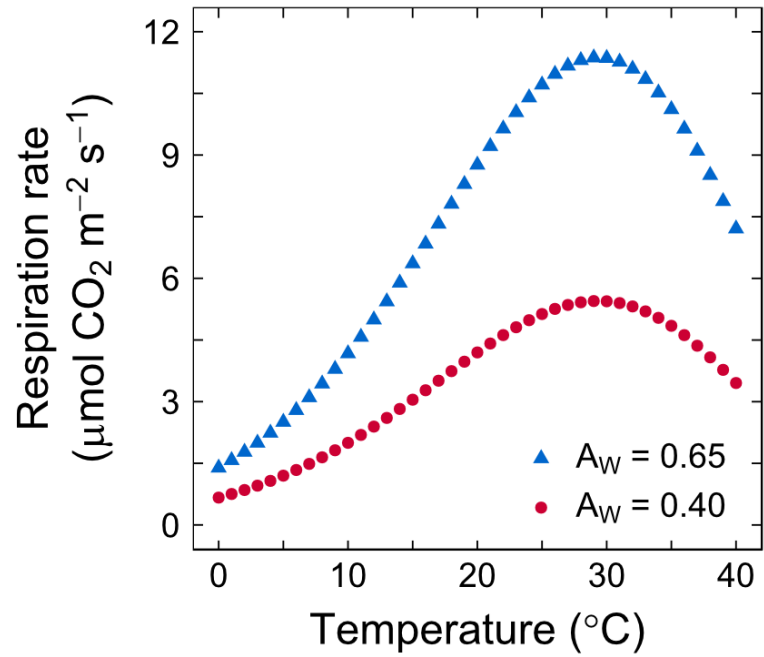


Figure 4.2: Respiration rate as a function of temperature and the effects of variation in water availability (A_w). Generated from Equation 4.1, with $R_{10} = 5 \mu\text{mol CO}_2 \text{ m}^{-2} \text{ s}^{-1}$ and Q_{10} varying as shown in Figure 4.1.

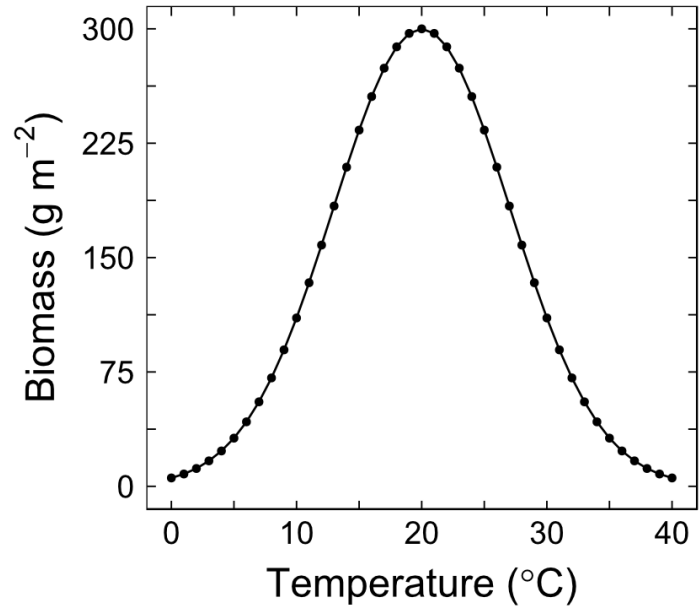


Figure 4.3: A theoretical pattern illustrating the effects of temperature on biomass.

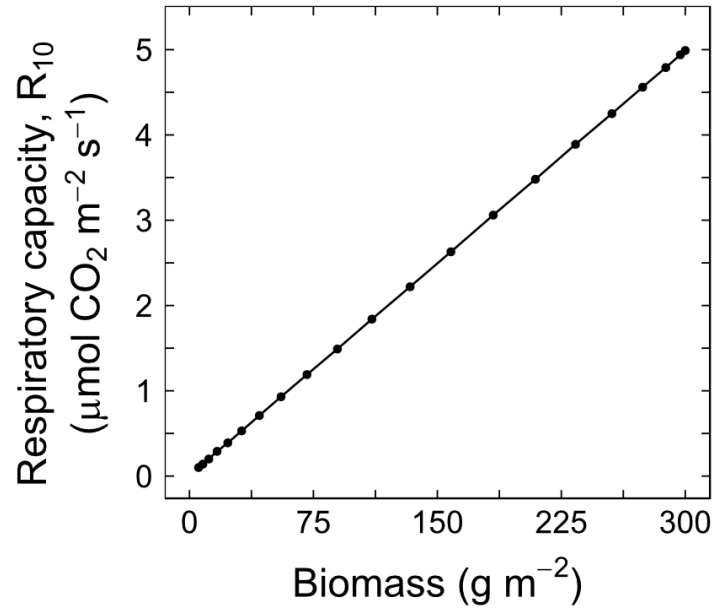


Figure 4.4: A theoretical pattern illustrating the effects of biomass on respiratory capacity (R_{10}).

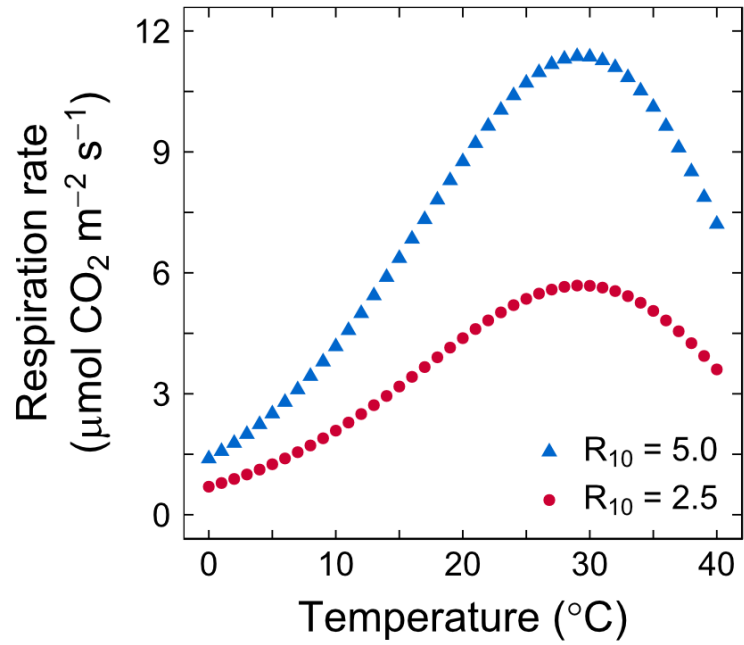


Figure 4.5: Respiration rate as a function of temperature and the effects of variation in respiratory capacity (R_{10}). Generated from Equation 4.1, with $A_w = 0.65$ and Q_{10} varying as shown in Figure 4.1.

4.2 Methods and materials

4.2.1 Field site description

As described in Chapter 2.

4.2.2 Environmental measurements

As described in Chapter 2.

4.2.3 Carbon dioxide flux

Ecosystem net CO₂ exchange was measured using an automated chamber system with clear chamber lids that are attached to soil collars (Carbone *et al.* 2008, Cai *et al.* 2010). The autochambers recorded the net ecosystem exchange rate once every 30 minutes on a continuous basis throughout the growing season period, from late April to early October. The measurements of net ecosystem CO₂ exchange was partitioned into estimates of ecosystem photosynthesis and total respiration using methods outlined in Cai *et al.* (2010). The daily values were used to calculate a 5-day average to remove some noise from the data. Results were assessed by repeated measures ANOVA using the 5-day average from every 5th day to look for statistically significant effect of treatment. Only the carbon dioxide flux measurements from the control and infrared heated plots were considered, due to potential inaccuracies in CO₂ measurements the open-top chambers caused by wind-related artifacts.

In addition to the autochamber measurements, soil respiration measurements were made manually at approximately two-week intervals over the

course of the growing season, using a portable gas exchange system (LI-6200, LI-COR Inc., Lincoln, NE, USA) and dynamic closed chamber (LI-6000-09 respiration chamber, LI-COR Inc.). The chamber was attached to plastic collars (10 cm tall) that were inserted into the soil to a depth of 5 cm. The collars enclosed a ground area of 71.6 cm² and one collar was located in each treatment plot. Living aboveground biomass in the collars was clipped 1-2 days prior to respiration measurements, and the clipped material was left in the collar, minimizing aboveground plant respiration without physically removing any organic material from the system (Flanagan *et al.* 2013). The chamber system measured the change in CO₂ concentration over a period of 30 seconds, during which a linear rise in CO₂ concentration was seen. This linear rise was used to calculate the respiration rate in $\mu\text{mol CO}_2 \text{ m}^{-2} \text{ s}^{-1}$. Results were averaged among all 9 plots to determine the seasonal pattern and were assessed using single-factor ANOVA, testing for statistically significant effects of day of year.

4.2.4 Soil sample collection

Soil samples from each treatment plot were taken four times over the course of the summer. Sampling dates corresponded approximately to the following ecosystem growth stages: active plant growth but prior to peak biomass (June 5, 2013 and June 27, 2013), near peak biomass (July 18, 2013), and soil dry-down prior to complete plant senescence (August 21, 2013). Samples were collected using sterile 1.9 cm aluminum pipes inserted to a depth of 15 cm. At each sampling date, five such soil cores were taken from each plot and combined in a sterile sample bag to form one sample per plot. The samples were kept in a

cooler until they could be returned to the laboratory. Each sample was broken up and mixed in the laboratory with a sterile spatula and stones, green plant biomass and large plant roots were removed. All soil processing was completed within 3 hours of sample collection.

Each soil sample was partitioned for three separate analyses. A subsample of approximately 0.25 g was used for DNA extraction. Four subsamples of approximately 1 g each were stored in a -80°C freezer to be used for enzyme assays. Finally, the remaining soil was evenly divided into four 30 mL pre-weighed beakers, to be used to determine microbial biomass via substrate-induced respiration.

4.2.5 Substrate-induced respiration

The beakers of soil were weighed to calculate the initial fresh weight of the soil. For each plot, there were two control samples and two samples to which substrate would be added. The control samples received 2 mL of sterile, distilled water, while the other two samples received 2 mL of a 10% w/v solution of yeast extract. The yeast extract solution was made from granulated, autolyzed yeast extract (EMD Chemicals Inc., Gibbstown, NJ, USA), which is a mixture of amino acids, peptides, water soluble vitamins and carbohydrates with a total carbon content of 39.7 ± 0.1 % and a total nitrogen content of 10.3 ± 0.02 % (average \pm standard error, n=4). The samples were then left for 24 hours at room temperature before respiration measurements were made. The 24-hour

incubation period allowed time for the soil to equilibrate after the disruption of sampling and adding solutions.

After the 24-hour incubation period, respiration was measured using a custom-made gas exchange system. The system consisted of a variety of components, connected with tubing for air flow. An air bag contained air with a known CO₂ concentration (396.5 ppm). Air from this bag was pumped into the system using a gas pump (Qubit F1000, Qubit Systems Inc., Kingston, ON, Canada) and then through a flow meter (Qubit G101, Qubit Systems Inc.), set to a flow rate of 0.5 L/min. After the flow meter, the air passed through a 500 mL mason jar containing a stainless steel temperature probe (Vernier Software & Technology, Beaverton, OR, USA). Next, the air moved through a temperature and humidity sensor (Qubit S161, Qubit Systems Inc.). The air then flowed through a container of Drierite (W.A. Hammond Drierite Company LTD., Xenia, OH, USA), to remove any water vapour, before flowing through the infrared gas analyzer (LI-820, LI-COR Inc., Lincoln, NE, USA). After passing through the gas analyzer, the air was vented to the room, creating an open system. Temperature and relative humidity probes, and the gas analyzer, were connected to a data logger (Vernier LabPro, Vernier Software & Technology) and visualized on a computer.

To measure respiration, the soil sample was placed in the mason jar. The pump was turned on, and the system was flushed with air from the air bag (396.5 ppm CO₂) until the CO₂ concentration equilibrated to a constant value, taking

approximately 5-10 minutes. At that point, the outflow tube from the gas analyzer was connected to the pump, in the place of the tube from the air bag, thus closing the system. Once the system was closed, after some initial fluctuations, the CO₂ concentration rose in a linear fashion for approximately 5 minutes. The change in CO₂ concentration or ΔCO₂ was calculated from the slope of the linear CO₂ increase (μmol CO₂ mol⁻¹ air min⁻¹). The soil samples were then dried at 100°C for 48 hours and weighed to determine their final dry mass.

The respiration rate of each soil sample was calculated using the ΔCO₂ value, the volume of the measuring system, the density of air and the mass of the soil:

$$\text{Respiration rate } (\mu\text{mol CO}_2 \text{ g}^{-1} \text{ min}^{-1}) = \frac{\Delta\text{CO}_2 (\mu\text{mol mol}^{-1} \text{ min}^{-1}) * \text{volume (m}^3) * \text{air density (mol m}^3)}{\text{soil dry mass (g)}} \quad (4.4)$$

The density of air is calculated from the Ideal Gas Law (Equation 4.5) and known values of temperature (T) and atmospheric pressure (P):

$$n/v = P/RT \quad (4.5)$$

where n is the number of moles of air (mol), v is the volume (m³), T is the absolute temperature (K), R is the gas constant (8.314 m³ Pa mol⁻¹ K⁻¹) and P is atmospheric pressure (90,000 Pa). Substrate-induced respiration of soil samples were averaged and assessed with a single-factor ANOVA test to determine if there were significant differences among samples collected on different days.

Before running tests on field samples, two preliminary tests were run to assess and optimize the methodology. First, a comparison was made between a 10% w/v sugar solution and a 10% w/v yeast extract solution to determine which would cause a greater stimulation of respiration. The yeast extract solution showed a 4.5-fold higher respiration rate than the sugar solution (Table 4.1) and was therefore chosen for the testing of field samples. The second test was to confirm that live microorganisms must be present for observed respiratory activity to be stimulated by added substrate. Yeast extract solution was added to both fresh and autoclaved soil. While the fresh soil showed significant increases in respiration due to the addition of substrate, the autoclaved soil with added substrate did not show higher respiration than the autoclaved soil with only water added (Table 4.2). This confirmed that living microorganisms must be present to show substrate-induced respiration.

4.2.6 Soil enzyme activity

Two enzymes were chosen to represent both fast and slow nitrogen cycling processes, β -1,4-*N*-acetylglucosaminidase (NAGase) and phenol oxidase, respectively (Phillips *et al.* 2011). Each soil sample was prepared for the assay by combining pre-weighed soil samples of approximately 1 g with 125 mL of 50 mM, pH 6 acetate buffer, and homogenizing in a small blender. These soil slurries were then immediately pipetted into the appropriate 96-well microplates for the assays, as described in the following sections.

4.2.6.1 β -1,4-*N*-acetylglucosaminidase assay

For the NAGase assay, black 96-well microplates were used. The reference standard was a 10 μ M 4-methylumbelliferone solution. The enzyme substrate was a 200 μ M 4-methylumbelliferyl *N*-acetyl- β -D-glucosaminide solution. There were 16 replicate wells for each of a blank control, a negative control and a reference standard. The blank control consisted of 250 μ L of acetate buffer. The negative control consisted of 200 μ L of acetate buffer and 50 μ L of substrate solution. The reference standard consisted of 200 μ L of acetate buffer and 50 μ L of reference standard solution.

For each soil sample, there were 8 replicate wells for each of a quench control and a soil blank control, and 16 replicate wells for the enzyme assay. The quench control consisted of 200 μ L of soil slurry and 50 μ L of reference standard solution. The soil blank control consisted of 200 μ L of soil slurry and 50 μ L of acetate buffer. The enzyme assay consisted of 200 μ L of soil slurry and 50 μ L of substrate solution. Two sets of plates were prepared for each soil sample; one was incubated for 2 hours at 23°C in the dark and the other was incubated for 4 hours at 10°C in the dark. After incubation, 10 μ L of 1.0 M NaOH was added to each well to stop the reaction. The plates were then immediately measured for fluorescence using a microplate reader (Varioskan Flash, Thermo Scientific, Waltham, MA, USA), with 365 nm excitation and 450 nm emission filters.

To determine the enzyme activity, the measurements from the replicate wells were first averaged for all controls and assays. Then, the average value for

the blank control was subtracted from all other average values. An emission coefficient was calculated using equation 4.6 in order to determine the amount of fluorescence per nmol of 4-methylumbelliferone (fluor/nmol). Next, a quench coefficient was calculated for each soil sample, using equation 4.7, to determine how much the soil slurry masked the fluorescence reading. The net fluorescence of each soil sample was then calculated using equation 4.8. Finally, the actual enzyme activity (nmol g⁻¹ h⁻¹) was calculated using equation 4.9, where 125 mL is the total volume of soil slurry and 0.2 mL is the volume of soil slurry in each assay well.

$$\text{emission coefficient (fluor/nmol)} = \frac{\text{reference standard}}{0.5 \text{ nmol}} \quad (4.6)$$

$$\text{quench coefficient} = \frac{\text{quench standard} - \text{sample control}}{\text{reference standard}} \quad (4.7)$$

$$\text{net fluor.} = \frac{\text{sample assay} - \text{sample control}}{\text{quench coefficient}} - \text{negative control} \quad (4.8)$$

$$\text{Activity (nmol g}^{-1} \text{ h}^{-1}\text{)} = \frac{\text{net fluor.} \times 125 \text{ mL}}{\text{emission coefficient (fluor/nmol)} \times 0.2 \text{ mL} \times \text{time (h)} \times \text{soil mass (g)}} \quad (4.9)$$

4.2.6.2 Phenol oxidase assay

For the phenol oxidase assay, clear 96-well microplates were used. The enzyme substrate was a 25 mM solution of L-dihydroxyphenylalanine (L-DOPA). There were 16 replicate wells for each of a blank control and a negative control. The blank control consisted of 250 µL of acetate buffer. The negative control consisted of 200 µL of acetate buffer and 50 µL of substrate solution. For each soil sample, there were 8 replicate wells for a soil blank control and 16 replicate

wells for the enzyme assay. The soil blank control consisted of 200 μL of soil slurry and 50 μL of acetate buffer. The enzyme assay consisted of 200 μL of soil slurry and 50 μL of substrate solution. Two sets of microplates were prepared for each soil sample; one was incubated for 12 hours at 23°C in the dark and the other was incubated for 24 hours at 10°C in the dark. After incubation, 175 μL of supernatant from each well was transferred to a second clear 96-well microplate, avoiding the sediment at the bottom of the wells. The microplates were then immediately measured for absorbance at 450 nm using a microplate reader (Varioskan Flash, Thermo Scientific).

In order to calculate phenol oxidase activity, it is necessary to know the extinction coefficient of the substrate being used. The extinction coefficient is the measured absorbance for a known amount of fully reacted substrate, giving units of absorbance per unit of reacted substrate. A clear, 96-well microplate was used with 16 replicate wells for each of a blank control and negative control, and 64 wells to measure an extinction coefficient. The substrate solution was a 0.5 mM solution L-DOPA, dissolved in 50 mM, pH 6 acetate buffer. The enzyme was Laccase (from *Trametes versicolor*), dissolved in 50 mM, pH 6 acetate buffer to a concentration of 1 mg/mL. The blank control consisted of 250 μL of acetate buffer. The negative control consisted of 200 μL of acetate buffer and 50 μL of enzyme solution. The extinction coefficient measurement consisted of 200 μL of L-DOPA solution and 50 μL of enzyme solution.

The microplate was incubated in the dark at 23°C for 12 hours. After the incubation, 175 µL of supernatant from each well was transferred to a second clear 96-well microplate. The plates were then immediately measured for absorbance at 450 nm using a microplate reader (Varioskan Flash, Thermo Scientific). The absorbance values for all replicate wells were averaged, and the average blank value was subtracted from all other average values. The absorbance of the negative control was then subtracted from the absorbance of the reacted L-DOPA. Finally, the average absorbance value of the reacted L-DOPA was divided by the amount of substrate in each well (0.1 µmol) to give an extinction coefficient, as per equation 4.10.

$$\text{Extinction coefficient (abs./}\mu\text{mol)} = \frac{\text{absorbance}}{\mu\text{mol substrate reacted}} \quad (4.10)$$

To determine the enzyme activity, the measurements from the replicate wells were first averaged for all controls and assays. Then, the average value for the blank control was subtracted from all other average values. Next, the optical density (OD) was calculated using equation 4.11 in order to determine the absorbance attributed to the reaction product and not the soil slurry itself. Finally, the actual enzyme activity ($\mu\text{mol g}^{-1} \text{h}^{-1}$) was calculated using equation 4.12, where 125 mL is the total volume of soil slurry produced and 0.2 mL is the volume of soil slurry in each assay well.

$$\text{OD} = \text{sample abs.} - \text{soil blank abs.} - \text{neg. control abs.} \quad (4.11)$$

$$\text{Activity } (\mu\text{mol g}^{-1} \text{h}^{-1}) = \quad (4.12)$$

$$\frac{\text{OD} \times 125 \text{ mL}}{\text{extinction coefficient (abs./}\mu\text{mol)} \times 0.2 \text{ mL} \times \text{time (h)} \times \text{soil mass (g)}}$$

4.2.6.3 Modeling seasonal enzyme activity

The two assay temperatures of 10°C and 23°C were chosen because they bracket the range of soil temperatures at the study site over the course of a growing season (Figure 4.6a). Using the rates of enzyme activity at these two temperatures, the Q_{10} for each enzyme was calculated using the following equation.

$$Q_{10} = \left(\frac{\text{Rate at } 23^{\circ}\text{C}}{\text{Rate at } 10^{\circ}\text{C}} \right)^{\left(\frac{10}{23^{\circ}\text{C} - 10^{\circ}\text{C}} \right)} \quad (4.13)$$

The value for Q_{10} was then used to model the activity of the enzymes over the course of the growing season, as a function of soil temperature, using equation 4.14,

$$\text{Enzyme activity (nmol g}^{-1} \text{ h}^{-1}) = R_{10} \times Q_{10}^{\left(\frac{T-10}{10} \right)} \quad (4.14)$$

where R_{10} is the measured rate of activity at 10°C and T is the soil temperature (°C) at a depth of 10 cm. Enzyme activity was modeled for each experimental plot, based on its specific R_{10} and Q_{10} values and its daily average soil temperature, producing the daily average rate of enzyme activity (nmol substrate $\text{g}^{-1} \text{ h}^{-1}$). The modeled daily average rates of enzyme activity were then plotted as a function of time, to show the seasonal pattern of modeled *in situ* enzyme activity. The measured activity at 10°C and 23°C and the calculated Q_{10} values were averaged across all 9 plots and tested for statistically significant effects of time using single-factor ANOVA.

4.2.7 Soil bacterial community composition

DNA extractions from soil samples were performed using the PowerSoil® DNA Isolation Kit (Mo-Bio, Carlsbad, CA, USA), as per the manufacturer's instructions. DNA was extracted from fresh soil within 6 hours of collection. The extracted DNA was then stored in the -80°C freezer, until all samples could be submitted for sequencing.

Sequencing was done by Molecular Research-DNA (Shallowater, TX, USA) and samples were aliquoted and shipped according to their standards. Amplicon pyrosequencing (bTEFAP®) was originally described by Dowd et al. (2008a) and has been employed in describing a wide range of microbiomes, both environmental and health related, such as intestinal populations in cattle (Dowd *et al.* 2008a, Callaway *et al.* 2010, Williams *et al.* 2010). In a modified version of the process, 16S universal eubacterial primers 27F-mod (5` - AGR GTT TGA TCM TGG CTC AG -3`) and 530R (5` - CCG CNG CNG CTG GCA C -3`) were used to amplify a ~500 bp region of the 16s rRNA gene. HotStarTaq Plus Master Mix Kit (Qiagen, Valencia, CA, USA) was used with a single-step 30 cycle PCR, under the following conditions: 94°C for 3 minutes, followed by 28 cycles of 94°C for 30 seconds, 53°C for 40 seconds and 72°C for 1 minute, and a final elongation step at 72°C for 5 minutes. Following PCR, all amplicon products from different samples were mixed in equal concentrations and purified using Agencourt Ampure beads (Agencourt Bioscience Corporation, MA, USA). Finally, samples were sequenced using Roche 454 FLX titanium instruments and reagents, following the manufacturer's guidelines.

The sequence data were processed using a proprietary analysis pipeline (MR DNA, Shallowater, TX, USA). Sequences were trimmed of barcodes and primers, and three types of sequences were removed: sequences shorter than 200 base pairs, sequences with ambiguous base calls and sequences with homopolymer runs exceeding 6 base pairs. Sequences were then denoised and chimeras were removed. Operational taxonomic units (OTUs) were defined after the removal of singleton sequences, clustering at 3% divergence or 97% similarity (Dowd *et al.* 2008a, Dowd *et al.* 2008b, Edgar 2010, Capone *et al.* 2011, Eren *et al.* 2011, Swanson *et al.* 2011). The final OTUs were taxonomically classified using BLASTn against a curated database derived from GreenGenes, RDPII and NCBI and compiled into each taxonomic level.

Species richness was calculated for each plot and sample date, as the number of species identified. Species diversity was also calculated using Simpson's index of diversity (Simpson 1949). The relative abundance of each identified bacterial phylum was calculated for each plot and sample date. Additionally, the relative abundance of each proteobacteria class was calculated for each plot and sample date. Species richness and diversity results, as well as relative abundance, were averaged and assessed for statistically significant effects of time using a single-factor ANOVA test.

Table 4.1: Comparison of the effects of sugar and yeast extract solutions (10% w/v) on the respiration rate of fresh soil, based on respiration rates measured 24 hours after the addition of the solution. Values represent mean \pm standard error, n=3.

Treatment	Respiration rate (nmol CO ₂ g ⁻¹ min ⁻¹)
Control	3.7 \pm 0.5
Substrate-induced: sugar	34.4 \pm 1.8
Substrate-induced: yeast extract	156.3 \pm 15.9

Table 4.2: Comparison of the effects of substrate addition on the respiration rate of autoclaved and fresh soil. Values represent mean \pm standard error, n=2.

Soil type	Treatment	Respiration rate (nmol CO ₂ g ⁻¹ min ⁻¹)
Autoclaved	Control	2.3 \pm 0.0
	Substrate-induced	2.7 \pm 0.5
Fresh	Control	4.0 \pm 0.5
	Substrate-induced	199.7 \pm 75.4

4.3 Results

4.3.1 Environmental conditions

The daily average soil temperature at a depth of 5 cm showed significant temporal changes during the growing season (Single-factor ANOVA: $F=212.7$, $df=35$, $p<0.001$; Figure 4.6a). Temperatures increased through May and June from about 12°C to about 21°C. The soil temperature then remained high from July to mid-September at around 20°C. It then declined through September and October down to approximately 6°C. Soil temperature at a depth of 10 cm showed an almost identical season pattern, and had a correlation with soil temperature at 5 cm of $r=0.997$ (data not shown). The daily average soil water content also showed significant seasonal variation (Single-factor ANOVA: $F=25.0$, $df=34$, $p<0.001$; Figure 4.6b). Soil moisture generally declined through the summer from a high of 0.35 m³ m⁻³ in May down to a low of 0.18 m³ m⁻³ in mid-September, with some minor increases due to occasional precipitation input. Additionally, there was dramatic increase back up to 0.34 m³ m⁻³ in September due to a very large influx of precipitation on day 270. In general, precipitation decreased over the season, with the exception of a high input in late September (Figure 4.6c). Total precipitation from May to October was 346 mm.

4.3.2 Carbon dioxide flux

All aspects of ecosystem carbon dioxide flux showed significant seasonal variation. Gross ecosystem productivity (GEP) rose relatively steadily through May and June from a low of 1 g C m⁻² d⁻¹, peaked at the beginning of July at a high of 8.6 g C m⁻² d⁻¹, and then declined for the remainder of the season back

down to a low of $0.2 \text{ g C m}^{-2} \text{ d}^{-1}$ in October (Single-factor ANOVA: $F=53.3$, $df=32$, $p<0.001$; Figure 4.7a). Total ecosystem respiration (TER) also rose through May and June from a low of $2.1 \text{ g C m}^{-2} \text{ d}^{-1}$, but remained high through July between $5.4 \text{ g C m}^{-2} \text{ d}^{-1}$ and $7.9 \text{ g C m}^{-2} \text{ d}^{-1}$, before dropping off quickly in mid-August and reaching a low of $1.3 \text{ g C m}^{-2} \text{ d}^{-1}$ in October (Single-factor ANOVA: $F=65.9$, $df=32$, $p<0.001$; Figure 4.7b).

Manual field measurements of soil respiration also showed significant variation over the course of the growing season (Single-factor ANOVA: $F=24.3$, $df=14$, $p<0.001$; Figure 4.8). It increased from $3.7 \mu\text{mol CO}_2 \text{ m}^{-2} \text{ s}^{-1}$ in May to $15.6 \mu\text{mol CO}_2 \text{ m}^{-2} \text{ s}^{-1}$ by late June. It then declined slightly to $12.1 \mu\text{mol CO}_2 \text{ m}^{-2} \text{ s}^{-1}$ by mid-July before showing a dramatic increase at the beginning of August, reaching $33.5 \mu\text{mol CO}_2 \text{ m}^{-2} \text{ s}^{-1}$. Finally, it declined sharply to $6.4 \mu\text{mol CO}_2 \text{ m}^{-2} \text{ s}^{-1}$ by mid-August, and then declined slowly for the remainder of the season, reaching $1.8 \mu\text{mol CO}_2 \text{ m}^{-2} \text{ s}^{-1}$ at the beginning of October.

There were two distinct components to the seasonal pattern of soil respiration: the overall curve, increasing in the early season and decreasing in the late season, as well as the spike occurring in mid-August, between day 212 and 221 (Figure 4.8). When looking for correlations between soil respiration and other measured values, the correlations were tested with and without the three measurements during the spike. When the high values in mid-August were included, there was a moderate positive correlation with soil temperature ($r=0.34$, $p<0.001$; Figure 4.9a) and no relationship with soil moisture ($r=0.08$,

$p > 0.1$; Figure 4.9b). The correlation between soil respiration and the product of soil temperature and moisture was stronger than either alone, but was still not very strong ($r = 0.47$, $p < 0.001$; Figure 4.9c). When the three values in mid-August were excluded, the correlation with soil temperature was slightly weaker ($r = 0.33$, $p < 0.001$; Figure 4.9a) while the correlation with soil moisture was stronger ($r = 0.36$, $p < 0.001$; Figure 4.9b). However, with the three high values excluded, soil respiration and the product of soil moisture and soil temperature showed a very strong positive relationship ($r = 0.78$, $p < 0.001$; Figure 4.4c).

4.3.3 Substrate-induced respiration

Substrate induced respiration showed a clear and statistically significant seasonal pattern (Single-factor ANOVA: $F = 6.6$, $df = 3$, $p = 0.001$; Figure 4.10). Respiration declined by approximately 30% from early June to late August, with average values decreasing from $72 \text{ nmol CO}_2 \text{ g}^{-1} \text{ min}^{-1}$ in June down to $51 \text{ nmol CO}_2 \text{ g}^{-1} \text{ min}^{-1}$ in August. There was a strong negative correlation between SIR and soil temperature at 5 cm ($r = -0.51$, $p < 0.01$; Figure 4.11a) and a strong positive correlation between substrate-induced respiration (SIR) and soil water content ($r = 0.62$, $p < 0.001$; Figure 4.11b). There was also a very strong negative correlation between soil temperature and soil water content ($r = -0.78$, $p < 0.001$; data not shown). This suggests that the negative correlation between SIR and soil temperature is a function of the relationship between soil temperature and soil moisture, because at these moderate temperatures respiration rates should increase with temperature (Figure 4.2). There was no significant correlation between SIR and gross ecosystem productivity ($r = 0.25$, $p > 0.1$; Figure 4.11c) and

no significant correlation between SIR and total ecosystem respiration ($r=0.33$, $p>0.1$; Figure 4.11d).

4.3.4 Soil enzyme activity

NAGase activity at 10°C showed a very clear seasonal trend as it began at approximately 106 nmol g⁻¹ h⁻¹ in June and dropped down to only about 58 nmol g⁻¹ h⁻¹ by late August (Single-factor ANOVA: $F=12.7$, $df=3$, $p<0.001$; Figure 4.12a). NAGase activity at 23°C followed the same seasonal pattern, but with higher activity levels of 246 nmol g⁻¹ h⁻¹ in June and 123 nmol g⁻¹ h⁻¹ in August (Single-factor ANOVA: $F=10.0$, $df=3$, $p<0.001$; Figure 4.12b). The approximate doubling of enzyme activity with a 13°C temperature difference corresponded to a calculated temperature sensitivity coefficient (Q_{10}) between 1.6 and 1.9, which remained relatively consistent through the season (Figure 4.12c). However, while the temperature sensitivity coefficient did not vary much, the slight decline over the course of the season was statistically significant (Single-factor ANOVA: $F=6.6$, $df=3$, $p=0.001$). NAGase activity at 10°C showed a moderate negative correlation with soil temperature ($r=-0.39$, $p<0.05$ Figure 4.13a) and a strong positive correlation soil moisture ($r=0.61$, $p<0.01$; Figure 4.13b). NAGase activity at 10°C was also strongly positively correlated to substrate-induced respiration ($r=0.77$, $p<0.01$; Figure 4.13e). NAGase activity at 10°C showed no significant correlation with GEP ($r=0.35$, $p>0.05$; Figure 4.13c) and a strong positive relationship with TER ($r=0.42$, $p<0.05$; Figure 4.13d). Correlations between NAGase activity at 23°C and soil temperature ($r=-0.47$, $p<0.01$), soil moisture ($r=0.61$, $p<0.001$), SIR ($r=0.74$, $p<0.001$), GEP ($r=-0.24$, $p>0.1$) and

TER ($r=0.30$, $p>0.1$) are all similar to those of NAGase activity at 10°C (data not shown).

Phenol oxidase activity showed more variability between replicate plots than NAGase activity, making seasonal patterns more difficult to discern. Activity at both 10°C and 23°C showed a peak in late July, at approximately 377 nmol g⁻¹ h⁻¹ and 1056 nmol g⁻¹ h⁻¹, respectively (Figure 4.12d,e). The activity at 23°C showed a significant seasonal pattern (Single-factor ANOVA: $F=4.2$, $df=3$, $p=0.01$), while activity at 10°C did not show a statistically significant pattern (Single-factor ANOVA: $F=2.4$, $df=3$, $p=0.09$). The calculated temperature sensitivity coefficient (Q_{10}) was higher for phenol oxidase than NAGase, ranging on average from 1.9 early in the season to 2.3 later in the season, although there was no statistically significant seasonal pattern (Single-factor ANOVA: $F=1.7$, $df=3$, $p=0.2$; Figure 4.12f). Phenol oxidase activity at 10°C showed no significant correlation to soil temperature ($r=-0.15$, $p>0.1$; Figure 4.14a) and a moderate positive correlation with soil moisture ($r=0.34$, $p<0.05$; Figure 4.14b). Phenol oxidase activity at 10°C was also moderately positively correlated to substrate-induced respiration ($r=0.39$, $p<0.05$; Figure 4.14e). Additionally, phenol oxidase activity at 10°C showed no significant correlation with GEP ($r=0.34$, $p>0.05$; Figure 4.14c) or with TER ($r=0.20$, $p>0.1$; Figure 4.14d). Correlations between phenol oxidase activity at 23°C and soil temperature ($r=0.19$, $p>0.1$), soil moisture ($r=-0.06$, $p>0.5$), SIR ($r=0.20$, $p>0.1$), GEP ($r=0.09$, $p>0.5$) and TER ($r=0.39$, $p>0.05$) were all similar to those of phenol oxidase activity at 10°C (data not shown).

When enzyme activity was modeled based on measured activity at 10°C (R_{10}), the calculated temperature sensitivity coefficient (Q_{10}) and soil temperature at 10 cm, the two enzymes showed different seasonal trends. Modeled NAGase activity showed a general downward trend through the summer, as would be expected based on the pattern of the measured activity (Figure 4.15a). The modeled NAGase activity showed a strong positive correlation with both GEP ($r=0.57$, $p<0.001$; Figure 4.16a) and TER ($r=0.58$, $p<0.001$; Figure 4.16b). Modeled phenol oxidase activity showed a peak at the end of July, also similar to the pattern of measured activity (Figure 4.15b). The modeled phenol oxidase activity showed no significant relationship with GEP ($r=0.18$, $p<0.1$; Figure 4.17a) and a strong positive correlation with TER ($r=0.46$, $p<0.001$; Figure 4.17b). However, the similarity in the seasonal patterns of GEP and the modeled phenol oxidase activity suggested a possible relationship. The correlation between modeled phenol oxidase activity and GEP was calculated for a range of different lag-times (eg. phenol oxidase activity with GEP from the same day (0-day lag), phenol oxidase activity with GEP from 1 day earlier (1-day lag), etc.). The strongest correlation occurred at a 23-day lag ($r=0.74$, $p<0.001$; Figure 4.18b), although the correlations from an 18-day lag to a 26-day lag were not significantly different, based on the standard error of the correlation coefficient (Figure 4.18a). The seasonal patterns of modeled phenol oxidase activity and GEP were very similar when modeled phenol oxidase activity was plotted at a 23-day lag (Figure 4.18c).

4.3.5 Soil bacterial community composition

The number of species identified (species richness) ranged from approximately 270 to 360, but there was no significant variation due to sampling date (Single-factor ANOVA: $F=0.9$, $df=3$, $p=0.5$; Figure 4.19a). Similarly, species diversity (measured as the Simpson's index of diversity) ranged from 0.97 to 0.985 and showed no significant variation associated with sampling time (Single-factor ANOVA: $F=2.8$, $df=3$, $p=0.06$; Figure 4.19b).

The primary component of the soil bacterial community was the *Proteobacteria* phylum, making up between 35 and 47% of the total identified sequences (Figure 4.20). The *Proteobacteria* abundance showed no significant variation over time (Single-factor ANOVA: $F=2.6$, $df=3$, $p=0.07$). The remainder of the community consisted primarily of 8 major phyla: *Bacteroidetes*, *Actinobacteria*, *Firmicutes*, *Acidobacteria*, *Chloroflexi*, *Gemmatimonadetes*, *Verrucomicrobia* and *Planctomycetes*. These, together with *Proteobacteria*, composed 98-99% of the total microbial community (Figure 4.20). The last 1-2% consisted of members of several phyla (*Nitrospirae*, *Fibrobacteres*, *Armatimonadetes*, *Cyanobacteria*, *Thermodesulfobacteria*, *Lentisphaerae*, *Spirochaetes*, *Synergistetes*, and *Tenericutes*) which were found in very small numbers in some samples, as well as some species which could not be identified or classified (data not shown).

Three phyla showed significant increases in abundance over time, four phyla showed significant decreases over the summer, and one phyla had no

significant seasonal pattern (Figure 4.21). *Bacteroidetes* abundance dropped from approximately 25% to 12% over the summer (Single-factor ANOVA: $F=15.4$, $df=3$, $p<0.001$). *Acidobacteria* abundance decreased from about 7% to 4% (Single-factor ANOVA: $F=6.5$, $df=3$, $p=0.001$). *Gemmatimonadetes* abundance decreased from approximately 3.5% to 2.25% (Single-factor ANOVA: $F=4.8$, $df=3$, $p=0.007$). *Verrucomicrobia* abundance dropped from 3.3% to 2.1% (Single-factor ANOVA: $F=6.9$, $df=3$, $p=0.001$). *Actinobacteria* abundance increased from approximately 11% to 23% (Single-factor ANOVA: $F=15.6$, $df=3$, $p<0.001$). *Chloroflexi* abundance rose from approximately 2.5% to 4.5% (Single-factor ANOVA: $F=12.6$, $df=3$, $p<0.001$). *Planctomycetes* abundance increased from 0.8% to 2.3% (Single-factor ANOVA: $F=18.6$, $df=3$, $p<0.001$). *Firmicutes* varied between approximately 2.5% and 4.5% (Single-factor ANOVA: $F=2.4$, $df=3$, $p=0.09$).

The four main classes within the *Proteobacteria* phylum (alpha, beta, gamma and delta) showed similar seasonal trends (Figure 4.22). *Alphaproteobacteria* abundance increased significantly from 13% to 19% (Single-factor ANOVA: $F=9.5$, $df=3$, $p<0.001$). *Betaproteobacteria* abundance decreased significantly from 10% to 7.5% (Single-factor ANOVA: $F=7.2$, $df=3$, $p<0.001$). *Gammaproteobacteria* abundance also declined significantly, from 10% to 6% (Single-factor ANOVA: $F=8.0$, $df=3$, $p<0.001$). *Deltaproteobacteria* abundance increased from 7% and 10%, but with no statistical significance (Single-factor ANOVA: $F=1.8$, $df=3$, $p=0.17$). Additionally, members of *Epsilonproteobacteria* were found in very low abundance in some samples (data not shown).

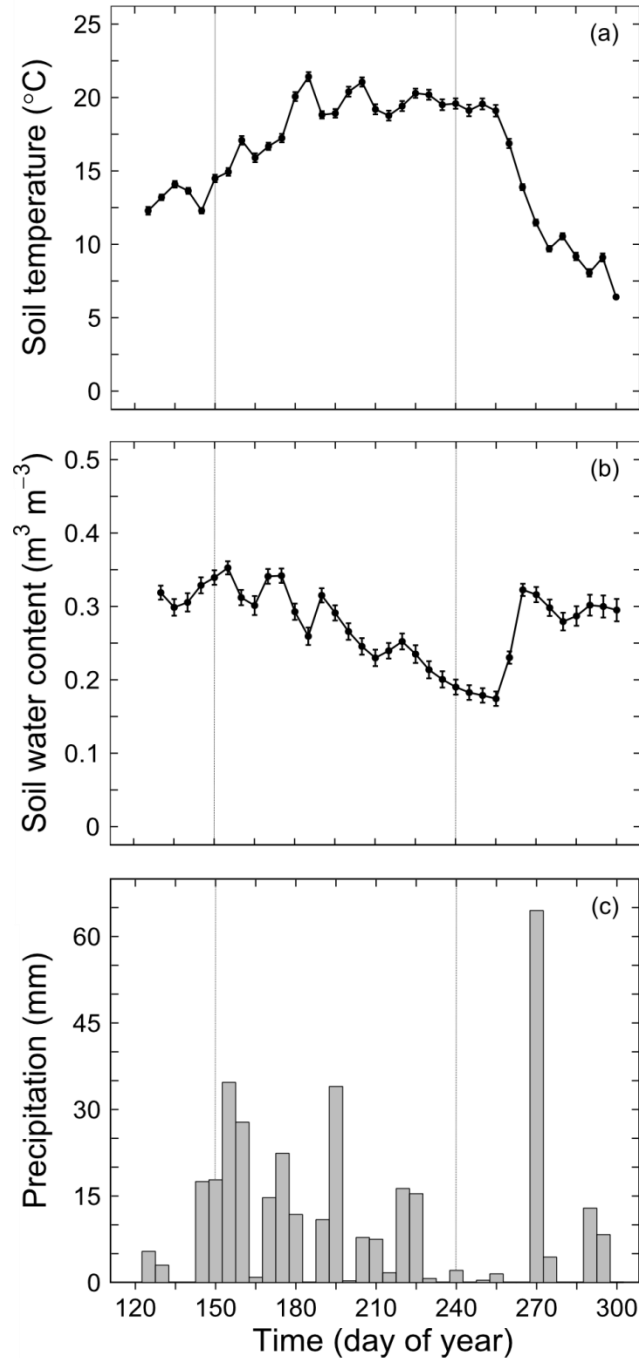


Figure 4.6: Seasonal variation in (a) daily average soil temperature at a depth of 5 cm, (b) daily average soil water content and (c) total daily precipitation at a grassland near Lethbridge, Alberta. Vertical lines mark June 1 and August 31, 2013, between which dates soil sampling was done. Values for soil temperature and water content represent 5-day averages \pm standard error, $n=9$. Statistical significance was based on single-factor ANOVA. (a) $F(35)=213$, $p<0.001$, (b) $F(34)=25$, $p<0.001$.

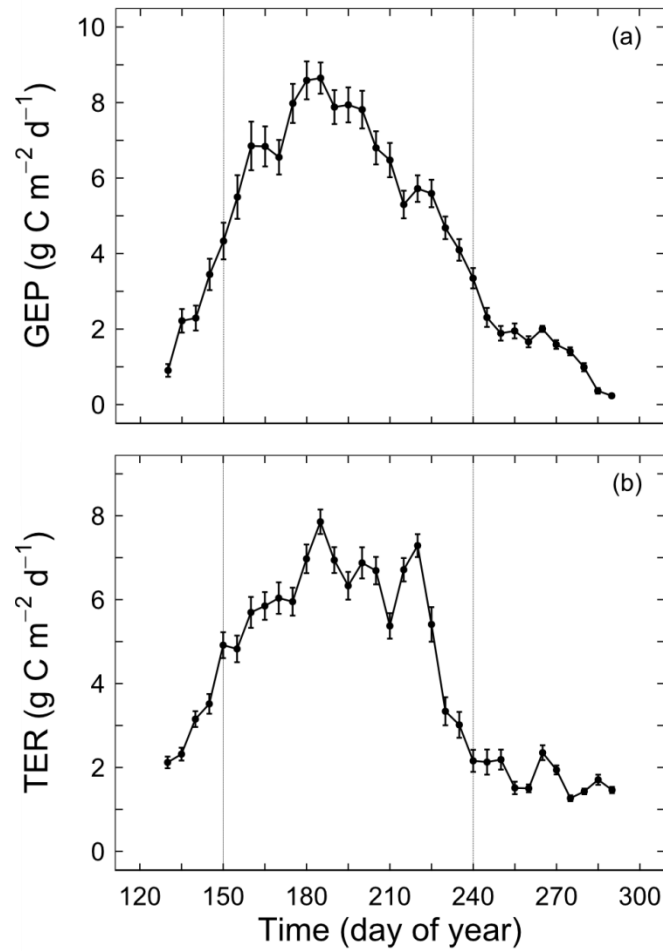


Figure 4.7: Seasonal variation in (a) gross ecosystem productivity (GEP) and (b) total ecosystem respiration (TER), calculated from half-hourly autochamber measurements. Vertical lines mark June 1 and August 31, 2013, between which dates soil sampling was done. Values represent 5-day averages \pm standard error, $n=6$. Statistical significance was based on single-factor ANOVA. (a) $F(32)=53.3$, $p<0.001$, (b) $F(32)=65.9$, $p<0.001$.

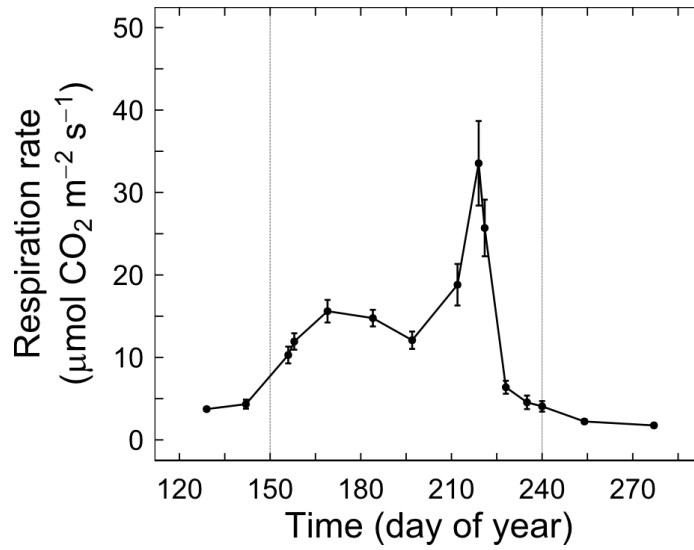


Figure 4.8: Seasonal variation in soil respiration, based on manual field measurements. Vertical lines mark June 1 and August 31, 2013, between which dates soil sampling was done. Values represent mean \pm standard error, $n=9$. Statistical significance was based on single-factor ANOVA. $F(14)=24.3$, $p<0.001$.

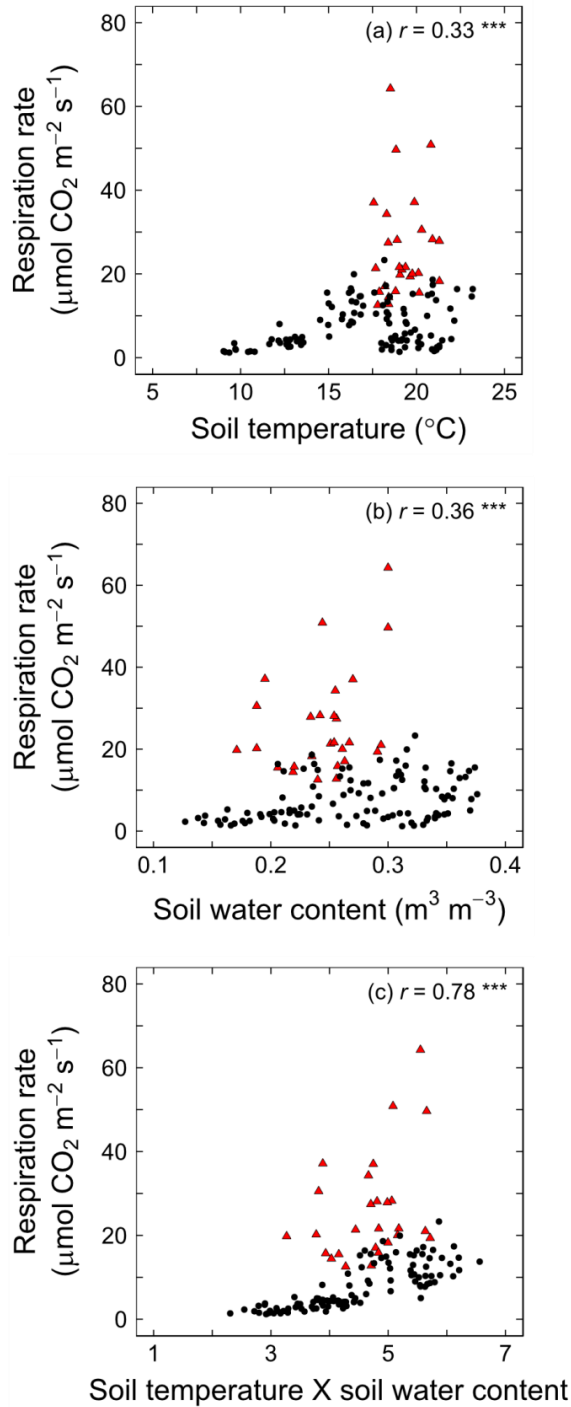


Figure 4.9: The relationship between soil respiration and (a) soil temperature at a depth of 5 cm, (b) soil water content at 0-15 cm soil depth, and (c) the product of soil temperature and water content. The red triangles represent the anomalous measurements from days 212 - 221, and were not included in the correlation calculation. Symbols after r value indicate statistical significant (NS - not significant, * - $p < 0.05$, ** - $p < 0.01$, *** - $p < 0.001$). $n=108$ when anomalous measurements are removed.

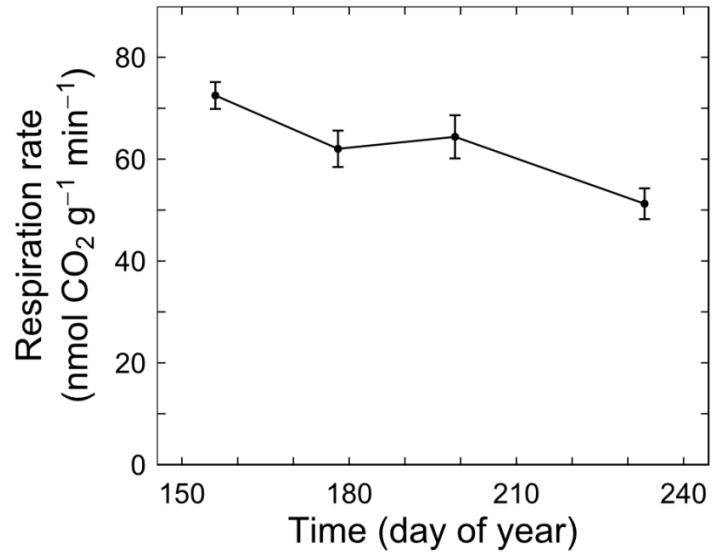


Figure 4.10: Seasonal variation in living soil microbial biomass, measured using substrate-induced respiration as a proxy. Values represent mean \pm standard error, $n=9$. Statistical significance was based on single-factor ANOVA. $F(3)=6.6$, $p=0.001$.

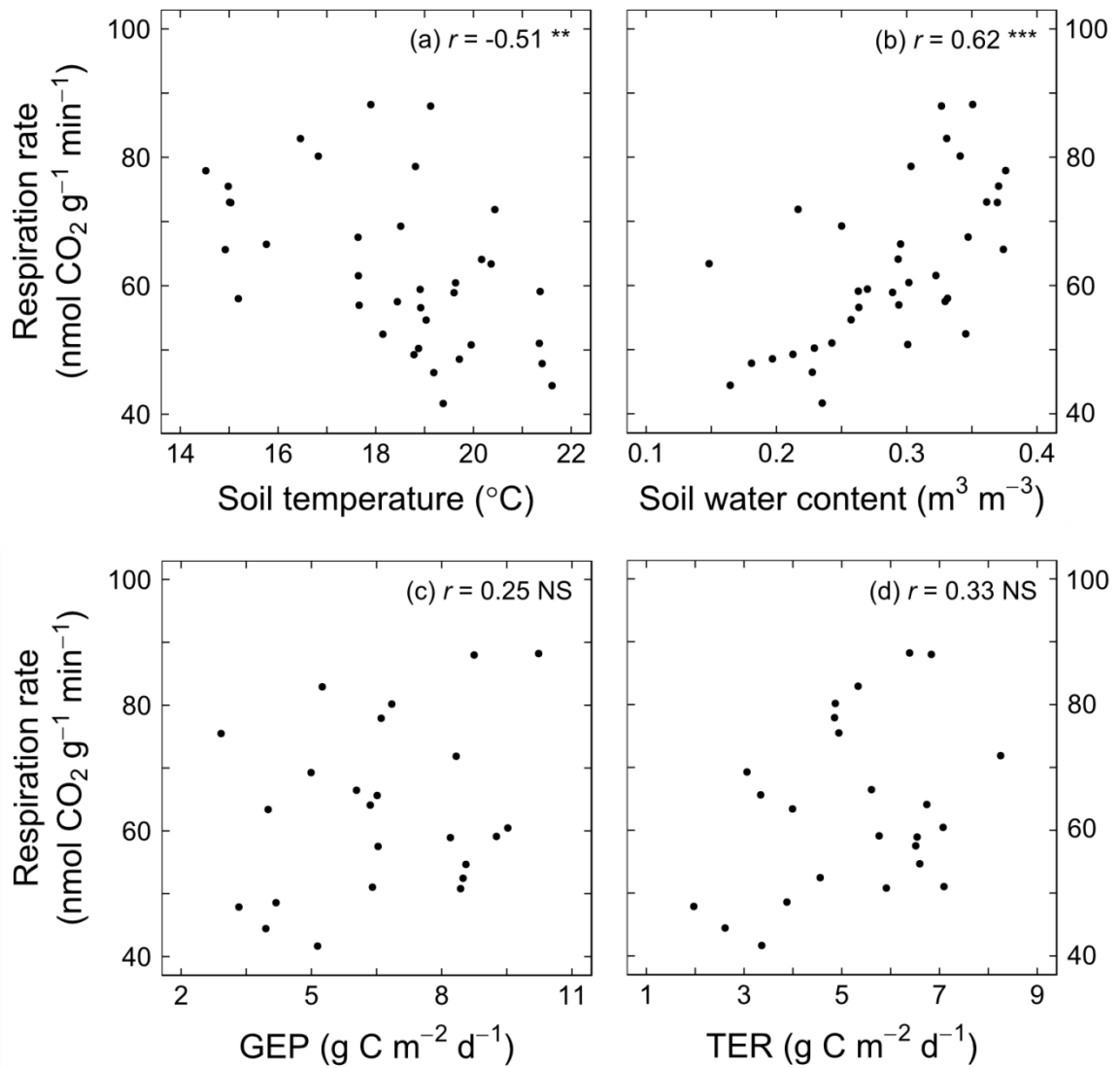


Figure 4.11: The relationship between substrate-induced respiration and (a) soil temperature at a depth of 5 cm, (b) soil water content, (c) gross ecosystem productivity, and (d) total ecosystem respiration. Symbols after r value indicate statistical significant (NS - not significant, * - $p < 0.05$, ** - $p < 0.01$, *** - $p < 0.001$). $n=36$ for (a) and (b), $n=24$ for (c) and (d).

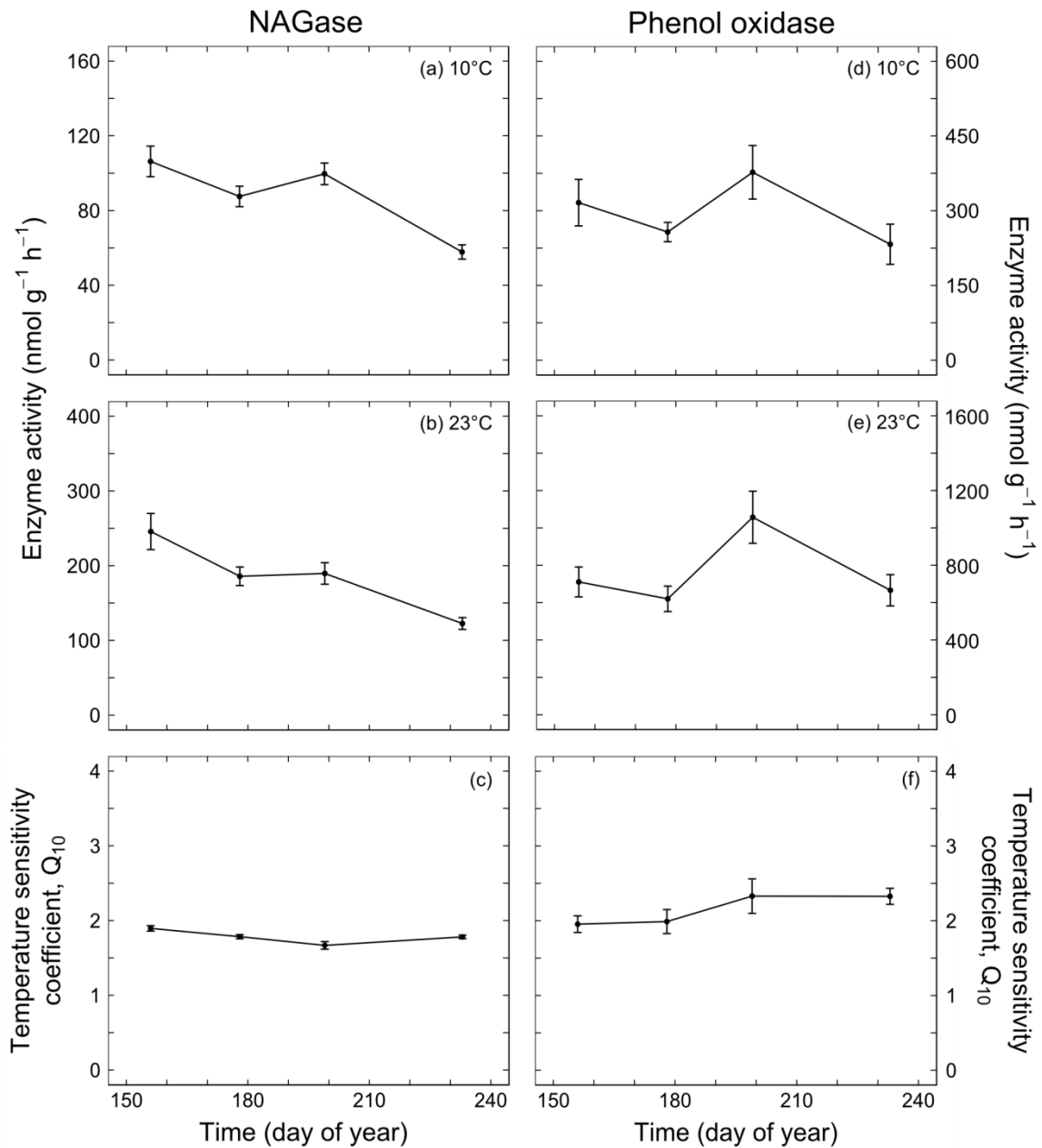


Figure 4.12: Seasonal variation in measured activity of NAGase (left) and phenol oxidase (right) at 10°C (a,d) and 23°C (b,e), and their calculated temperature sensitivity coefficients (c,f). Values represent mean \pm standard error, n=9.

Statistical significance was based on single-factor ANOVA. (a) $F(3)=12.7$, $p<0.001$, (b) $F(3)=10.0$, $p<0.001$, (c) $F(3)=6.6$, $p=0.001$, (d) $F(3)=4.2$, $p=0.01$, (e) $F(3)=2.4$, $p=0.09$, (f) $F(3)=1.7$, $p=0.2$.

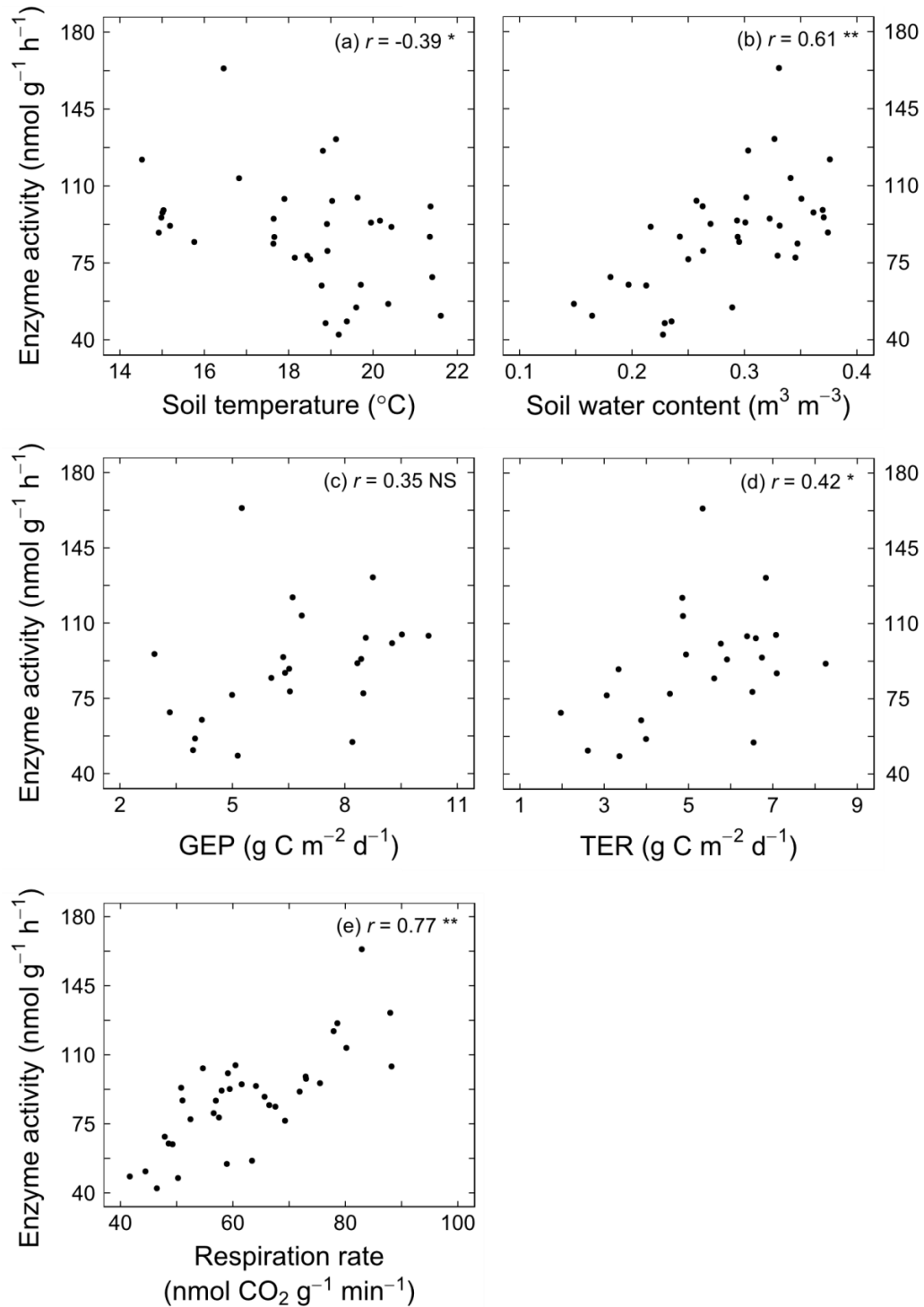


Figure 4.13: The relationship between NAGase activity at 10°C and (a) soil temperature at a depth of 5 cm, (b) soil water content, (c) gross ecosystem productivity (GEP), (d) total ecosystem respiration (TER), and (e) substrate-induced respiration (e). Symbols after r value indicate statistical significant (NS - not significant, * - $p < 0.05$, ** - $p < 0.01$, *** - $p < 0.001$). $n = 36$ for (a), (b) and (e), $n = 24$ for (c) and (d).

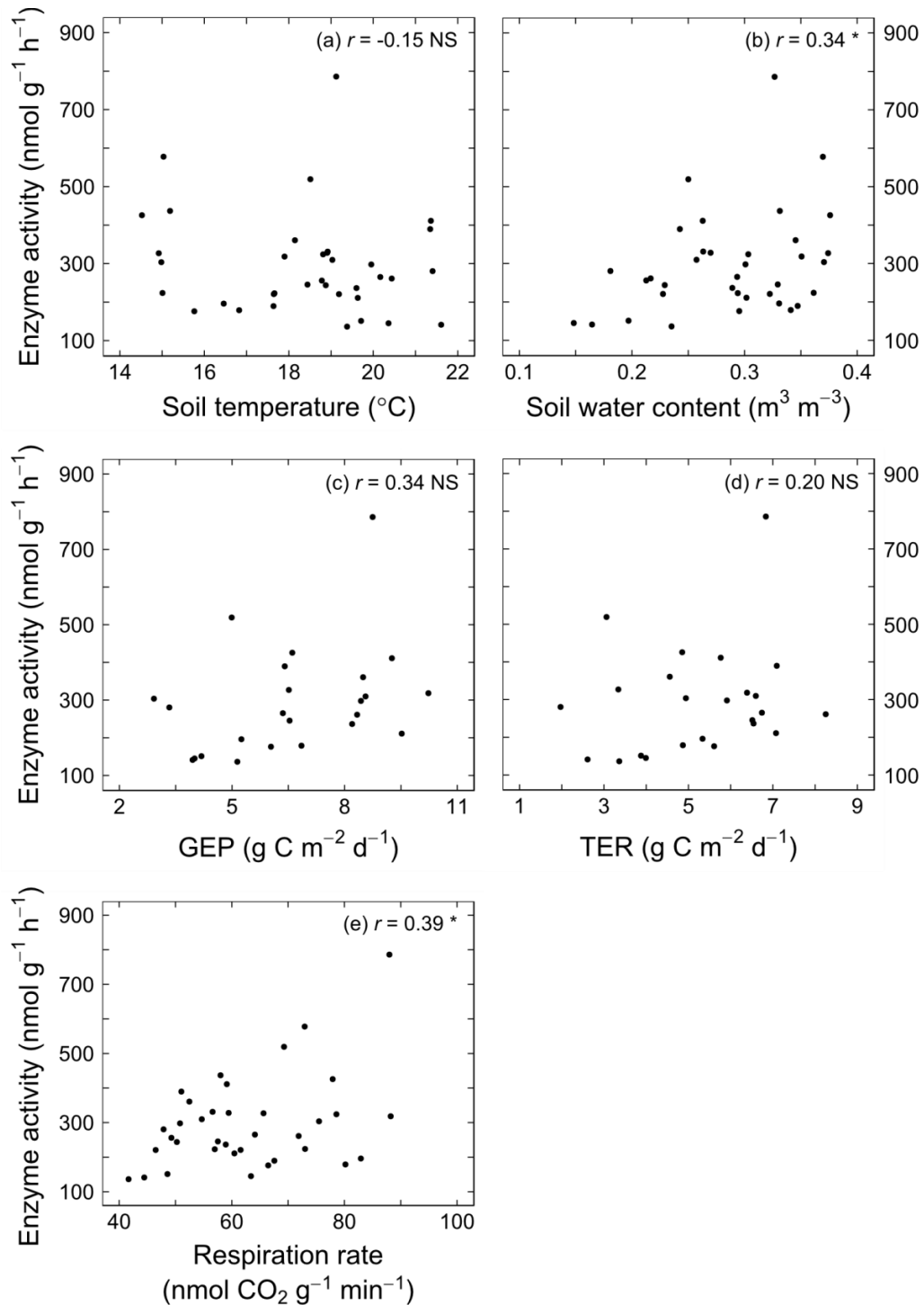


Figure 4.14: The relationship between phenol oxidase activity at 10°C and (a) soil temperature at a depth of 5 cm, (b) soil water content, (c) gross ecosystem productivity (GEP), (d) total ecosystem respiration (TER), and (e) substrate-induced respiration (e). Symbols after r value indicate statistical significant (NS - not significant, * - $p < 0.05$, ** - $p < 0.01$, *** - $p < 0.001$). $n = 36$ for (a), (b) and (e), $n = 24$ for (c) and (d).

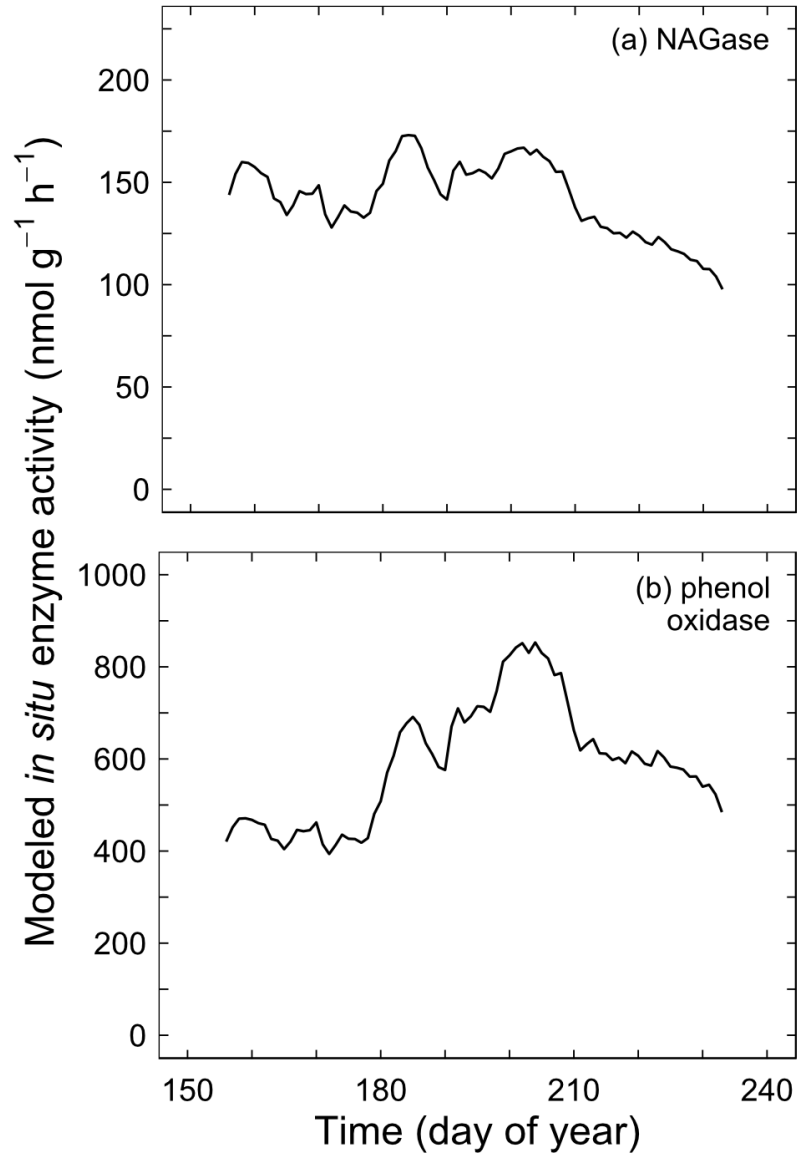


Figure 4.15: Seasonal variation of modeled *in situ* enzyme activity of (a) NAGase and (b) phenol oxidase, calculated based on activity rate at 10°C, temperature sensitivity coefficient and actual daily average soil temperature at a depth of 10 cm, as shown in Equation 4.14. Values represent the average across plots (n=9).

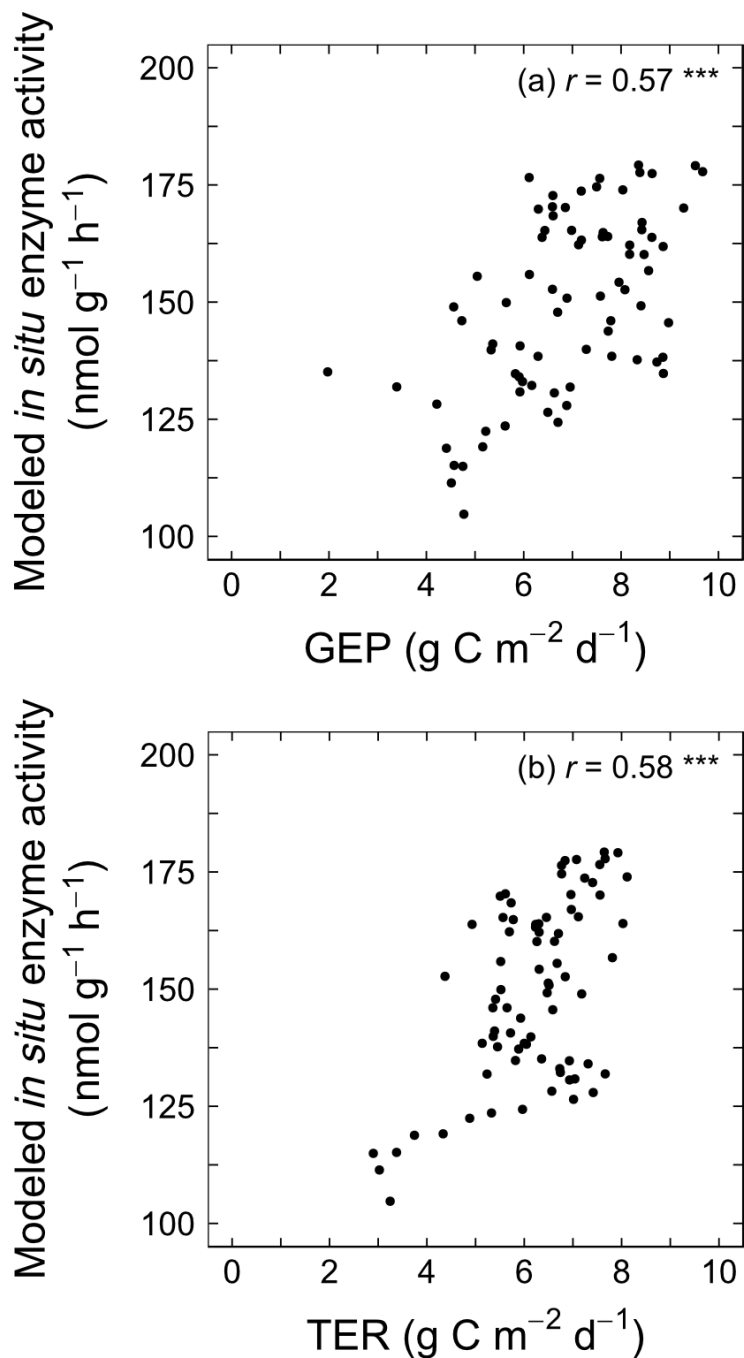


Figure 4.16: The relationship between modeled *in situ* NAGase activity and (a) gross ecosystem productivity (GEP) and (b) total ecosystem respiration (TER). Values represent the daily average, averaged across plots (n=6). Symbols after *r* value indicate statistical significant (NS - not significant, * - $p < 0.05$, ** - $p < 0.01$, *** - $p < 0.001$). n=78.

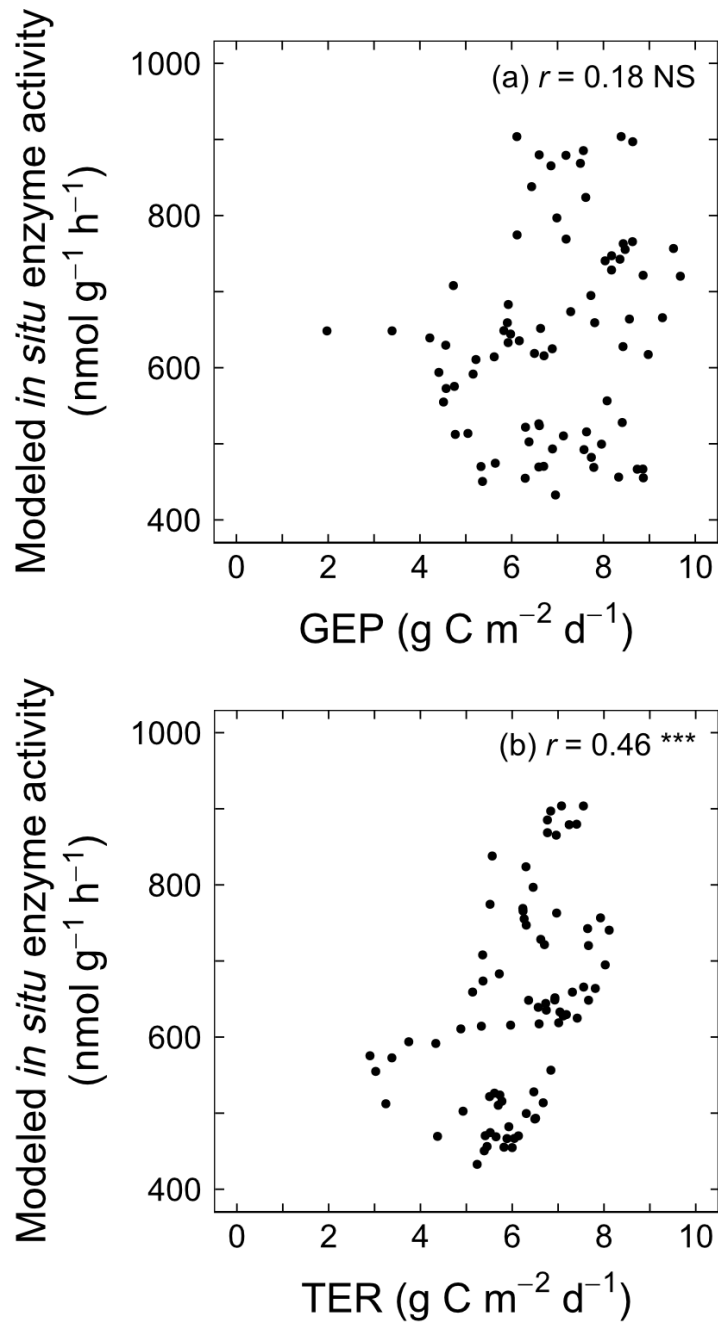


Figure 4.17: The relationship between modeled *in situ* phenol oxidase activity and (a) gross ecosystem productivity (GEP) and (b) total ecosystem respiration (TER). Values represent the daily average, averaged across plots (n=6). Symbols after r value indicate statistical significant (NS - not significant, * - $p < 0.05$, ** - $p < 0.01$, *** - $p < 0.001$). n=78.

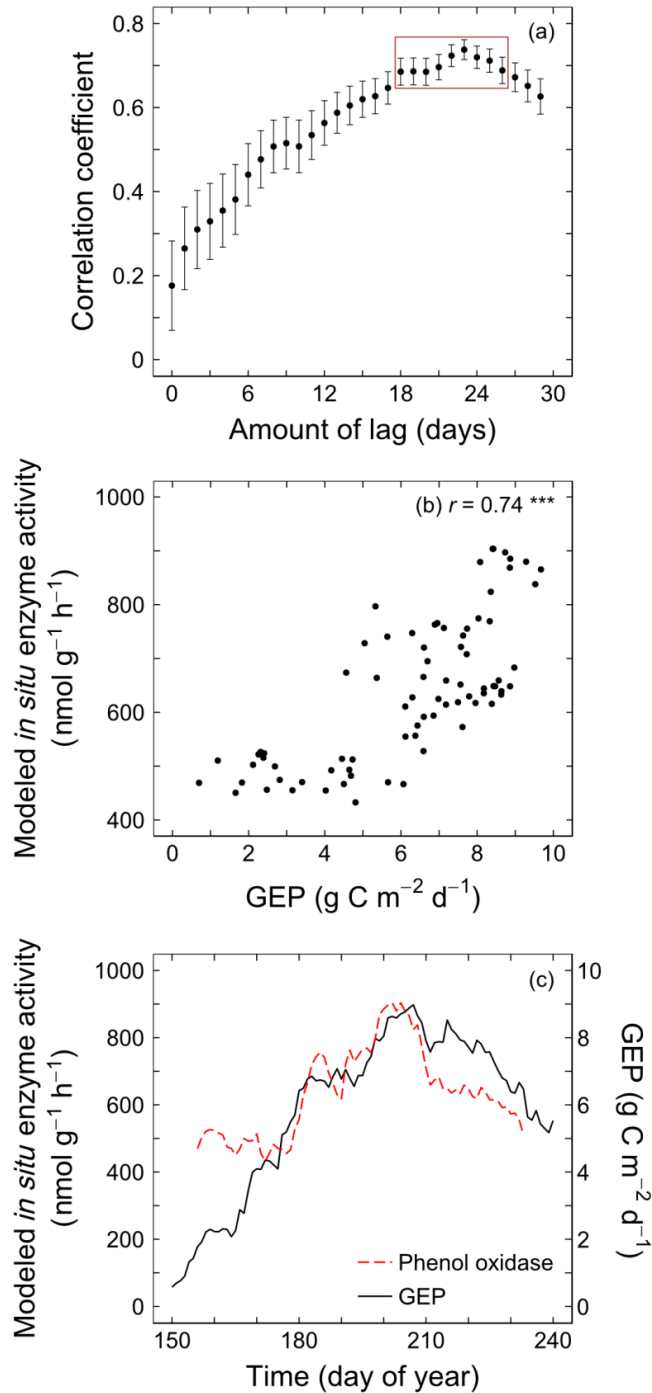


Figure 4.18: (a) Correlation coefficients between modeled *in situ* phenol oxidase activity and gross ecosystem productivity (GEP) as a function lag-time (1-day lag means phenol oxidase activity is compared to GEP from one day earlier). Boxed values are not significantly different from the peak value, based on standard error of the correlation coefficient. (b) The relationship between modeled *in situ* phenol oxidase activity and mean GEP, using 23-day lag, $n=78$. (c) Seasonal variation in modeled *in situ* phenol oxidase activity and GEP, where DOY for GEP = DOY + 23, to account for lag.

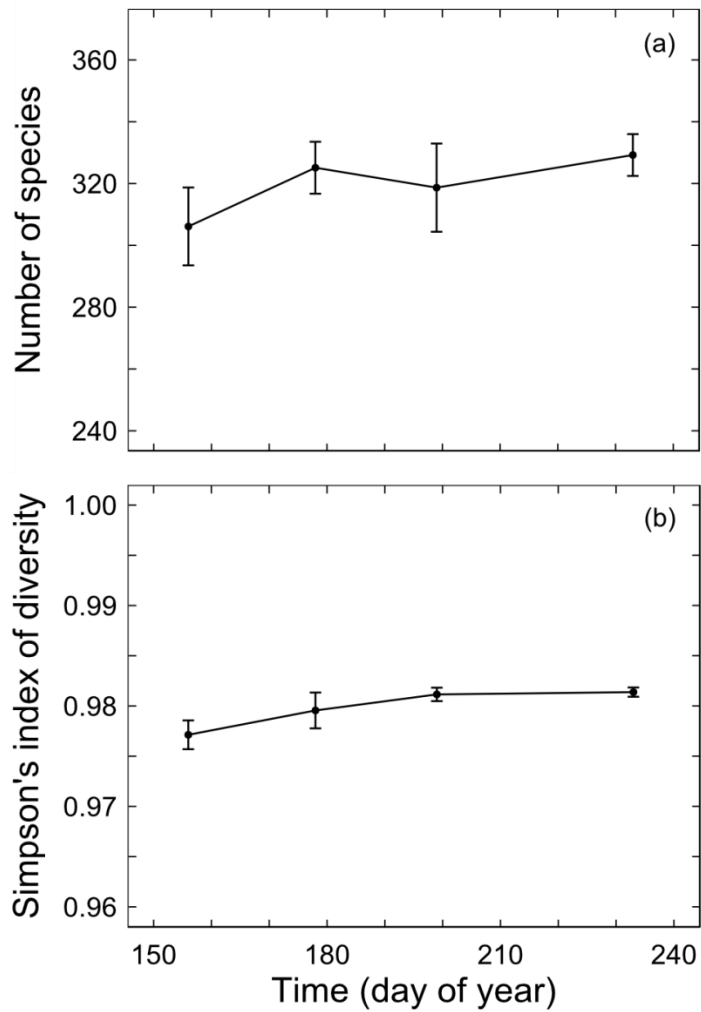


Figure 4.19: Seasonal variation in (a) species richness and (b) species diversity of the soil bacterial community. Values represent mean \pm standard error, $n=9$. Statistical significance was based on single-factor ANOVA. (a) $F(3)=0.9$, $p=0.5$, (b) $F(3)=2.8$, $p=0.06$.

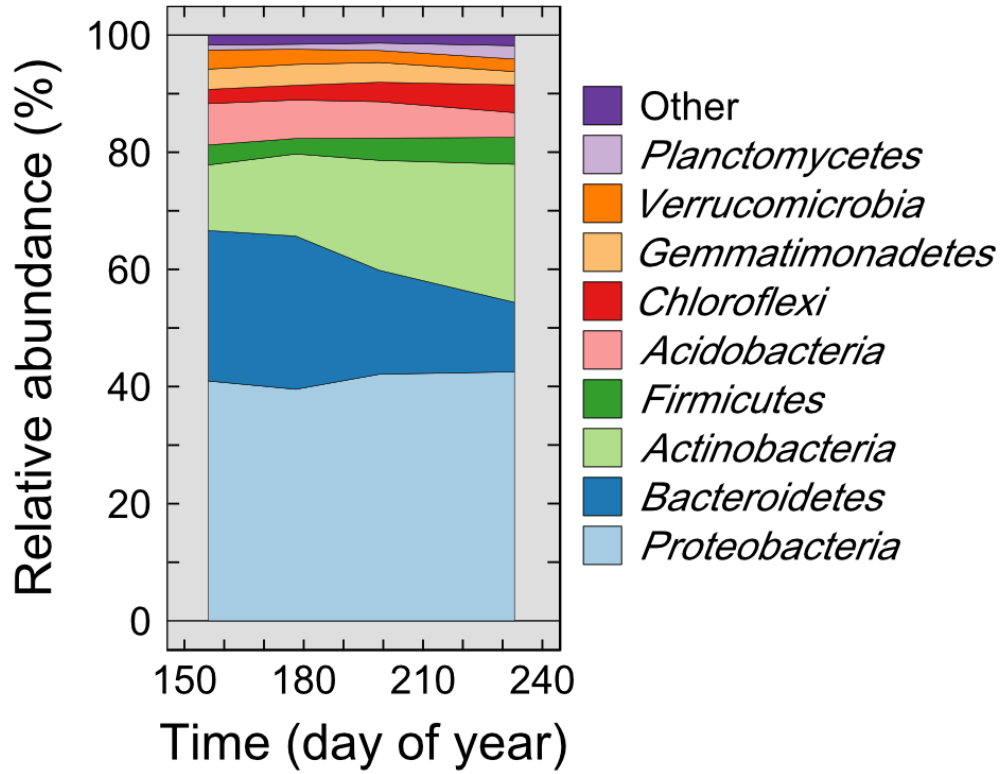


Figure 4.20: Seasonal variation in the relative abundance of the major bacterial phyla. Values represent the mean (n=9).

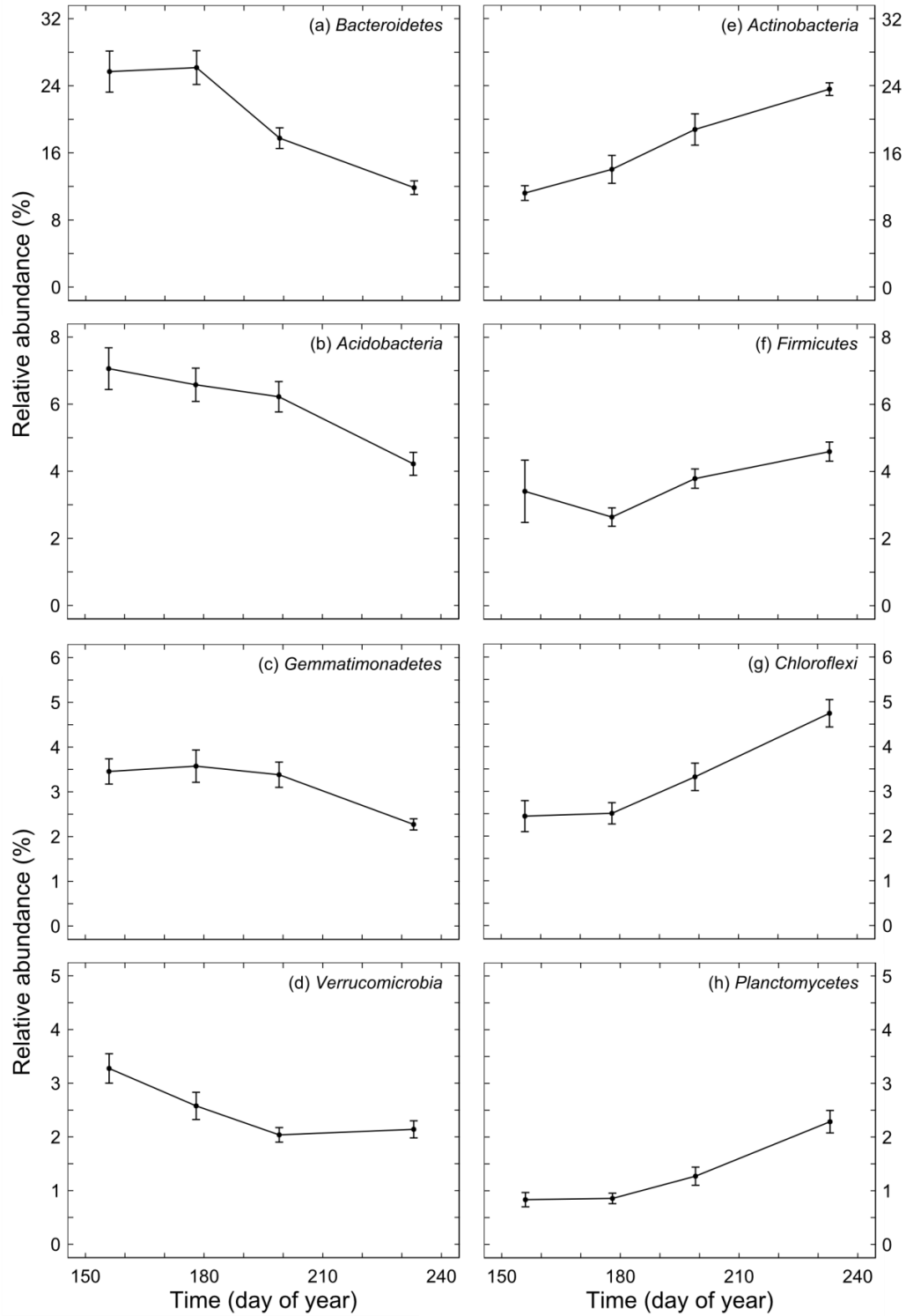


Figure 4.21: Seasonal variation in the relative abundance of 8 major bacterial phyla. Values represent mean \pm standard error (n=9). Statistical significance was based on single-factor ANOVA. (a) $F(3)=15.4$, $p<0.001$, (b) $F(3)=6.5$, $p=0.001$, (c) $F(3)=4.8$, $p=0.007$, (d) $F(3)=6.9$, $p=0.001$, (e) $F(3)=15.6$, $p<0.001$, (f) $F(3)=2.4$, $p=0.09$, (g) $F(3)=12.6$, $p<0.001$, (h) $F(3)=18.6$, $p<0.001$.

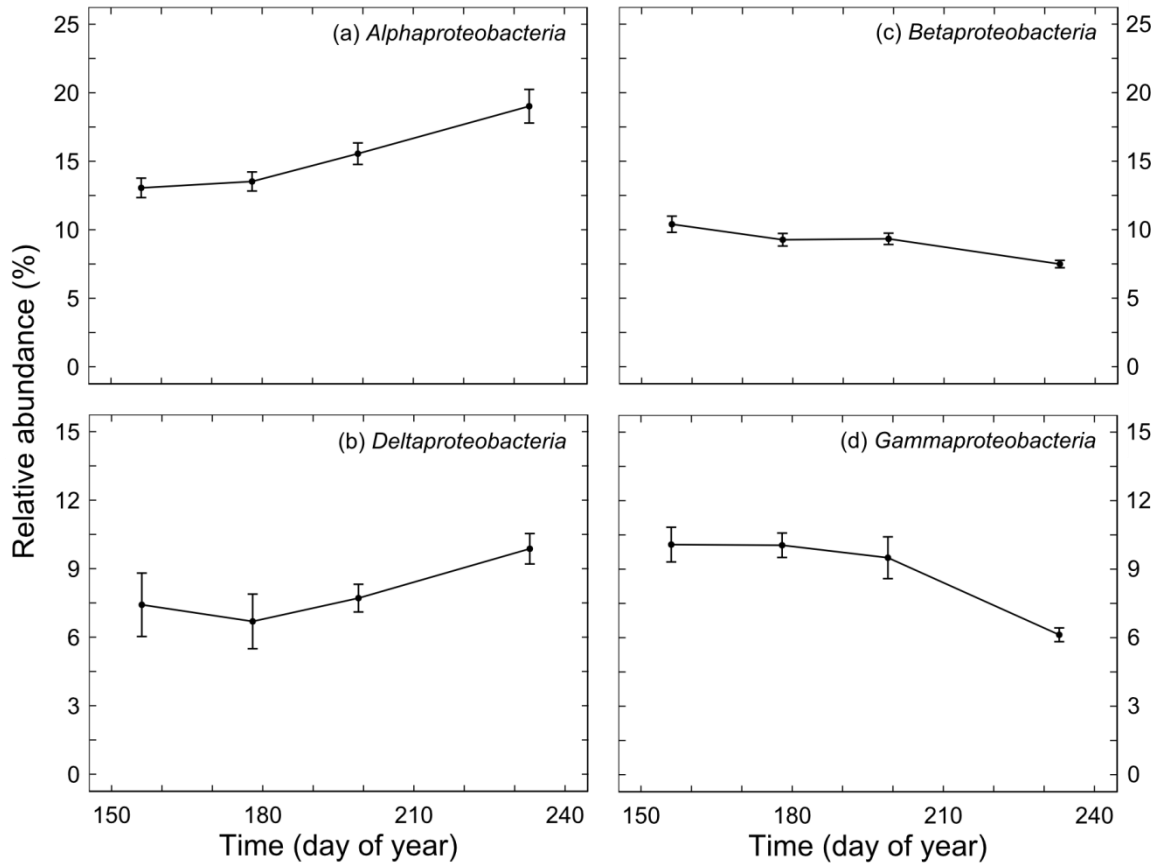


Figure 4.22: Seasonal variation in the relative abundance of the four major *Proteobacteria* classes. Values represent mean \pm standard error (n=9). Statistical significance was based on single-factor ANOVA. (a) $F(3)=9.5$, $p<0.001$, (b) $F(3)=1.9$, $p=0.17$, (c) $F(3)=7.2$, $p<0.001$, (d) $F(3)=8.0$, $p<0.001$.

4.4 Discussion

The purpose of this study was to investigate the direct effects of seasonal variations in soil temperature and soil moisture on soil respiration, as well as the indirect effects of microbial biomass, bacterial species community composition, extracellular enzyme activity, and substrate availability. Conceptually, it is understood that soil respiration is directly affected by both soil temperature and soil moisture (Equation 4.1; Figure 4.2). However, there are also a variety of ways that soil temperature and water availability can indirectly influence soil respiration. Variations in the soil's respiratory capacity (R_{10}) will affect the total rate of soil respiration (Equation 4.1). Respiratory capacity is influenced by root and microbial biomass, as well as substrate availability. Therefore, any seasonal variations within the ecosystem that influence biomass or substrate availability will impact soil respiratory capacity, representing indirect effects on soil respiration. This study examined soil microbial biomass, extracellular enzyme activity within the soil, and the species community composition of the soil bacterial community, looking for correlations with soil temperature and soil moisture, which could represent indirect effects on soil respiration rates.

4.4.1 Soil respiration

Over the course of the growing season, soil temperature and soil moisture showed significant variation (Figure 4.6a,b). It is expected that the seasonal variations in soil temperature and soil moisture will drive the seasonal pattern of soil respiration, either directly or indirectly. Studies have shown that over the course of a season, the combination of temperature and soil moisture explain

most of the variation in soil respiration (Carbone *et al.* 2008). Consistent with these results, my study showed a very strong correlation between soil respiration and the product of soil temperature and water content (Figure 4.9c).

There was one aspect of the seasonal pattern of soil respiration that cannot be explained by the relationship with soil temperature and soil moisture: the 3- to 4-fold increase in soil respiration rates in August (Figure 4.8). The timing of the increase was consistent with the timing of a late increase in gross ecosystem productivity and total ecosystem respiration on day 220 (Figure 4.7), which may have been due to precipitation input (Figure 4.6c). However, the magnitude of the increases in soil respiration was not consistent with that of total ecosystem respiration measured by either the autochambers (Figure 4.7b) or eddy covariance (Flanagan *et al.* 2014). Soil collars used to measure soil respiration have been shown to overestimate respiration rates under certain situations, such as pressure imbalances, and these effects can be amplified in dry, porous soil (Davidson *et al.* 2002, Pumpanen *et al.* 2004). Sudden and short lived increases in soil respiration have been observed at this field site in previous years, although they have generally been spatially and temporally inconsistent (L.B. Flanagan, personal communication, October 2014). In this study, a variety of factors may have interacted to produce consistent but anomalous data that was not part of the overall seasonal pattern, and while the timing of the increase may have been real, the magnitude was inconsistent with all other data and should not be considered significant.

Therefore, it was the overall seasonal pattern and its correlation to soil temperature and soil moisture that were analysed for this study. However, correlations do not determine the cause of the relationship, nor if the relationship represents direct or indirect effects of soil temperature and soil moisture. The possible indirect effects include changes in root biomass, soil microbial biomass and substrate availability. Substrate availability may be affected by plant activity, extracellular enzyme activity in the soil, and the species composition of the soil microbial community.

4.4.2 Substrate-induced respiration

Soil microbial biomass is controlled by a variety of factors, including soil moisture, temperature, nutrient availability, soil pH, and plant activity (Wardle 1992). Therefore, as many of these factors vary throughout the growing season, microbial biomass can also be expected to show seasonal patterns. For example, in a Mediterranean grassland in California, microbial respiration was at its highest in the wet, winter months and at its lowest in the dry summer months, and soil water content explained a significant portion of the variability (Waldrop and Firestone 2006). Similarly, Liu *et al.* (2009) showed that microbial biomass and respiration in a temperate steppe ecosystem were reduced by warming when water was limiting, but that increases in precipitation increase biomass and respiration. My measurements of soil microbial biomass by substrate-induced respiration showed a similar correlation with soil moisture (Figure 4.11b).

Biomass affects the respiratory capacity (R_{10}) of the soil, thereby affecting soil respiration. Biomass includes both root and microbial biomass, and both root and microbial respiration contribute to total soil respiration (Hanson *et al.* 2000, Luo and Zhou 2006). A study by Lee and Jose (2003) showed that soil respiration in a cottonwood stand was positively correlated with both fine root biomass production and soil microbial biomass. A study of a Swiss grassland showed that elevated levels of atmospheric CO₂ increased overall rates of soil respiration, but it was due to an increase in microbial biomass as opposed to an increase in the activity of individual microorganisms (Sowerby *et al.* 2000). The correlation between soil respiration and soil temperature and soil moisture may be due to the indirect effect of moisture on microbial biomass, as well as the negative correlation between soil moisture and soil temperature.

4.4.3 Soil enzyme activity

In addition to the amount of microbial biomass present in the soil, the activity of the microorganisms is important to any ecosystem, as they are the primary decomposers of organic matter and recyclers of nutrients. Of the wide variety of extracellular enzymes produced by these microorganisms, those involved in the cycling of nitrogen are particularly important, as nitrogen is often a limiting nutrient. My focus was on two such enzymes, phenol oxidase and β -1,4-*N*-acetylglucosaminidase (NAGase). The activity of these two enzymes is influenced by many factors, some shared between them and some unique to each enzyme. In general, enzyme activity increases with temperature, due to the effects of temperature on biochemical processes (Brzostek and Finzi 2012). Both

enzymes are also influenced by soil pH, with NAGase activity benefitting from low pH while phenol oxidase activity benefits from higher pH (Sinsabaugh *et al.* 2008). The activity of NAGase was primarily regulated by microclimate and soil characteristics (Boerner *et al.* 2005). Similar to NAGase activity, microbial biomass was correlated with soil temperature and moisture (Figure 4.11). Studies have shown that NAGase activity was positively correlated with total microbial biomass and total bacteria, as well as related to potential soil respiration (Waldrop and Firestone 2006, Brockett *et al.* 2012). Similarly, my results show a strong positive correlation between NAGase activity and substrate-induced respiration.

In contrast, phenol oxidase activity was controlled by the quality and availability of substrate for decomposition (Boerner *et al.* 2005). Specifically, phenol oxidase activity was influenced by lignin content in soil organic matter, the concentration of soluble phenolic compounds and nitrogen availability (Sinsabaugh 2010). As well, phenol oxidase can be increased weeks or months after a large input of carbon, where the amount of carbon added exceeds the amount of carbon in microbial biomass and nitrogen remains limited, in what is called a real priming effect (Blagodatskaya and Kuzyakov 2008). Such an input of carbon can cause increased microbial activity that requires the breakdown of SOM to fulfill nitrogen requirements and can also cause an increase in microbial biomass (Blagodatskaya and Kuzyakov 2008). Root exudates introduce a larger amount of carbon than nitrogen to the soil, which can cause this real priming effect (Klein *et al.* 1988, Mench and Martin 1991, Nardi *et al.* 2000,

Blagodatskaya and Kuzyakov 2008). The products of photosynthesis are transported belowground and metabolized within hours of initial assimilation, and exudation intensity is high when photosynthetic activity is high (Kuzyakov and Cheng 2001). Photosynthesis is tightly coupled with priming effects, which suggests that root exudates are primarily responsible for rhizosphere priming (Kuzyakov and Cheng 2001).

Several of my results are consistent with a real priming effect. Substrate-induced respiration indicated that microbial biomass increased slightly on day 199 from day 178, in contrast to the overall downward trend of substrate-induced respiration over the course of the season. This may correspond to the expected increase in microbial biomass due to a real priming effect (Blagodatskaya and Kuzyakov 2008). The lag of approximately 23 days between peak GEP (and exudation rates) and the peak in phenol oxidase activity was also consistent with the time frame described by Blagosatskaya and Kuyakov (2008). A priming effect also tends to cause an increase in soil respiration, although in my study, this increase could have been masked by the artificially high spike in soil respiration in August.

Substrate availability in the soil is one component of the soil's respiratory capacity. One study has shown that when soil temperature and soil moisture are ideal, the rate of soil respiration is limited by the amount of biologically available substrate and not the microbial biomass (Wang *et al.* 2003). Soil temperature and soil moisture can have an impact on enzyme activity directly, or via root

exudation rates and priming effects. The resulting effect of soil temperature and soil moisture on soil respiration through the soil's respiratory capacity is indirect.

4.4.4 Soil bacterial community composition

My study showed no significant change in species richness or alpha diversity over the course of the summer of 2013 (Figure 4.19). However, there was a shift in the composition of the microbial community (Figure 4.20). As well, specific bacterial phyla and classes could be seen to increase or decrease in relative abundance over the course of the summer. *Proteobacteria* was the largest component of the community, and while its abundance did not change, the abundance of its constituent classes did. Both *Alphaproteobacteria* and *Deltaproteobacteria* increased in abundance, while *Gammaproteobacteria* and *Betaproteobacteria* decreased in abundance (Figure 4.22). Similarly, the other major bacterial phyla tended to show either an increase or a decrease in abundance over the summer. Specifically, the phyla *Bacteroidetes*, *Acidobacteria*, *Gemmatimonadetes* and *Verrucomicrobia* all showed decreases in abundance while the phyla *Actinobacteria*, *Firmicutes*, *Chloroflexi* and *Planctomycetes* all showed increases in abundance (Figure 4.21).

Waldrop and Firestone (2006) studied both an oak canopy ecosystem and a grassland ecosystem and found that season had a significant effect on microbial community composition. Their study also indicated that differences in microbial community composition stemming from differences between the oak canopy and grassland ecosystem were primarily related to difference in soil moisture.

Different microorganisms are better suited to different environmental conditions, and water availability can determine which microbial community is active in the soil (Voroney 2007). For example, *Actinobacteria* are aerobes and well suited to low resource availability, and are therefore generally found in lower abundance when soils are wet (Cruz-Martinez *et al.* 2009). This fact explains the observed increase in *Actinobacteria* abundance through the summer, as soil moisture levels declined. In contrast, *Bacteroidetes*, *Betaproteobacteria*, and *Gammaproteobacteria* tend to be favoured in soils that remain moist, consistent with my data that showed these three groups declined over the summer in correlation with reduction in soil moisture (Cruz-Martinez *et al.* 2009). Xiong *et al.* (2014) showed that the abundance of *Actinobacteria* increased and *Acidobacteria* and *Bacteroidetes* decreased in abundance in response to a warming treatment in a high alpine meadow, which significantly lowered soil moisture.

An increase in the availability of organic carbon in the soil can stimulate an increase in the activity of an opportunistic subset of the soil bacterial community, thereby increasing soil respiration (Cleveland *et al.* 2007). Environmental warming can also benefit the soil fungal community through an increase in substrate quantity and a decrease in nitrogen availability, causing an increase in the soil fungal contribution to soil respiration (Zhang *et al.* 2005). Fungi generally have greater efficiency at assimilating carbon, reducing their CO₂ output by lowering their R_{10} value (Zhang *et al.* 2005). Therefore, changes in the species composition of the soil microbial community may affect soil respiration

either through a change in substrate availability or a direct change in respiratory capacity.

4.5 Conclusion

The strong positive relationship between soil respiration and the product of soil temperature and soil moisture is controlled by both the direct and indirect effects of temperature and moisture on respiration rates. The seasonal patterns of soil temperature and soil moisture are correlated with seasonal patterns of plant activity, soil microbial biomass, extracellular enzyme activity and the species composition of the soil bacterial community, which may be responsible for variations in soil respiration either through biomass abundance or substrate availability. The relationships between the different components of the soil ecosystem and their relationships with the aboveground ecosystem and the atmosphere are numerous and complex. Soil respiration is an important component of the global carbon cycle, and has the potential to increase under warming conditions, further increasing atmospheric carbon dioxide levels. It is important to understand both the direct and indirect effects of temperature and moisture on soil respiration in order to accurately predict future consequences of climate change.

CHAPTER 5. CONCLUSION

The anthropogenic increase of carbon dioxide in the atmosphere will lead to a variety of changes to the global climate system, including increases in the average global temperature, alterations to precipitation regimes, and changes in the timing and amount of water availability (Barnett *et al.* 2005, Rosenzweig *et al.* 2008). These changes in climate will cause changes in ecosystem functioning, which might then cause a feedback loop to further increase atmospheric CO₂. Scientists are working to understand how these changes will affect terrestrial ecosystems, but accurate data must be collected from field experiments to produce accurate models and predictions.

Warming experiments performed in the field allow us to observe how increased temperatures affect ecosystems in otherwise natural conditions. It is very important to choose the best warming treatment for the ecosystem and the measurements being made so that the data produced will be helpful in climate and ecosystem models. It is also important to plan for long-term warming studies, as applying a warming treatment for only one growing season may not produce any changes in the ecosystem, as was seen in this study. Since interannual variation in environmental conditions such as precipitation and water availability may be significant, long-term studies allow scientists to see the effects of warming under a variety of natural conditions. As water availability changes with global climate change, it may affect the ability of an ecosystem to acclimate to warming conditions, particularly in a semi-arid grassland like the study site. Soil temperature and soil moisture are also controlling factors of

many aspects of the soil microbial community, from active microbial biomass and enzyme activity to the species composition of the community. Any changes in climate that affect water availability and subsequently, plant activity, may cause shifts in these microbial communities and their activities. These alterations may cause shifts in the carbon intake and output of the ecosystem, shifting the balance between carbon source and carbon sink, and the ecosystem's role in the global carbon cycle.

As this project continues, and interannual variation in precipitation and temperature are seen, it may also be important to examine additional aspects of the ecosystem. It would be valuable to examine the contribution of the soil fungal community as well as different extracellular enzymes in the soil to further understand the soil microbial community's composition and activities. As well, the consideration of nitrogen or other nutrient availability and its effects on both the plant and microbial community would be worthwhile.

In conclusion, it is important to choose a warming treatment carefully based on what is being measured and to conduct long-term warming studies that consider both the direct and indirect effects of temperature and moisture on ecosystems. Well planned studies will allow better predictions about the impact of future global climate change on the biosphere.

REFERENCES

- An, Y. A., S. Q. Wan, X. H. Zhou, A. A. Subedar, L. L. Wallace, and Y. Q. Luo. 2005. Plant nitrogen concentration, use efficiency, and contents in a tallgrass prairie ecosystem under experimental warming. *Global Change Biology* **11**:1733-1744.
- Aronson, E. L., and S. G. McNulty. 2009. Appropriate experimental ecosystem warming methods by ecosystem, objective, and practicality. *Agricultural and Forest Meteorology* **149**:1791-1799.
- Aronson, E. L., and S. G. McNulty. 2010. Reply to comment on "Appropriate experimental ecosystem warming methods by ecosystem, objective, and practicality" by Aronson and McNulty. *Agricultural and Forest Meteorology* **150**:499-500.
- Atkin, O. K., and M. G. Tjoelker. 2003. Thermal acclimation and the dynamic response of plant respiration to temperature. *Trends in Plant Science* **8**:343-351.
- Badri, D. V., and J. M. Vivanco. 2009. Regulation and function of root exudates. *Plant Cell and Environment* **32**:666-681.
- Barnett, T. P., J. C. Adam, and D. P. Lettenmaier. 2005. Potential impacts of a warming climate on water availability in snow-dominated regions. *Nature* **438**:303-309.
- Bell, C. W., V. Acosta-Martinez, N. E. McIntyre, S. Cox, D. T. Tissue, and J. C. Zak. 2009. Linking microbial community structure and function to seasonal differences in soil moisture and temperature in a Chihuahuan desert grassland. *Microbial Ecology* **58**:827-842.
- Berry, J., and O. Bjorkman. 1980. Photosynthetic response and adaptation to temperature in higher-plants. *Annual Review of Plant Physiology and Plant Molecular Biology* **31**:491-543.
- Blagodatskaya, E., and Y. Kuzyakov. 2008. Mechanisms of real and apparent priming effects and their dependence on soil microbial biomass and community structure: critical review. *Biology and Fertility of Soils* **45**:115-131.
- Boerner, R. E. J., J. A. Brinkman, and A. Smith. 2005. Seasonal variations in enzyme activity and organic carbon in soil of a burned and unburned hardwood forest. *Soil Biology & Biochemistry* **37**:1419-1426.
- Boone, R. D., K. J. Nadelhoffer, J. D. Canary, and J. P. Kaye. 1998. Roots exert a strong influence on the temperature sensitivity of soil respiration. *Nature* **396**:570-572.
- Boval, M., and R. M. Dixon. 2012. The importance of grasslands for animal production and other functions: a review on management and methodological progress in the tropics. *Animal* **6**:748-762.
- Bowes, G. 1993. Facing the inevitable: plants and increasing atmospheric CO₂. *Annual Review of Plant Biology* **44**:309-332.
- Brockett, B. F. T., C. E. Prescott, and S. J. Grayston. 2012. Soil moisture is the major factor influencing microbial community structure and enzyme activities across seven biogeoclimatic zones in western Canada. *Soil Biology and Biochemistry* **44**:9-20.

- Brzostek, E. R., and A. C. Finzi. 2012. Seasonal variation in the temperature sensitivity of proteolytic enzyme activity in temperate forest soils. *Journal of Geophysical Research-Biogeosciences* **117**:G01018, 10.1029/2011JG001688.
- Burke, I. C., W. K. Lauenroth, and W. J. Parton. 1997. Regional and temporal variation in net primary production and nitrogen mineralization in grasslands. *Ecology* **78**:1330-1340.
- Cai, T. E. B., L. B. Flanagan, and K. H. Syed. 2010. Warmer and drier conditions stimulate respiration more than photosynthesis in a boreal peatland ecosystem: Analysis of automatic chambers and eddy covariance measurements. *Plant Cell and Environment* **33**:394-407.
- Callaway, T. R., S. E. Dowd, T. S. Edrington, R. C. Anderson, N. Krueger, N. Bauer, P. J. Kononoff, and D. J. Nisbet. 2010. Evaluation of bacterial diversity in the rumen and feces of cattle fed different levels of dried distillers grains plus solubles using bacterial tag-encoded FLX amplicon pyrosequencing. *Journal of Animal Science* **88**:3977-3983.
- Cao, G., Y. Tang, W. Mo, Y. Wang, Y. Li, and X. Zhao. 2004. Grazing intensity alters soil respiration in an alpine meadow on the Tibetan plateau. *Soil Biology and Biochemistry* **36**:237-243.
- Capone, K. A., S. E. Dowd, G. N. Stamatias, and J. Nikolovski. 2011. Diversity of the human skin microbiome early in life. *The Journal of Investigative Dermatology* **131**:2026-2032.
- Carbone, M. S., G. C. Winston, and S. E. Trumbore. 2008. Soil respiration in perennial grass and shrub ecosystems: Linking environmental controls with plant and microbial sources on seasonal and diel timescales. *Journal of Geophysical Research-Biogeosciences* **113**:G02022, 10.1029/2007jg000611.
- Carlson, P. J. 2000. Seasonal and inter-annual variation in carbon dioxide exchange and carbon balance in a mixed grassland. M.Sc. Thesis. University of Lethbridge, Lethbridge, AB, Canada.
- Castro, H. F., A. T. Classen, E. E. Austin, R. J. Norby, and C. W. Schadt. 2010. Soil microbial community responses to multiple experimental climate change drivers. *Applied and Environmental Microbiology* **76**:999-1007.
- Ciais, P., C. Sabine, G. Bala, L. Bopp, V. Brovkin, J. Canadell, A. Chhabra, R. DeFries, J. Galloway, M. Heimann, C. Jones, C. Le Quère, R. B. Myneni, S. Piao, and P. Thornton. 2013. Carbon and Other Biogeochemical Cycles. *In* T. F. Stocker, D. Qin, G.-K. Plattner, M. Tignor, S. K. Allen, J. Boschung, A. Nauels, Y. Xia, V. Bex, and P. M. Midgley, editors. *Climate Change 2013: The Physical Science Basis. Contribution of Working Group I to the Fifth Assessment Report of the Intergovernmental Panel on Climate Change*. Cambridge University Press, Cambridge, United Kingdom and New York, NY, USA.
- Cleveland, C. C., D. R. Nemergut, S. K. Schmidt, and A. R. Townsend. 2007. Increases in soil respiration following labile carbon additions linked to rapid shifts in soil microbial community composition. *Biogeochemistry* **82**:229-240.

- Cornwell, W. K., J. H. C. Cornelissen, K. Amatangelo, E. Dorrepaal, V. T. Eviner, O. Godoy, S. E. Hobbie, B. Hoorens, H. Kurokawa, N. Perez-Harguindeguy, H. M. Quested, L. S. Santiago, D. A. Wardle, I. J. Wright, R. Aerts, S. D. Allison, P. van Bodegom, V. Brovkin, A. Chatain, T. V. Callaghan, S. Diaz, E. Garnier, D. E. Gurvich, E. Kazakou, J. A. Klein, J. Read, P. B. Reich, N. A. Soudzilovskaia, M. V. Vaieretti, and M. Westoby. 2008. Plant species traits are the predominant control on litter decomposition rates within biomes worldwide. *Ecology Letters* **11**:1065-1071.
- Corre, M. D., R. R. Schnabel, and W. L. Stout. 2002. Spatial and seasonal variation of gross nitrogen transformations and microbial biomass in a Northeastern US grassland. *Soil Biology & Biochemistry* **34**:445-457.
- Cruz-Martinez, K., K. B. Suttle, E. L. Brodie, M. E. Power, G. L. Andersen, and J. F. Banfield. 2009. Despite strong seasonal responses, soil microbial consortia are more resilient to long-term changes in rainfall than overlying grassland. *The ISME Journal: Multidisciplinary Journal of Microbial Ecology* **3**:738-744.
- Curiel Yuste, J., D. D. Baldocchi, A. Gershenson, A. Goldstein, L. Misson, and S. Wong. 2007. Microbial soil respiration and its dependency on carbon inputs, soil temperature and moisture. *Global Change Biology* **13**:2018-2035.
- Davidson, E. A., and I. A. Janssens. 2006. Temperature sensitivity of soil carbon decomposition and feedbacks to climate change. *Nature* **440**:165-173.
- Davidson, E. A., I. A. Janssens, and Y. Q. Luo. 2006. On the variability of respiration in terrestrial ecosystems: moving beyond Q_{10} . *Global Change Biology* **12**:154-164.
- Davidson, E. A., K. Savage, L. V. Verchot, and R. Navarro. 2002. Minimizing artifacts and biases in chamber-based measurements of soil respiration. *Agricultural and Forest Meteorology* **113**:21-37.
- Dhakhwa, G. B., and C. L. Campbell. 1998. Potential effects of differential day-night warming in global climate change on crop production. *Climatic Change* **40**:647-667.
- Dilkes, N. B., D. L. Jones, and J. Farrar. 2004. Temporal dynamics of carbon partitioning and rhizodeposition in wheat. *Plant Physiol* **134**:706-715.
- Dowd, S. E., T. R. Callaway, R. D. Wolcott, Y. Sun, T. McKeehan, R. G. Hagevoort, and T. S. Edrington. 2008a. Evaluation of the bacterial diversity in the feces of cattle using 16S rDNA bacterial tag-encoded FLX amplicon pyrosequencing (bTEFAP). *BMC Microbiology* **8**:125.
- Dowd, S. E., Y. Sun, R. D. Wolcott, A. Domingo, and J. A. Carroll. 2008b. Bacterial tag-encoded FLX amplicon pyrosequencing (bTEFAP) for microbiome studies: bacterial diversity in the ileum of newly weaned Salmonella-infected pigs. *Foodborne Pathogens and Diseases* **5**:459-472.
- Edgar, R. C. 2010. Search and clustering orders of magnitude faster than BLAST. *Bioinformatics* **26**:2460-2461.
- Environment Canada. 2015. Climate Data Online. Available at: http://climate.weather.gc.ca/climate_normals/index_e.html. (accessed 09 April 2015).

- Eren, A. M., M. Zozaya, C. M. Taylor, S. E. Dowd, D. H. Martin, and M. J. Ferris. 2011. Exploring the diversity of *Gardnerella vaginalis* in the genitourinary tract microbiota of monogamous couples through subtle nucleotide variation. *PLoS One* **6**:e26732.
- Falkowski, P., R. J. Scholes, E. Boyle, J. Canadell, D. Canfield, J. Elser, N. Gruber, K. Hibbard, P. Hogberg, S. Linder, F. T. Mackenzie, B. Moore, T. Pedersen, Y. Rosenthal, S. Seitzinger, V. Smetacek, and W. Steffen. 2000. The global carbon cycle: A test of our knowledge of earth as a system. *Science* **290**:291-296.
- Fitter, A. H., G. K. Self, T. K. Brown, D. S. Bogie, J. D. Graves, D. Benham, and P. Ineson. 1999. Root production and turnover in an upland grassland subjected to artificial soil warming respond to radiation flux and nutrients, not temperature. *Oecologia* **120**:575-581.
- Flanagan, L. B., and A. C. Adkinson. 2011. Interacting controls on productivity in a northern Great Plains grassland and implications for response to ENSO events. *Global Change Biology* **17**:3293-3311.
- Flanagan, L. B., and G. D. Farquhar. 2014. Variation in the carbon and oxygen isotope composition of plant biomass and its relationship to water-use efficiency at the leaf- and ecosystem-scales in a northern Great Plains grassland. *Plant Cell and Environment* **37**:425-438.
- Flanagan, L. B., and B. G. Johnson. 2005. Interacting effects of temperature, soil moisture and plant biomass production on ecosystem respiration in a northern temperate grassland. *Agricultural and Forest Meteorology* **130**:237-253.
- Flanagan, L. B., E. J. Sharp, and J. A. Gamon. 2014. Application of the photosynthetic light-use efficiency model in a northern Great Plains grassland. Submitted to: *Remote Sensing of Environment*.
- Flanagan, L. B., E. J. Sharp, and M. G. Letts. 2013. Response of plant biomass and soil respiration to experimental warming and precipitation manipulation in a Northern Great Plains grassland. *Agricultural and Forest Meteorology* **173**:40-52.
- Flanagan, L. B., L. A. Wever, and P. J. Carlson. 2002. Seasonal and interannual variation in carbon dioxide exchange and carbon balance in a northern temperate grassland. *Global Change Biology* **8**:599-615.
- Frank, A. B., M. A. Liebig, and J. D. Hanson. 2002. Soil carbon dioxide fluxes in northern semiarid grasslands. *Soil Biology & Biochemistry* **34**:1235-1241.
- Gebrekirstos, A., M. van Noordwijk, H. Neufeldt, and R. Mitlöhner. 2011. Relationships of stable carbon isotopes, plant water potential and growth: an approach to assess water use efficiency and growth strategies of dry land agroforestry species. *Trees* **25**:95-102.
- Godfree, R., B. Robertson, T. Bolger, M. Carnegie, and A. Young. 2011. An improved hexagon open-top chamber system for stable diurnal and nocturnal warming and atmospheric carbon dioxide enrichment. *Global Change Biology* **17**:439-451.
- Hanson, P. J., N. T. Edwards, C. T. Garten, and J. A. Andrews. 2000. Separating root and soil microbial contributions to soil respiration: A review of methods and observations. *Biogeochemistry* **48**:115-146.

- Heimann, M., and M. Reichstein. 2008. Terrestrial ecosystem carbon dynamics and climate feedbacks. *Nature* **451**:289-292.
- Hogberg, P., A. Nordgren, N. Buchmann, A. F. S. Taylor, A. Ekblad, M. N. Hogberg, G. Nyberg, M. Ottosson-Lofvenius, and D. J. Read. 2001. Large-scale forest girdling shows that current photosynthesis drives soil respiration. *Nature* **411**:789-792.
- Holland, J. N., W. Cheng, and D. A. Crossley, Jr. 1996. Herbivore-induced changes in plant carbon allocation: assessment of below-ground C fluxes using carbon-14. *Oecologia* **107**:87-94.
- Hollister, R. D., and P. J. Webber. 2000. Biotic validation of small open-top chambers in a tundra ecosystem. *Global Change Biology* **6**:835-842.
- Hopkins, F. M., M. S. Torn, and S. E. Trumbore. 2012. Warming accelerates decomposition of decades-old carbon in forest soils. *Proceedings of the National Academy of Sciences of the United States of America* **109**:E1753-E1761.
- IPCC. 2013a. Annex III: Glossary [Planton, S. (ed.)]. *In* T. F. Stocker, D. Qin, G.-K. Plattner, M. Tignor, S. K. Allen, J. Boschung, A. Nauels, Y. Xia, V. Bex, and P. M. Midgley, editors. *Climate Change 2013: The Physical Science Basis. Contribution of Working Group I to the Fifth Assessment Report of the Intergovernmental Panel on Climate Change*. Cambridge University Press, Cambridge, United Kingdom and New York, NY, USA.
- IPCC. 2013b. Summary for Policymakers. *In* T. F. Stocker, D. Qin, G.-K. Plattner, M. Tignor, S. K. Allen, J. Boschung, A. Nauels, Y. Xia, V. Bex, and P. M. Midgley, editors. *Climate Change 2013: The Physical Science Basis. Contribution of Working Group I to the Fifth Assessment Report of the Intergovernmental Panel on Climate Change*. Cambridge University Press, Cambridge, United Kingdom and New York, NY, USA.
- Janssens, I. A., and K. Pilegaard. 2003. Large seasonal changes in Q_{10} of soil respiration in a beech forest. *Global Change Biology* **9**:911-918.
- Kahmen, A., D. Sachse, S. K. Arndt, K. P. Tu, H. Farrington, P. M. Vitousek, and T. E. Dawson. 2011. Cellulose $\delta^{18}O$ is an index of leaf-to-air vapor pressure difference (VPD) in tropical plants. *Proceedings of the National Academy of Sciences of the United States of America* **108**:1981-1986.
- Kimball, B. A. 2005. Theory and performance of an infrared heater for ecosystem warming. *Global Change Biology* **11**:2041-2056.
- Kimball, B. A. 2011. Comment on the comment by Amthor et al. on "Appropriate experimental ecosystem warming methods" by Aronson and McNulty. *Agricultural and Forest Meteorology* **151**:420-424.
- Kimball, B. A., M. M. Conley, S. Wang, X. Lin, C. Luo, J. Morgan, and D. Smith. 2008. Infrared heater arrays for warming ecosystem field plots. *Global Change Biology* **14**:309-320.
- King, G. M. 2011. Enhancing soil carbon storage for carbon remediation: potential contributions and constraints by microbes. *Trends in Microbiology* **19**:75-84.
- Klein, D. A., B. A. Frederick, M. Biondini, and M. J. Trlica. 1988. Rhizosphere microorganism effects on soluble amino acids, sugars and organic acids in

- the root zone of *Agropyron cristatum*, *A. smithii* and *Bouteloua gracilis*. *Plant and Soil* **110**:19-25.
- Kowalchuk, G. A. 2012. Bad news for soil carbon sequestration? *Science* **337**:1049-1050.
- Kucera, C. L., and D. R. Kirkham. 1971. Soil respiration studies in tallgrass prairie in Missouri. *Ecology* **52**:912-915.
- Kuzyakov, Y., and W. Cheng. 2001. Photosynthesis controls of rhizosphere respiration and organic matter decomposition. *Soil Biology & Biochemistry* **33**:1915-1925.
- Lee, K. H., and S. Jose. 2003. Soil respiration, fine root production, and microbial biomass in cottonwood and loblolly pine plantations along a nitrogen fertilization gradient. *Forest Ecology and Management* **185**:263-273.
- Lin, D. L., J. Y. Xia, and S. Q. Wan. 2010. Climate warming and biomass accumulation of terrestrial plants: a meta-analysis. *New Phytologist* **188**:187-198.
- Liu, W. X., Z. Zhang, and S. Q. Wan. 2009. Predominant role of water in regulating soil and microbial respiration and their responses to climate change in a semiarid grassland. *Global Change Biology* **15**:184-195.
- Luo, Y. 2007. Terrestrial carbon-cycle feedback to climate warming. *Annual Review of Ecology, Evolution, and Systematics* **38**:683-712.
- Luo, Y., and X. Zhou. 2006. Chapter 9 - Separation of source components of soil respiration. *In* Y. Luo and X. Zhou, editors. *Soil Respiration and the Environment*. Academic Press, Burlington. Pages 187-214.
- Meehl, G. A., and C. Tebaldi. 2004. More intense, more frequent, and longer lasting heat waves in the 21st century. *Science* **305**:994-997.
- Mench, M., and E. Martin. 1991. Mobilization of cadmium and other metals from two soils by root exudates of *Zea mays* L., *Nicotiana tabacum* L. and *Nicotiana rustica* L. *Plant and Soil* **132**:187-196.
- Mokany, K., R. J. Raison, and A. S. Prokushkin. 2006. Critical analysis of root: shoot ratios in terrestrial biomes. *Global Change Biology* **12**:84-96.
- Nardi, S., G. Concheri, D. Pizzeghello, A. Sturaro, R. Rella, and G. Parvoli. 2000. Soil organic matter mobilization by root exudates. *Chemosphere* **41**:653-658.
- Niu, S. L., X. R. Xing, Z. Zhang, J. Y. Xia, X. H. Zhou, B. Song, L. H. Li, and S. Q. Wan. 2011. Water-use efficiency in response to climate change: from leaf to ecosystem in a temperate steppe. *Global Change Biology* **17**:1073-1082.
- Olszyk, D. M., T. W. Tibbitts, and W. M. Hertzberg. 1980. Environment in open-top field chambers utilized for air-pollution studies. *Journal of Environmental Quality* **9**:610-615.
- Phillips, R. P., A. C. Finzi, and E. S. Bernhardt. 2011. Enhanced root exudation induces microbial feedbacks to N cycling in a pine forest under long-term CO₂ fumigation. *Ecol Lett* **14**:187-194.
- Polley, H. W. 2002. Implications of atmospheric and climatic change for crop yield and water use efficiency. *Crop Science* **42**:131-140.
- Pumpanen, J., P. Kolari, H. Ilvesniemi, K. Minkkinen, T. Vesala, S. Niinisto, A. Lohila, T. Larmola, M. Morero, M. Pihlatie, I. Janssens, J. C. Yuste, J. M.

- Grunzweig, S. Reth, J. A. Subke, K. Savage, W. Kutsch, G. Ostreng, W. Ziegler, P. Anthoni, A. Lindroth, and P. Hari. 2004. Comparison of different chamber techniques for measuring soil CO₂ efflux. *Agricultural and Forest Meteorology* **123**:159-176.
- Roberts, P., R. Bol, and D. L. Jones. 2007. Free amino sugar reactions in soil in relation to soil carbon and nitrogen cycling. *Soil Biology & Biochemistry* **39**:3081-3092.
- Rosenzweig, C., D. Karoly, M. Vicarelli, P. Neofotis, Q. G. Wu, G. Casassa, A. Menzel, T. L. Root, N. Estrella, B. Seguin, P. Tryjanowski, C. Z. Liu, S. Rawlins, and A. Imeson. 2008. Attributing physical and biological impacts to anthropogenic climate change. *Nature* **453**:353-357.
- Rustad, L. E., J. L. Campbell, G. M. Marion, R. J. Norby, M. J. Mitchell, A. E. Hartley, J. H. C. Cornelissen, J. Gurevitch, and Gcte-News. 2001. A meta-analysis of the response of soil respiration, net nitrogen mineralization, and aboveground plant growth to experimental ecosystem warming. *Oecologia* **126**:543-562.
- Rustad, L. E., T. G. Huntington, and R. D. Boone. 2000. Controls on soil respiration: Implications for climate change. *Biogeochemistry* **48**:1-6.
- Schimel, D. S. 1995. Terrestrial ecosystems and the carbon cycle. *Global Change Biology* **1**:77-91.
- Schlesinger, W. H., and J. A. Andrews. 2000. Soil respiration and the global carbon cycle. *Biogeochemistry* **48**:7-20.
- Schmidt-Rohr, K., J. D. Mao, and D. C. Olk. 2004. Nitrogen-bonded aromatics in soil organic matter and their implications for a yield decline in intensive rice cropping. *Proceedings of the National Academy of Sciences of the United States of America* **101**:6351-6354.
- Shaver, G. R., J. Canadell, F. S. Chapin, J. Gurevitch, J. Harte, G. Henry, P. Ineson, S. Jonasson, J. Melillo, L. Pitelka, and L. Rustad. 2000. Global warming and terrestrial ecosystems: A conceptual framework for analysis. *Bioscience* **50**:871-882.
- Simpson, E. H. 1949. Measurement of diversity. *Nature* **163**:688-688.
- Sinsabaugh, R. L. 2010. Phenol oxidase, peroxidase and organic matter dynamics of soil. *Soil Biology & Biochemistry* **42**:391-404.
- Sinsabaugh, R. L., C. L. Lauber, M. N. Weintraub, B. Ahmed, S. D. Allison, C. Crenshaw, A. R. Contosta, D. Cusack, S. Frey, M. E. Gallo, T. B. Gartner, S. E. Hobbie, K. Holland, B. L. Keeler, J. S. Powers, M. Stursova, C. Takacs-Vesbach, M. P. Waldrop, M. D. Wallenstein, D. R. Zak, and L. H. Zeglin. 2008. Stoichiometry of soil enzyme activity at global scale. *Ecology Letters* **11**:1252-1264.
- Smith, P. 2014. Do grasslands act as a perpetual sink for carbon? *Global Change Biology* **20**:2708-2711.
- Solomon, S., G.-K. Plattner, R. Knutti, and P. Friedlingstein. 2009. Irreversible climate change due to carbon dioxide emissions. *Proceedings of the National Academy of Sciences of the United States of America* **106**:1704-1709.
- Sowerby, A., H. Blum, T. R. G. Gray, and A. S. Ball. 2000. The decomposition of *Lolium perenne* in soils exposed to elevated CO₂: comparisons of mass loss

- of litter with soil respiration and soil microbial biomass. *Soil Biology & Biochemistry* **32**:1359-1366.
- Swanson, K. S., S. E. Dowd, J. S. Suchodolski, I. S. Middelbos, B. M. Vester, K. A. Barry, K. E. Nelson, M. Torralba, B. Henrissat, P. M. Coutinho, I. K. Cann, B. A. White, and G. C. Fahey, Jr. 2011. Phylogenetic and gene-centric metagenomics of the canine intestinal microbiome reveals similarities with humans and mice. *The ISME Journal* **5**:639-649.
- Tjoelker, M. G., J. Oleksyn, and P. B. Reich. 2001. Modelling respiration of vegetation: evidence for a general temperature-dependent Q_{10} . *Global Change Biology* **7**:223-230.
- Townsend, A. R., P. M. Vitousek, and S. E. Trumbore. 1995. Soil organic matter dynamics along gradients in temperature and land-use on the island of Hawaii. *Ecology* **76**:721-733.
- van't Hoff, J. H. 1898. Lectures on theoretical and physical chemistry. *In* R. A. Lehfeldt, editor. *Chemical Dynamics: Part 1*. Edward Arnold, London, UK. Pages 224-229 (translated from German).
- Voroney, R. P. 2007. 2 - The Soil Habitat. *In* E. A. Paul, editor. *Soil Microbiology, Ecology and Biochemistry (Third Edition)*. Academic Press, San Diego. Pages 25-49.
- Waldrop, M. P., and M. K. Firestone. 2006. Seasonal dynamics of microbial community composition and function in oak canopy and open grassland soils. *Microbial Ecology* **52**:470-479.
- Walker, T. S., H. P. Bais, E. Grotewold, and J. M. Vivanco. 2003. Root exudation and rhizosphere biology. *Plant Physiology* **132**:44-51.
- Wallenstein, M. D., S. K. McMahon, and J. P. Schimel. 2009. Seasonal variation in enzyme activities and temperature sensitivities in Arctic tundra soils. *Global Change Biology* **15**:1631-1639.
- Wallenstein, M. D., and M. N. Weintraub. 2008. Emerging tools for measuring and modeling the in situ activity of soil extracellular enzymes. *Soil Biology & Biochemistry* **40**:2098-2106.
- Wang, W. J., R. C. Dalal, P. W. Moody, and C. J. Smith. 2003. Relationships of soil respiration to microbial biomass, substrate availability and clay content. *Soil Biology & Biochemistry* **35**:273-284.
- Wardle, D. A. 1992. A comparative assessment of factors which influence microbial biomass carbon and nitrogen levels in soil. *Biological Reviews of the Cambridge Philosophical Society* **67**:321-358.
- Wardle, D. A. 1998. Controls of temporal variability of the soil microbial biomass: A global-scale synthesis. *Soil Biology & Biochemistry* **30**:1627-1637.
- Wever, L. A., L. B. Flanagan, and P. J. Carlson. 2002. Seasonal and interannual variation in evapotranspiration, energy balance and surface conductance in a northern temperate grassland. *Agricultural and Forest Meteorology* **112**:31-49.
- Whitehead, F. H. 1962. Experimental studies of the effect of wind on plant growth and anatomy. *New Phytologist* **61**:59-62.
- Williams, W. L., L. O. Tedeschi, P. J. Kononoff, T. R. Callaway, S. E. Dowd, K. Karges, and M. L. Gibson. 2010. Evaluation of in vitro gas production and

- rumen bacterial populations fermenting corn milling (co)products. *Journal of Dairy Science* **93**:4735-4743.
- Xiong, J., H. Sun, F. Peng, H. Zhang, X. Xue, S. M. Gibbons, J. A. Gilbert, and H. Chu. 2014. Characterizing changes in soil bacterial community structure in response to short-term warming. *FEMS Microbiology Ecology* **89**:281-292.
- Xu, L. K., and D. D. Baldocchi. 2004. Seasonal variation in carbon dioxide exchange over a Mediterranean annual grassland in California. *Agricultural and Forest Meteorology* **123**:79-96.
- Yvon-Durocher, G., J. I. Jones, M. Trimmer, G. Woodward, and J. M. Montoya. 2010. Warming alters the metabolic balance of ecosystems. *Philosophical Transactions of the Royal Society B-Biological Sciences* **365**:2117-2126.
- Zeglin, L. H., M. Stursova, R. L. Sinsabaugh, and S. L. Collins. 2007. Microbial responses to nitrogen addition in three contrasting grassland ecosystems. *Oecologia* **154**:349-359.
- Zhang, L., H. Guo, G. Jia, B. Wylie, T. Gilmanov, D. Howard, L. Ji, J. Xiao, J. Li, W. Yuan, T. Zhao, S. Chen, G. Zhou, and T. Kato. 2014. Net ecosystem productivity of temperate grasslands in northern China: An upscaling study. *Agricultural and Forest Meteorology* **184**:71-81.
- Zhang, L., B. K. Wylie, L. Ji, T. G. Gilmanov, L. L. Tieszen, and D. M. Howard. 2011. Upscaling carbon fluxes over the Great Plains grasslands: Sinks and sources. *Journal of Geophysical Research. Biogeosciences* **116**:G00J03, 10.1029/2010JG001504.
- Zhang, W., K. M. Parker, Y. Luo, S. Wan, L. L. Wallace, and S. Hu. 2005. Soil microbial responses to experimental warming and clipping in a tallgrass prairie. *Global Change Biology* **11**:266-277.